Biobased polycarbonates derived from L-menthol

DISSERTATION

zur Erlangung des akademischen Grades eines
Doktors der Naturwissenschaften (Dr. rer. nat.)
in der Bayreuther Graduiertenschule für Mathematik und Naturwissenschaften
(BayNAT)
der Universität Bayreuth

vorgelegt von

Adrian Wambach
aus Nürnberg
Bayreuth, 2022

Die vorliegende Arbeit wurde in der Zeit von April 2018 bis Dezember 2021 in Bayreuth am Lehrstuhl Makromolekulare Chemie II unter Betreuung von Herrn Professor Dr. Andreas Greiner angefertigt.

Vollständiger Abdruck der von der Bayreuther Graduiertenschule für Mathematik und Naturwissenschaften (BayNAT) der Universität Bayreuth genehmigten Dissertation zur Erlangung des akademischen Grades eines Doktors der Naturwissenschaften (Dr. rer. nat.).

Dissertation eingereicht am:	17.03.2022
Zulassung durch das Leitungsgremium:	13.04.2022
Wissenschaftliches Kolloquium:	10.10.2022

Amtierender Direktor: Prof. Dr. Hans Keppler

Prüfungsausschuss:

Prof. Dr. Andreas Greiner	(Gutachter/in)
Prof. Dr. Matthias Breuning	(Gutachter/in)
Prof. Dr. Peter Strohriegl	(Vorsitz)
Prof. Dr. Birgit Weber	

Die vorliegende Arbeit ist als Monographie verfasst.

Teile der Arbeit sind bereits in der folgenden Publikation erschienen:

Synthesis of Biobased Polycarbonate by Copolymerization of Menth-2-ene Oxide and CO_2 with Exceptional Thermal Stability

Wambach, A.; Agarwal, S.; Greiner, A. Synthesis of Biobased Polycarbonate by Copolymerization of Menth-2-ene Oxide and CO_2 with Exceptional Thermal Stability. *ACS Sustainable Chem. Eng.* **2020**, *8* (39), 14690–14693.

DOI: 10.1021/acssuschemeng.0c04335

Diese Publikation ist in der vorliegenden Arbeit mit der Literaturstelle [165] zitiert.

Abbreviations

atm	unit of atmospheric pressure
bdi	2,6-ethylphenyl-β-diketiminato ligand
[(bdi)Zn(OAc)]	β-diketiminato zinc acetate complex
BINAP	2,2′-bis(diphenylphosphino)-1,1′-binaphthyl
bisBP	bis-4-benzophenyl adipate
BO	butene oxide
BPA	bisphenol A
BPA-PC	bisphenol A polycarbonate
°C	degree Celcius
cBC	cyclic butene carbonate
CHO	cyclohexene oxide
CO_2	carbon dioxide
COD	cyclo octadiene
COS	carbonylsulfide
COSY	correlation spectroscopy
cPC	cyclic propylene carbonate
d	day
Đ	dispersity ($\frac{\bar{M}_n}{\bar{M}_w}$)
DBP	dibutyl phthalate
DCM	dichloromethane
DEHS	di(2-ethylhexyl) sebacate
DFT	density-functional theory
DMF	dimethylformamide
DMP	dimethyl phthalate
DMSO	dimethyl sulfoxide
DPP	2,6-diphenylphenol
ECH	epichlorohydrine
EO	ethylene oxide
FGE	furanyl glycidyl ether
GC	gas chromatography
GMA	glycidyl methacrylate

h	hour
HMQC	heteronuclear multiple-quantum correlation spectroscopy
HO	hexene oxide
IR	infrared
*i*Pr	*iso*-propyl moiety
LimO	limonene oxide
*m*CPBA	*meta*-chloroperbenzoic acid
MenO	menth-2-ene oxide (mixture of diastereomers)
[M]/[I]	molar monomer to initiator ratio
$\bar{M}_n$	numerical average molecular weight
M_p	peak molecular weight
$\bar{M}_w$	weight average molecular weight
NBS	*N*-bromosuccinimide
NMR	nuclear magnetic resonance spectroscopy
OAc	acetate
OO	octene oxide
p	pressure
PAN	polyacrylonitrile
PBC	poly(butene carbonate)
PBO	poly(butene oxide)
PCHC	poly(cyclohexene carbonate)
PE	polyethylene
PET	poly(ethylene thelephthalate)
PI	polyimide
PLA	polylactide
PLimC	poly(limonene oxide)
PMenBC	poly(menth-2-ene carbonate-*co*-butene carbonate-*co*-butene oxide)
PMenC	poly(menth-2-ene carbonate)
PO	propylene oxide
PPC	poly(propylene carbonate)
ppm	parts per million

[PPN]Cl	bis(triphenylphosphine)iminium chloride
t	time
T	temperature
*t*Bu	*tert*-butyl moiety
TEB	triethylborane
T_g	glass transition temperature
THF	tetrahydrofuran
TMEDA	tetramethylethylenediamine
TOF	turn over frequency
TPE	thermoplastic elastomer
w	weight fraction
WAXS	wide-angle X-ray scattering
wt.%	weight percent

Table of Contents

1 Introduction

Sustainability is having enough for everybody forever and can be viewed from a social, economic or environmental perspective. The UN general assembly summarized these aspects in 17 so-called “Sustainable Development Goals” in 2015, including the end of poverty and hunger, availability of education, healthy lives, gender equality, water and infrastructure, inclusion, protection of terrestrial and aquatic ecosystems and a general collaboration of different countries.[1] Goal 12 of this list demands sustainable consumption and production patterns. This goal is threatened drastically by our dependency on fossil resources. Over 88 million barrels in 2020 and almost 95 million barrels of oil in 2019 were produced per day. If humanity continues to consume oil at this rate, the currently known reservoirs will be depleted in under 54 years.[2] A majority goes into transportation, electricity generation and heating.[3] Burning it for energy adds to the continuously rising carbon dioxide (CO_2) levels, which again requires actions to reduce accelerating climate change as described in goal 13. A big part of the remainder goes into the production of polymers. At least 368 Mt of plastics were produced worldwide in 2019, but only about 2.1 Mt were so-called bioplastics.[4,5] Predictions for 2026 might indicate an increase in demand and production to 7.6 Mt, but a closed circular economy is not in sight.[6] The term bioplastics additionally combines biobased and biodegradable polymers in this case, so that portion of renewable plastics is hard to grab.

Sustainable polymers produced in the most considerable margin are by percentage starch blends, polylactide (PLA), poly(butylene adipate terephthalate) (PBAT), polyamides (PA), polyethylene (PE) and poly(ethylene terephthalate) (PET).[5] Ethylene from steam cracking or natural gas for the production of PET and PE can be substituted by ethylene produced by catalytic dehydration of natural ethanol, making these polymers more sustainable.[7,8] Still, their lack of environmental degradation remains a problem and they are not entirely biobased. On the other hand, PLA degrades at least in special waste treatment plants. Its monomer, lactic acid, can be produced by the fermentation of glucose.[9] Fatty acids of castor oil or isolated from algae are used as starting materials for different long-chain polyamides.[10,11] Although no or fewer petrochemicals are used, the substitutes are generally not less problematic. Especially glucose has to be reviewed critically since its production from starch is always in competition with human food consumption. Although food production is currently

sufficient to feed the world population and the distribution into areas with low incomes is a problem, further competition on the market of carbohydrate-rich foods might increase the prices, making it less affordable. Higher demands of these seemingly sustainable alternatives could be in contradiction to end hunger.[1] Other resources have to be unlocked.

Investigations in this thesis are dedicated to accessing new polymers from renewable sources. Terpenes are an exciting class of natural products with a wide known variety of structures and functionalities. Natural rubber or polyisoprene is with a production of 10 Mt the commercially most relevant terpene polymer.[12] Still, others as α- or β-pinene, α-methylene-γ-butyrolactone or limonene were also tested as potential monomers.[13–15] The combination of limonene with the abundant building block CO_2 showed its potential as the starting material for polycarbonates and opened the field of research for even more sustainable materials.[16,17] Since the atom economy of this copolymerization is optimal and the properties were promising, other terpene-derived polycarbonates are of interest. L-menthol is a terpenoid, widely available from natural and synthetic sources and not in competition with food production. These points make it a promising candidate as the carbon source for synthesizing new polycarbonates by copolymerization with CO_2, which will be presented in the following.

2 Theoretical Background

2.1 Polycarbonates in General

Polycarbonates have been known since 1898 when Einhorn reacted resorcinol or hydroquinone with phosgene, but the term polycarbonate (PC) usually refers to polycarbonate, which is synthesized starting from bisphenol A (BPA).[18] Schnell at Farbenfabrik Bayer and Fox at General Electric Company independently developed this specific polymer in 1946, which was introduced to the market in 1958. Although commercial BPA-PC only has weight-average molar masses ($\bar{M}_w$) of 18000-35000, it shows an ideal set of properties. Low conductivity, heat resistance and flame-retardant properties its main application are found in electronic hardware. Low weight, durability and high transparency make it a highly demanded material for the construction industry. Data storage in the form of CDs, DVDs and Blu-ray disks, safety glasses, and some mobile phones might be the most prominent contact of customers with this material.[19]

In general, there are two industrially relevant synthesic routes towards general-purpose grade BPA-PC, interfacial polycondensation and melt transesterification. BPA is dissolved in the alkaline, aqueous phase to form sodium bisphenolate and phosgene is dissolved in an organic phase for the polycondensation (Scheme 1). Phosgene has to be used in slight excess of 10 – 20 mol% to compensate hydrolysis to NaCl and Na_2CO_3, which dissolve in the aqueous phase. The addition of monofunctional phenol controls molecular masses by chain termination. A clean copolymer solution is then obtained by separating the phases and washing the organic phase first with diluted acids and later with ion-free water. BPA-PC itself is isolated either by precipitation or evaporation of the solvent in a water bath or extruder. Reaction temperatures of 20 – 40 °C make this process mild and easy to handle, but the use of phosgene, a toxic gas, is a significant safety hazard. Losses due to the necessary excess of phosgene and sodium salts as couple-product give this process a poor atom economy, which should be avoided in terms of green chemistry. Furthermore, the general use of chlorinated solvents raises environmental concerns.[19–22]

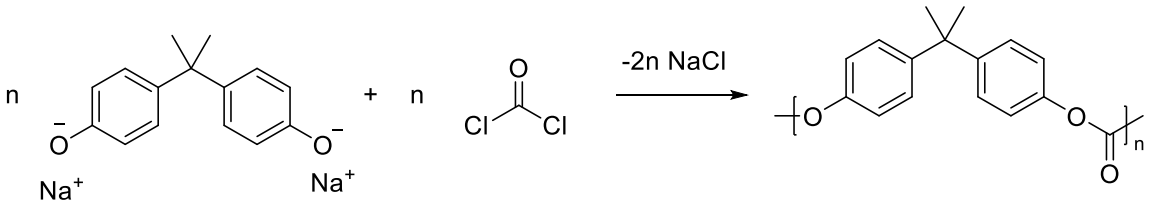

Scheme 1. Synthesis of BPA-PC by interfacial polycondensation.

The other process of melt transesterification circumvents many of these problems. No solvent is necessary and phosgene is substituted by diphenyl carbonate (Scheme 2). This can be synthesized by transesterification of dimethyl carbonate, which again is a product of a catalyzed reaction of carbon monoxide and methanol. Since phenol is removed during the reaction, both alcohols could, in principle, be recycled during the process.[23] One drawback of this process is that after a precondensation phase at approximately 200 °C, the temperature has to be raised to 290 – 310 °C to compensate for the high melt viscosity. These high temperatures might result in defects due to the Fries rearrangement, which is not present in the interfacial process. Furthermore, low pressures of 1 mbar are necessary to remove the phenol from the reaction mixture requiring sufficient equipment.[19–22]

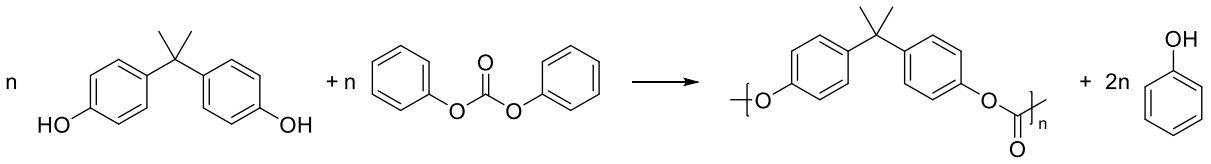

Scheme 2. Synthesis of BPA-PC by melt condensation.

Although other polycarbonates are known and could be produced in similar processes from butane, pentane or hexanediol, BPA remains the monomer with the highest throughput due to its superior mechanical and thermal properties.[22,24] Concerns were rising in the last years that BPA might act as an endocrine disruptor, which led to a rethinking of its general use, especially in drinking bottles and thermal printing paper.[25,26]

2.2 Biobased Polycarbonates

2.3 Biobased polycarbonates

Several biobased polycarbonates were synthesized by the polycondensing of a bio-derived diol with phosgene derivatives. Monoterpenes can be reacted with phenol to give terpene diphenol. Polycarbonates of this monomer showed an even higher glass transition temperature (T_g) than BPA-PC (147 °C).[27] Other diols were obtained by dimerizing L-tyrosine or protecting and reducing tartaric acid.[28,29] Many potential monomers are derived from sugar alcohols. D-mannitol is protected with camphor and its T_g with 164 °C is higher than BPA-PC.[30] Isosorbide was also used as a sugar-derived diol.[31]

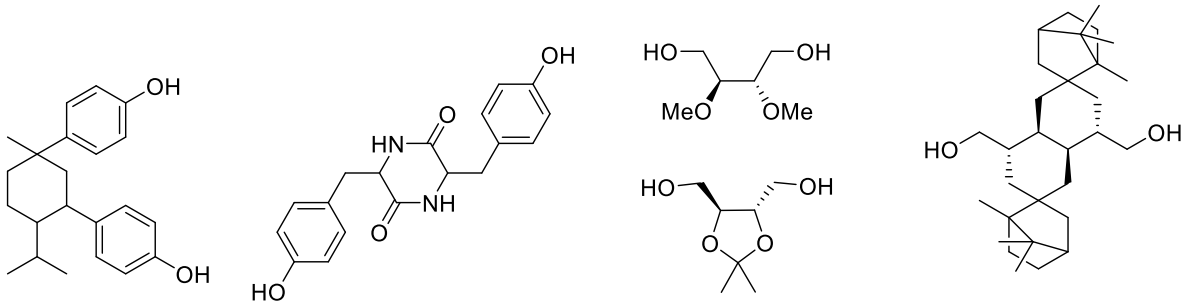

Figure 1. Sustainable diols for the polycondensation of biobased polycarbonates.

The ongoing development of catalysts for the copolymerization of epoxides and CO_2 (see Chapter 2.4) led to the synthesis of new polycarbonates based on metabolites or other compounds found in nature. One of these metabolites is ethanol, produced industrially from the fermentation of carbohydrate-rich plants. After elimination, biobased ethylene can either be directly epoxidized to ethylene oxide (EO) or oligomerized to produce 1-butene, 1-hexene or 1-octane.[32–35] The hazardous properties of EO, including mutagenicity, toxicity and carcinogenicity, limited its investigations in academia, although it is applied in several industrial processes as diol for polyurethane production.[36,37] More studies can be found on butene oxide (BO), hexene oxide (HO) and octene oxide (OO), but the number of publications is far less than those of propylene oxide (PO) and cyclohexene oxide (CHO).[38–40] The epoxidation product of soybean oil is also investigated as a sustainable source of linear aliphatic monomers.[41]

Glycerin is a waste product of bio-diesel production and can be transformed into epichlorohydrin.[42] Despite its high toxicity and mutagenicity, several reports of its

alternating copolymer with CO_2 exist.[43–45] The high reactivity of this epoxide, in general, requires perfectly tunes catalysts and carefully selected conditions to achieve a selectivity towards the polycarbonate. Its ethers enable further modifications and the polymerization of other biomaterials. Furfuryl glycidyl ether (FGE) and its hydrogenated analog were used as monomers.[46,47] FGE can act as a diene for Diels-Alder reactions and was applied for the synthesis of insoluble crosslinked networks by Frey and coworkers.[46]

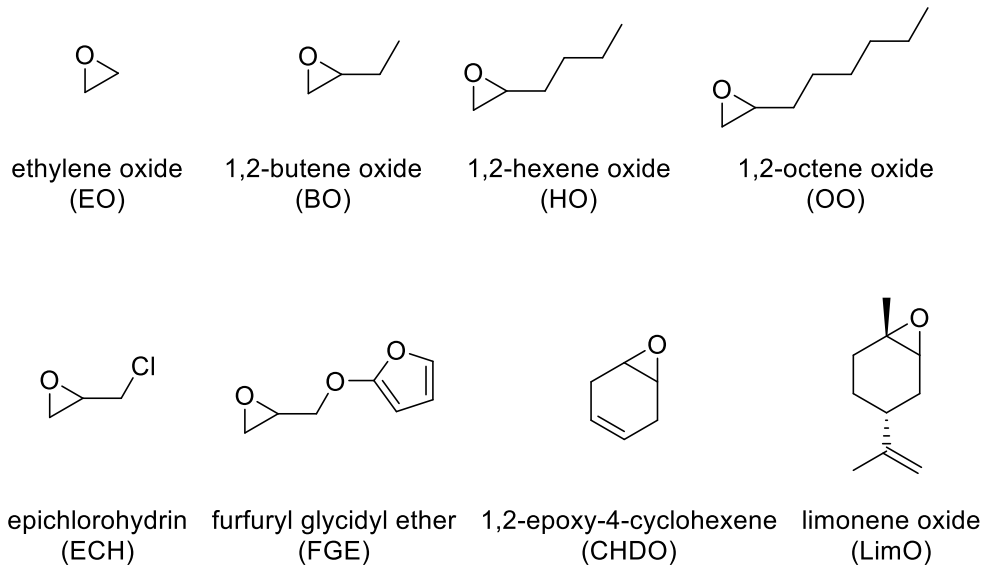

Figure 2. Sustainable epoxides for the copolymerization with CO_2.

1,2-epoxy-4-cyclohexene (CHDO) is promoted as a sustainable alternative to CHO. It can be produced by selective oxidation from 1,4-cyclohexadiene, a waste product of self-metathesis of polyunsaturated fatty acids. The second double bond can later be modified by thiol-ene-click reactions and other addition reactions.[48,49]

Limonene is another sustainable starting material, which can be directly epoxidized to limonene oxide (LimO). Coates and coworkers took the first approach towards the copolymerization of LimO and CO_2.[16] Tests with their β-diketiminate zinc catalyst (structure Figure 5), which shows exceptional activity with CHO, revealed that it could also copolymerize this renewable monomer with CO_2. Although a new polymer with promising properties was obtained, it lacked complete conversions and thus higher molecular weights. Hauenstein et al. were able to eliminate the problem of the conversion by noticing that only the *trans*-isomer is consumed and that inhibiting impurities with protic moieties are present in the used monomer.[17] A diastereoselective route for the monomer synthesis was exploited, resulting in primarily the desired

isomer. The impurities had to be masked by drying the whole mixture over sodium hydride and scavenging the present alkoxide species with iodomethane in a Williamson ether synthesis. Fixing these problems made synthesis on a kilogram scale with molecular weights up to 100 kDa possible.

Modifications of the properties of PlimC were achieved by using analogous polymer reactions at the double bond or by using modified monomers.[50] There are several examples published modifying the double bond, ranging from crosslinking it with sulfur bridges to introducing quaternary ammonium ions for anti-bacterial properties.[50–53] Thiol-ene-click chemistry is often exploited to perform these reactions. Modified monomers are much rarer reported. Several publications are applying the polymerization of limonene dioxide and its post-polymerization modifications. Another important modificaton is the use of selectively hydrogenated limonene oxide. The resulting polymer PMen1C is much more resistant against discolorations and crosslinking under processing conditions than unmodified PLimC.[50]

2.4 Metal-based Catalysts for the Copolymerization of Epoxides and CO_2

Another synthetic route for the production of polycarbonates was introduced by Inoue *et al*.[54] After their successful copolymerization of epoxides and anhydrides, they postulated that CO_2 as the anhydride of the carbonic acid could react similarly to other anhydrides. Two reaction steps were necessary for the copolymerization. First, CO_2 has to react with a propagating alkoxide chain end and then has to be able to open another epoxide with the formed carbonate from the first reaction. The viability of both reaction steps and the polymerization under 50 - 60 atm pressure of CO_2 was shown with a diethylzinc-water mixture as the catalyst.[54]

Since then, many refinement iterations on the catalytic system have been reported. Combinations of diethylzinc and many different H-acidic compounds, *e.g*., water, primary amines, diaminobenzene thioresorcinol, phenols with more than one hydroxyl or carboxylate moieties.[55–59] These catalysts do not have a uniform structure and consist of coordination oligomers or complex networks, which tend to be insoluble in common laboratory solvents. Only some of these examples have a verified structure. Harsher conditions are necessary to maintain a successful copolymerization. Diethyl zinc is not always essential as a reactive and expensive starting material but can be substituted by zinc oxide, hydroxide or double metal cyanides without losing activity.[60–63] A copolymerization was also accomplished with zinc acetate as the catalyst, although the reaction proceeded slowly, even at 80 °C.[64] Similar systems with trialkyl aluminium as cheaper alternatives to diethyl zinc were investigated but resulted in polymers with low polycarbonate content. The combination with Lewis bases or onium-halide salts increased the carbonate content.[65,66] A group of the KAUST identified that the catalyst consisted of a Lewis pair and simplified the catalyst design by splitting these components into an initiating Lewis base and a catalytic Lewis acid. Their first approach was the combination of lithium salts or organolithium compounds with triisobutylaluminium. Attractive polymer architectures were accessible due to the possibility to synthesize macroinitiators easily, e.g., polystyryl lithium or polyisoprenyl lithium, by anionic polymerization.[65] Lithium additionally promoted the reaction of an epoxide with CO_2, but the overall reaction was sluggish and showed a low activity.[67]

The next step in this ongoing line of developments was the introduction of single-site metal complexes. The first, tetraphenylporphyrin aluminium chloride complex, was introduced by Inoue and coworkers.[68] It synthesized alternating copolymers of PO or

CHO with CO_2 in combination with quaternary phosphonium or ammonium salts as a cocatalyst. Narrow dispersities and a clear correlation of the monomer to catalyst ratio showed the living character of the polymerization. Further catalysts with aluminium as active center were synthesized, tested and showed their potential for the ring-opening copolymerization but were restricted by their overall low activity and the high polyether content of the yielded polymers.[69]

Besides zinc and aluminium, chromium and cobalt acetates showed catalytic activity for the coupling of PO and CO_2. Therefore, it was no surprise that homogeneous catalysts of these were synthesized. In the beginning, chromium porphyrins were tested but showed only moderate activity and required cocatalysts.[70] Complexes with salen ligands showed increased activities in the copolymerization of PO or CHO with CO_2, if methyl imidazole or DMAP are added in a certain amount.[71,72]

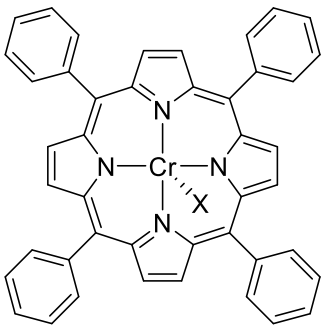

Kruper, Dellar, 1995
X= Cl or O

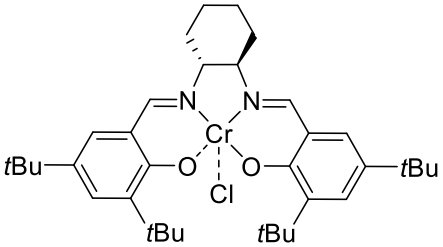

Darensbourg, Yarbrough, 2002
Eberhardt *et al.*, 2003

Figure 3. Chromium catalyst for the CO_2/epoxide copolymerization by Kruper and Dellar[70] (left), Darensbourgh and Yarbrough[71] (right).

The first cobalt salen complex, which catalyzed the copolymerization, was introduced by Coates and coworkers.[73] No cyclic by-products and high carbonate linkages were observed, but high pressures of 55 atm were necessary to sustain a reaction. The group of Lu achieved further improvements. A simple change of a ligand with an electron-withdrawing group and the addition of quaternary ammonium bromides, chlorides or acetates increased the turnover-frequencies (*TOF*) to 248 h^{-1} at lower pressures of 20 atm. Kinetic resolution at the chiral catalyst resulted even in moderate enantioselectivity.[74] Peak activities of cobalt catalysts with *TOF* up to 26000 h^{-1} were reached by the covalent attachment of the cocatalyst to the ligand system.[75] This was attributed to the coulombic attraction of the positively charged cocatalyst cation and the negatively charged propagating species. The propagating species thus is kept in

proximity to the catalytic center, which inhibits chain transfers. Additionally, the initiation and propagation occur at close points in space. The reaction rate is first-order dependent on the catalyst concentration compared to fractional orders for conventional catalysts.[76] Although their catalytic performance is superior, the multi-step synthesis of these complexes makes their use cumbersome and is unfavorable for an application.

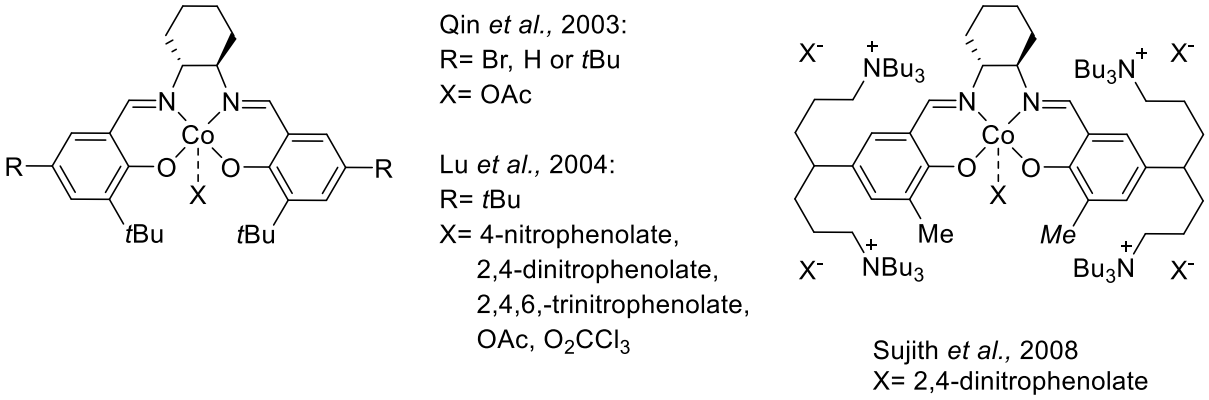

Figure 4. Ground structures of Co(salen) complexes for CO_2/epoxide copolymerization by Qin et al.[73], Lu et al.[74](left) and Sujith et al.[75](right).

Besides the more or less dispersed zinc catalysts systems, discrete zinc complexes were also developed. Darensbourg reported the first one in 1995.[77] It was a complex of zinc with two 2,6-diphenyl phenol ligands and was able to catalyze the copolymerization of CHO and CO_2 with high content of carbonate linkages, although only broad distributions and *TOF*s were achieved. Complexes with benzoate, salicylaldiminato or substituted cyclopentadienyl ligands could reach high molecular weights but still showed broad distributions and slow reaction rates.[78–80] A pyridine alkoxide zinc acetate complex showed narrower distributions and higher rates for the copolymerization of CHO and CO_2 but could only reach unusually low carbonate contents of 63%.[81] Higher reaction rates for CHO without a loss in selectivity could be realized with β-diketiminato zinc complexes.[82] Different initiating ligands are possible by the same synthetic route. Depending on the steric demand of the ligand, these complexes either are monomers, dimers or exist in an equilibrium of both. This can also be different for reactions in solid-state or in solutions.[83–85] Rate studies propose the involvement of a dimeric species during the polymerization, although a monomeric transition state could not be excluded.[81] This led to developing a bimetallic zinc catalyst to avoid dependence on a monomer-dimer equilibrium. Lee and coworker published a bis(anilido-aldimide) complex of zinc, which showed an excellent high *TOF* of 312 h^{-1}.[86]

Macrocycles with two zinc centers were also reported and reached an even higher *TOF* of 9130 h^{-1} without compromising the selectivity.[87]

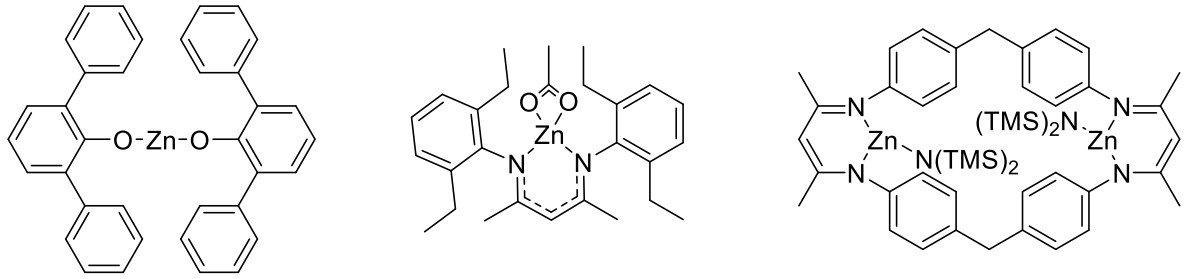

Darensbourg *et al.,* 1995 Moore *et al*., 2003 Lehenmeier *et al.* 2013

Figure 5. A selection of zinc complexes for the CO_2/epoxide copolymerization by Darensbourg et al.(left)[77], Moore et al.(middle)[82], Lehenmeier et al.(right)[87].

Besides dinuclear zinc catalysts, dinuclear Co(III), Mg(II) and Fe(III) catalysts showed their capability in the CO_2 epoxide copolymerization at 1 bar CO_2 pressure.[88–90] Experimental data and theoretical calculations suggested a chain shuttling mechanism.[91] The polymer chain is attached to one metal atom and moves to the other one with every monomer insertion. This discovery led to the development of heterodinuclear complexes since each metal center appears to have a distinct role of either epoxide activation or carbonate coordination and heterodinuclear complexes might tune the electronic properties to increase the activity even further. Indeed, mixed Zn(II)/Mg(II) catalysts showed higher activities than their homonuclear counterparts.[92] Synergetic effects also were observed for combinations of Zn(II)/Ln(III), Co(II)/Mg(II), Co(III)/K or Zn(II)/Na.[93–95] Especially, the Co(II)/Mg(II) catalyst was a significant advancement since it reached a *TOF* of up to 12460 h^{-1}.[96]

2.5 Borane-based Catalysts for the Copolymerization of Epoxides and CO_2

Since the critical features of the metal-based catalyst are their prominent Lewis acidity and trialkylaluminium compounds already showed their potential as a catalyst for the copolymerization of CO_2 and epoxides, alternative acidic molecules were examined. Triethylborane (TEB) was introduced as an alternative Lewis acid, thus opening a field of organocatalytic CO_2/epoxide copolymerization. TEB coordinates to epoxides and salts containing a low coordinating cation, which acts as the initiator, were able to open the three-membered ring to an alkoxide (Scheme 3, I). CO_2 inserts into the coordinative bond between the alkoxide and the boron (Scheme 3, II) before reacting with another epoxide activated by TEB (Scheme 3, III). The coordination strength of TEB is just right to allow the insertion steps but to reduce the nucleophilicity of the alkoxide to stop backbiting (Scheme 3, IV) or homopolymerization. Copolymerizations of CO_2 with PO or CHO were possible in the original publication of Zhang *et al.* Molecular weights up to 50000 for poly(propylene carbonate) (PPC) and 76400 for PCHC were achieved.[67] Molecular weights were further increased by drying the CO_2 with triethyl aluminium. Although these distributions were unimodal, this procedure was not adopted due to the high flammability of the drying agent.[97] Experimental data indicated that two equivalents of the catalyst TEB were necessary for a successful reaction.[67] Succeding theoretical studies showed that one equivalent activates the epoxide in the reaction mixture, while the other one stabilizes the growing chain end. This stabilization reduces the basicity of the alkoxide, which otherwise might undergo homopolymerization forming the polyether or backbite to form the cyclic organic carbonate.[98] Other studies on phenyl glycidyl ether and styrene oxide as alternative monomers indicated that even more equivalents might be necessary to meet the requirements of other building blocks.[99] If the initiator is chosen wisely, even recycling of the catalyst was demonstrated as viable.[100]

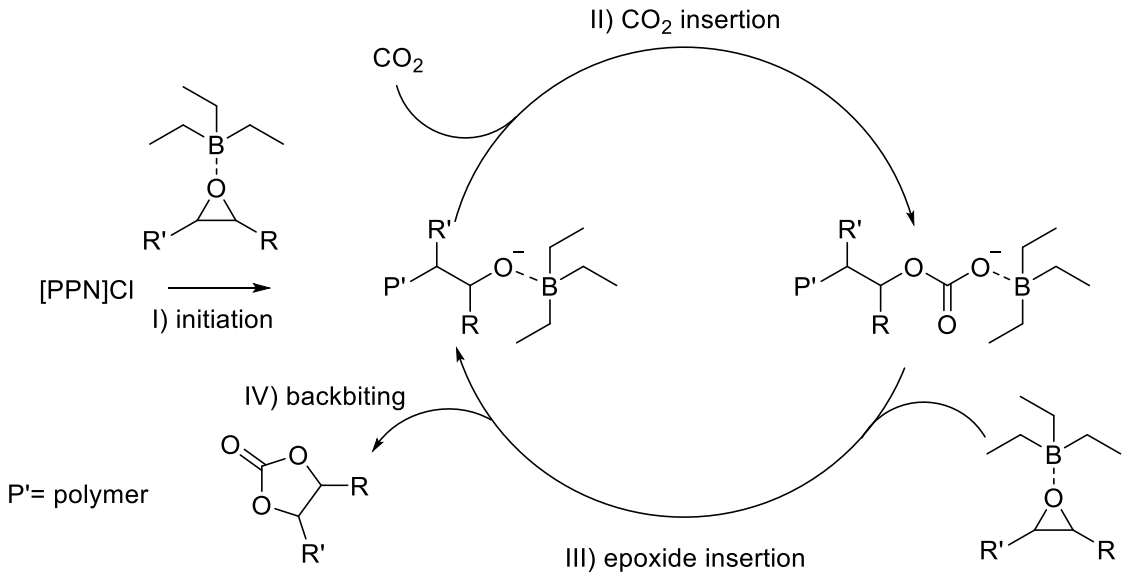

Scheme 3. The proposed mechanism of the TEB catalyzed copolymerization of CO_2 and epoxides with its three general steps of I) initiation, II) CO_2 insertion and III) epoxide insertion. IV) demonstrates the potential production of cyclic carbonates by backbiting. Bis(triphenylphosphine)iminium chloride ([PPN]Cl) was depicted as the exemplary initiator.

The splitting of activation and initiation also splits the design of these parts of the reaction. Varying the structure of the initiator enables a high number of potential polymer architectures. A successful synthesis of polycarbonate diols, triols or tetraols was achieved by utilizing multivalent carboxylates.[101] These were prepared by the reaction of carboxylic acids with tetra *n*-butyl ammonium hydroxide. The same trick was applied to the carboxylic acids of poly(methacrylic acid), allowing the synthesis of graft polymers.[102]

Another approach towards different polymer architectures was accomplished by utilizing the living character of the reaction and the versatility of the system. Anhydrides could be used instead of CO_2 to synthesize polyesters or polyethers.[103,104] These properties were applied in the synthesis of block copolymers and thermoplastic elastomers (TPE).[105–109] Star block copolymers with a degradable core were prepared by this route as well.[110] Heteroallenes as carbonyl sulfide or isocyanates provide access to thiocarbonates or polyurethanes with enhanced thermal or metal-binding properties.[111,112]

In recent years the drastically increased efficiency of catalysts, in which the active center is covalently bonded to the initiator cation, showed that ionic attractions between the anionic growing polymer chain and the catalyst cation are beneficial for high reaction rates.[39,75,76,113] Wu and co-workers presented a bifunctional organoboron catalyst (Figure 6, left) and its preparation in a cost-effective kilogram scale by

alkylation of a tertiary amine and subsequent hydroboration.[114] *TOF* of 710 h^{-1} were achieved with this bifunctional catalyst, while a combination of two model compounds for the initiator and the catalyst parts only reached 12 h^{-1}. DFT calculations supported a drastic increase in the synergetic effect. A high selectivity towards the polycarbonate without a significant cyclic carbonate formation was achieved for CHO. A structurally similar catalyst (Figure 6, middle) was utilized for the selective conversion of PO into the cyclic carbonate (cPC).[115] Since the borane acts as an activator for the epoxide and has to stabilize the chain end to suppress backbiting and homopolymerization, a higher number of boranes per initiator might be necessary, especially for more active monomers. Adding three further boron substituents by a similar synthetic pathway enabled the copolymerization of epichlorohydrin with CO_2 with high selectivities towards the alternating copolymer (Figure 6, right).[45]

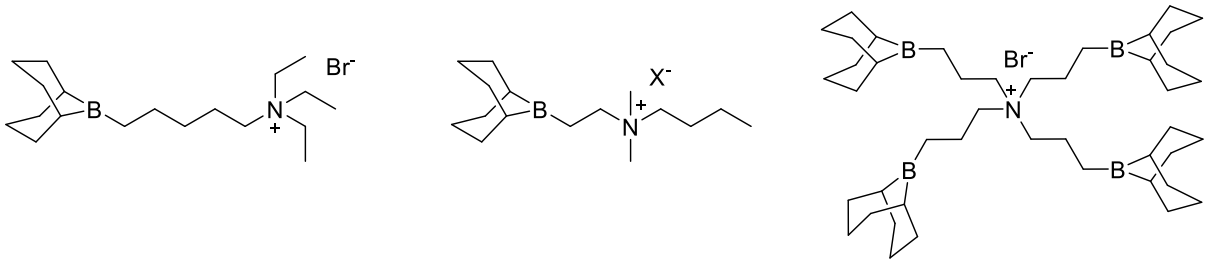

Yang *et al.*, 2020 Zhang *et al.*, 2020 Yang *et al.*, 2021

Figure 6. Multifunctional borane catalyst for the coupling of CO_2 and epoxides by Yang et al.[45,114] (left, right), Zhang et al. [115](middle).

2.6 Menthol from Natural and Industrial Synthesis

Menthol is a monocyclic terpene alcohol, naturally found in corn mint, spearmint and other plants of the genus *Mentha*.[116] Due to its three stereogenic centers, eight diastereomers are possible (see Figure 7). The most important one is L-menthol. It has the strongest odor and shows a cooling sensation when it comes in contact with skin, making it a commonly used ingredient for cosmetics, cough medicines, aftershaves, perfumery, or antipruritics.[116] Its chiral structure makes this molecule also a widely used chiral auxiliary in organic chemistry.[117,118]

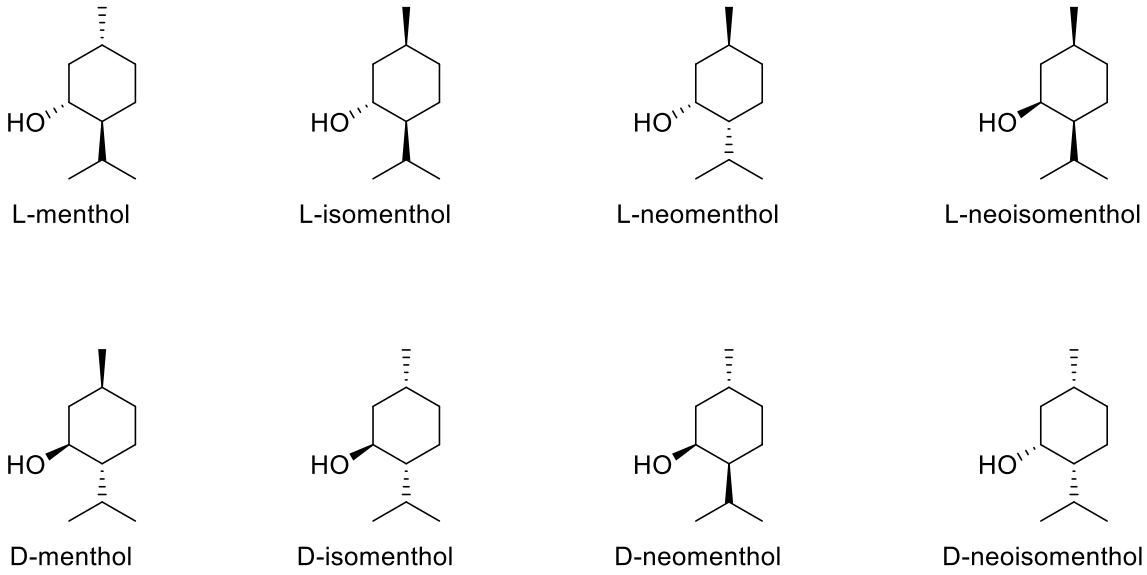

Figure 7. Diastereomers of menthol.

Due to its broad applicability, there is a high demand for menthol and the market was valued at 838.7 million USD in 2020.[119] A significant portion of this market is supplied by harvesting plants of the genus *Mentha* and extraction of the L-menthol-rich essential oil by steam distillation. After removal of water and solids by filtration, the crude mint oil is distilled under reduced pressure and subsequently cooled to -40 °C. At this temperature, menthol crystallizes and can be removed from the dementholized oil. Then the obtained powder is dissolved in small amounts of the oil and cooled to -10 °C over several days until big crystals form.[120]

One of the traditional processes for the production of menthol is the Haarmann-Reimer process. The first step of this procedure is the alkylation of *m*-cresol with propene, followed by unselective hydrogenation. Since an achiral substrate is used and no asymmetric catalyst is used, a mixture of the racemates of menthol, neomenthol, isomenthol and neoisomenthol is obtained. This mixture is rich in DL-menthol. A

consequent fractional distillation to separate the isomers is possible due to sufficient differences in boiling points of the racemates. L-Menthol can be obtained from the racemate by fractional crystallization of the benzoate ester. The efficiency of this process is increased by recycling R-menthol and the other diastereomers and thus achieves an overall yield in the range of 90%. Recycling the less demanded isomers is realized by reintroducing them into the hydrogenation step, where a re-equilibration to the DL-menthol-rich mixture occurs.[121]

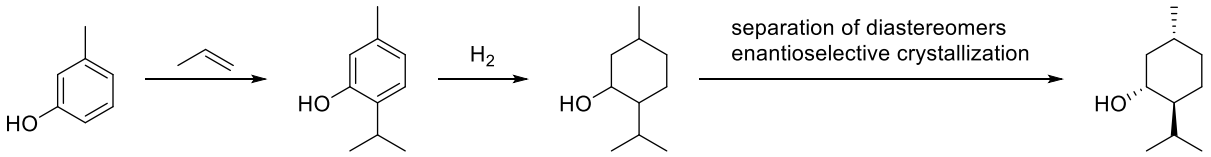

Scheme 4. Schematic depiction of the synthesis of menthol in the Haarmann-Reiman process.

The Takasago process can use a more sustainable and broader range of resources. The terpene β-pinene, extracted from pine resin, is thermally cracked or dimerization of isoprene gives myrcene the starting material for this synthetic pathway. Myrcene is treated with *N*,*N*-diethylamine in the presence of *n*-butyllithium as the catalyst. This 1,4-conjugated addition results in the formation of *N*,*N*-diethylgeranylamine, which is isomerized to *N*,*N*-diethylenamine of D-citronellal by an enantiomerically pure rhodium catalyst with BINAP-ligand.

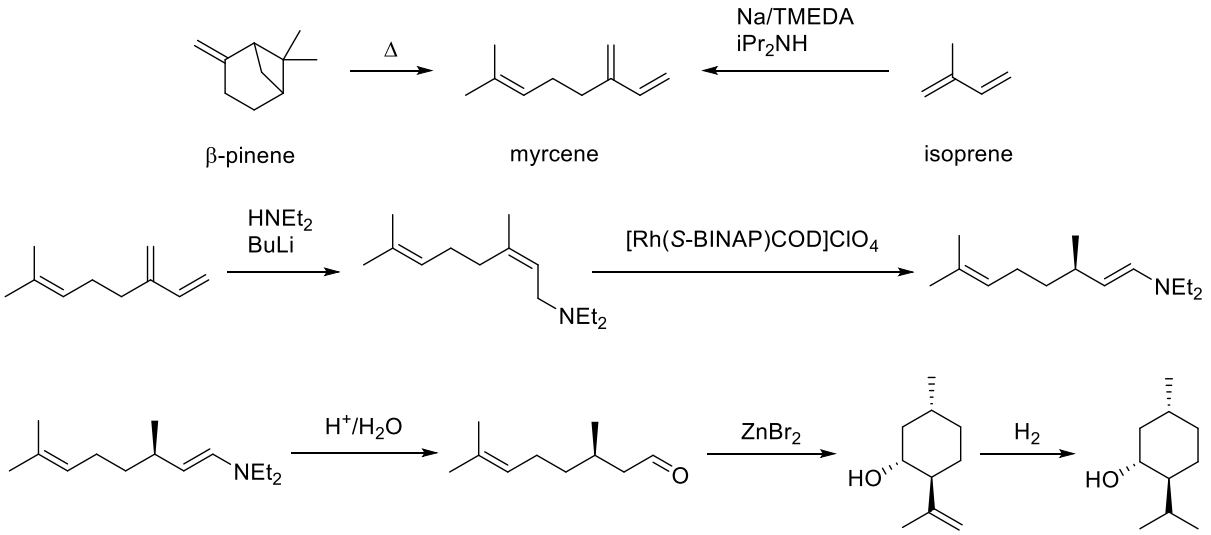

Scheme 5. Schematic depiction of the menthol synthesis in the Takasago process.

The introduction of the first enantiomeric center, quantitative yields, high optical purity, high turn-over numbers, and the catalyst's recyclability makes this step an outstanding example for successful asymmetric catalysis. Acidic hydrolysis removes the enamine, zinc bromide or zinc chloride catalyzes a diastereoselective cyclization by a carbonyl-

ene reaction and the resulting isopulegol is reduced to give highly optically pure L-menthol.[122]

BASF developed the newest industrially relevant processes for the production of L-menthol. The company already produced the starting material citral and this is initially reduced to give a mixture of nerol and geraniol. Both isomers are further reduced in the presence of different Ru-BINAP catalysts resulting in both cases in (*R*)-citronellol. It is further oxidized to (*R*)-citronellal, cyclized similar to the Takasago process utilizing a Lewis acid and again reduced to L-menthol. A direct reduction of geranial and neral to (*R*)-citronellal could be performed with the application of suitable rhodium-Chiraphos catalysts.[122]

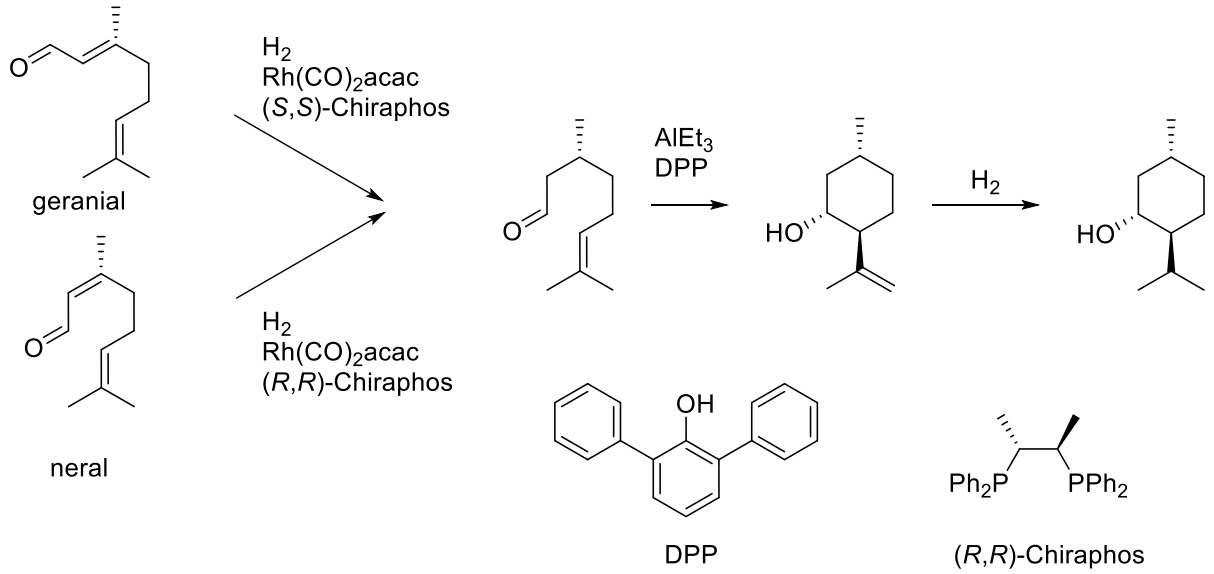

Scheme 6. Schematic depiction of the menthol synthesis in BASF process with stereoselective hydrogenation of citral.

Although L-menthol is a broadly available and cheap building block applied on several occasions in organic synthesis as a chiral auxiliary, its application in polymer science is very limited. Most publications dealing with menthol use it as a bulky and/or chiral side chain in vinyl polymers.[123–125] They could be polymerized at low temperatures and showed a rotation of linear polarized light. Modifications in other positions are complex because the hydroxyl moiety represents the only functional group in the molecule. Hence, some more polymerization types are known, starting from the menthol-derived ketone menthone.[15,126–129] In theory, this could be obtained by selective oxidation of menthol but is also available from natural sources since it is a by-product of the biosynthesis of menthol. Several publications perform a Baeyer-Villiger-oxidation with menthone and use the resulting lactone as a building block for aliphatic polyesters with

exceptional low T_gs.[15,126] Combinations with high T_g or crystalline polyesters was a possible approach on biobased block copolymers with TPE-like properties. A lactam can be obtained if menthone is used in a Beckmann rearrangement. This can be used in anionic ring-opening polymerizations of polyamides. These show high thermal stability up to 400 °C and high melting temperatures around 300 °C, which is even higher than Nylon-6.[127–129]

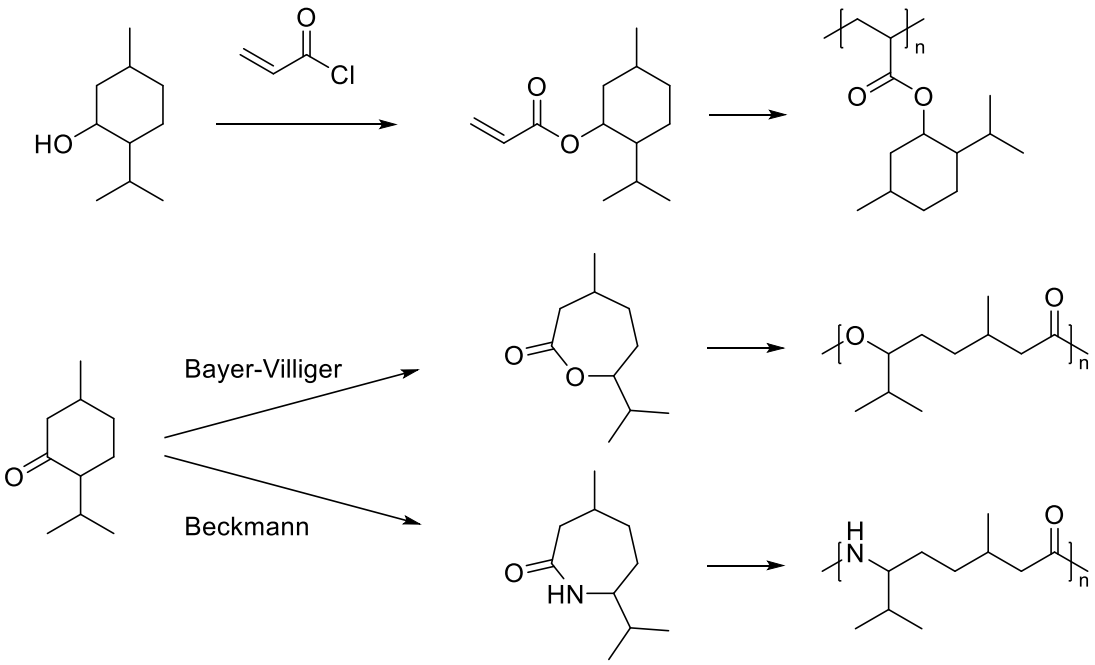

Scheme 7. Synthesis of known menthol-based polymers.

2.7 Principles and Applications of Electrospun Nanofibers

Electrospinning is a method to produce fibers on a nano- to micrometer scale and a wide range of morphologies. Although a publication from 1887[130] and patents by Cooley[131] and Morten[132] from the early 1900s describe the principles behind this method, it took a further ninety years to establish it as a widespread manufacturing practice. Noteworthy are the patents of Formhals[133], which showed the applicability of the method, and the theoretical works of Sir Geoffrey Taylor, which led to the understanding of the shape of droplets in a strong electrical field.[134] The research took off in the 1990s with Doshi and Renecker.[135] Alone in 2021, electrospinning contributed 6446 publications according to Scifinder.[136]

Fibers are produced by the deformation and stretching of a droplet to a fiber in a strong electric field. A polymer solution is usually loaded inside a syringe and continuously ejected through a cannula, which also works as the electrode. At its end, a droplet is formed and if a sufficient voltage is applied, first a Taylor-cone is formed on the surface, which then results in the formation of the jet. This jet is accelerated towards the counter electrode. Either this is connected to the electrical ground or a small negative voltage is applied. Due to the acceleration and the additional fast evaporation of solvent from the drastically increased surface of the newly formed fiber, it decreases until dry fibers in the lower micrometer or nanometer scale are obtained.

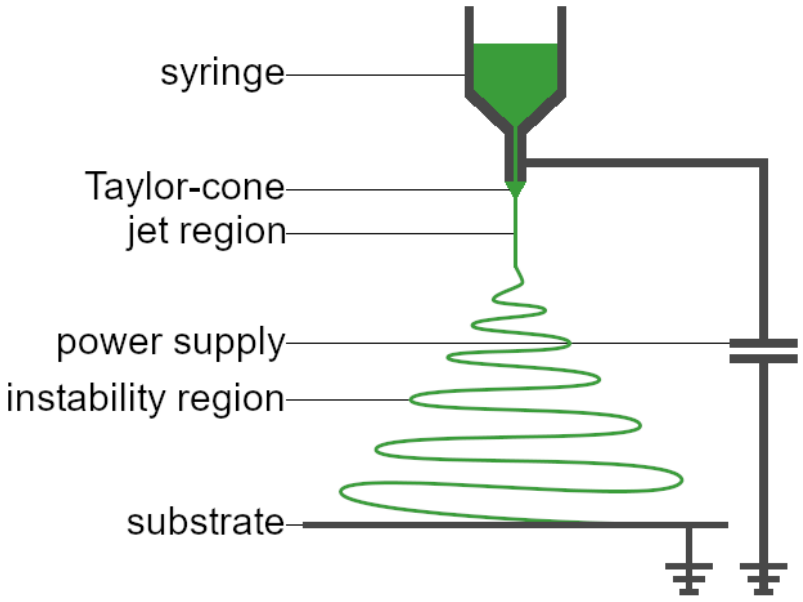

Figure 8. Schematic depiction of the electrospinning process.

Electric repulsion of likely charged jet segments adds up to a force perpendicular to the electrical field, called bending instabilities, and deflects the jet on an increasingly

complex trajectory. Repulsion becomes stronger with decreasing fiber diameter, which increases the diameter of the spiral even further. Elongations up to the factor of 10^5 are possible.[137]

Many parameters influence the continuity and shape of the generated fibers. Besides the apparent voltage difference, flow rates have to be adjusted to supply sufficient amounts of the polymer solution without the formation of drops. The diameter of the cannula also influences the process as well as the distance between syringe and collector. Temperatures are another parameter since it significantly affects the evaporation of the solvent and the properties of the solution itself. The viscosity of the solution, solvent, conductivity, surface tension, but also the polymer and its molecular weight play a massive role in the preparation of continuous straight fibers or fibers with the content of beads. High humidity could result in highly structured fibers but also helps to discharge the jet.[138]

Due to the nanometer scale of electrospun fibers, membranes with tiny pores in the micro to nano scale form, which result in good filtration properties of these materials. Especially dust removal from air polluted by industrial processes is still an active field of research.[139] Also, filtration of aqueous media is an important topic. Polystyrene particles with a diameter of 10 µm could be removed efficiently from solutions with polysulfone or polyvinylidene fluoride fibers.[140,141] Modifications of the polymer by introducing anchor groups for nanoparticles or heavy metals can also remove these selectively.[142,143] A study by Shin and Chase demonstrated the coalescence filtration of secondary emulsions with water droplets smaller than 50 µm. The main parameters, fiber diameter and wettability could be controlled during the electrospinning process and an appropriate selection of the polymer.[144]

Furthermore, the high surface area of the electrospun non-wovens can be utilized in the biomedical field by the slow and controlled release of therapeutically active substances over an extended period.[145] This reduces toxicity and facilitates medication. This effect can even be enhanced by using microparticles spun together with a carrier solution.[146]

The high porosity of the obtained non-wovens is exploited in developing materials for lithium-ion batteries.[147] Examples of novel silicon anodes were prepared by coaxial electrospinning of silicon nanoparticles and polyacrylonitrile (PAN) and subsequent pyrolization of the polymer matrix.[148] Gelled membranes of poly(vinylidene difluoride)

electrospun fibers showed their potential as a separator.[149] Similar, carbon nanotube-enforced carbon nanofibers with active platinium on the surface could be used as electrode material in fuel cells.[150]

Furthermore, short-cut electrospun fibers can be processed to sponges with low density, high porosity, and substantial internal volumes. Jiang *et al*. presented the preparation of polyimide (PI) sponges with a low density between 7.6 and 10.1 mg/cm^3 and high thermal insulating properties even under compression by freeze-drying of a solution of short-cut PI fibers.[151] Tai *et al.* pyrolyzed a PAN/silica sponge to obtain a superhydrophobic sponge for oil and water potential separation.[152]

Another application is the use as a template. Whenever thin fibers of the material are required but cannot be produced directly, electrospun fibers with suitable additives can be used as templates. So covalent organic frameworks, which are usually solid, could be grown on the surface of thin PAN fibers and were obtained as a dispersible powder after removal of the template.[153] Also, hollow poly(*para*-xylylene) fibers loaded with gold nanoparticles could be produced by chemical vapor deposition coating gold-loaded electrospun fibers.[154] TiO_2 or copper fibers could also be produced by adding precursors to the spinning solution.[155,156] Biodegradable non-wovens can be used for tissue engineering.[157] Nanofibers are here used as scaffolds mimicking the fibrillar structure of the extracellular matrix.[147] Properties can easily be adjusted to meet requirements in mechanical properties, cell attachment, diffusion of nutrients or alignment and additives, *e.g.,* the addition of hydroxyapatite nanoparticles and bone morphogenetic protein 2 facilitated the differentiation of human bone-marrow-derived mesenchymal stem cells to form bones.[147]

3 Motivation

Polymers are ubiquitous and necessary for the modern lifestyle, but commodity plastics are at this point no sustainable solution. They are synthesized from petrol-based monomers and are usually not biodegradable. Environmental concerns have become a more and more severe issue. Thus circular economies, biobased materials and sustainability, in general, are rising to the most important research topics of the following decades. This thesis is dedicated to accessing materials from renewable resources and may be motivating others to contribute to the scope of biobased polymers. The utilization of limonene, which is the main component of citrus oils, in combination with CO_2 showed that readily available biobased byproducts of other industrial processes could be used to synthesize novel polycarbonates. As the topic of CO_2 copolymerization is mainly dominated by propylene and cyclohexene oxide, this more sustainable choice of monomer is a welcome alternative. Limonene is a terpene, which is a class of natural compounds that are formally built up by isoprene units. PLimC and a polycarbonate derived from α-pinene have been the only published terpene-based polycarbonates at the start of the work for this thesis. Other terpenes could be potential candidates for sustainable polymers with interesting new properties. Here, the terpene alcohol menthol was chosen. It is the major component of essential oils of plants of the genus *Mentha*, cultivated on a large scale. There is an already working and established industry for the extraction of natural menthol. Menthol is used in several products, *e.g.,* drinks, toothpaste, mouthwash, but is only as a flavoring agent. A potential new material on its basis thus is not in conflict with food production like other bioplastics, *e.g.,* poly(lactic acid), bio-polyethylene, bio-poly(ethylene terephthalate). Industrial synthesis can compensate for disadvantages of plant-based materials like poor harvests due to droughts or extreme weather and ensure the supply. Menthol is a common auxiliary in organic chemistry and thus, plenty of publications are available for the modification and elimination of the hydroxyl group. Furthermore, the two elimination products are isomers to the already studied menth-1-en, which already showed good properties for processing. These properties might be further improved and deduced from the altered structure.

4 Aim and Objectives

The main goal of this work is the synthesis and application of a novel sustainable polycarbonate. Starting materials have to be chosen carefully to achieve the goal of sustainability. As far as possible, every used component should come, at least in theory, from a regenerative source and be neither toxic nor harmful. Natural L-menthol was chosen as the primary biobased carbon source for the backbone.

In consideration of sustainability, the copolymerization of CO_2 with epoxides was chosen for the synthesis of the polycarbonate since it adds an excellent atom economy. This objective consists of two parts. First, a synthetic pathway has to be established to transform menthol into an epoxide efficiently. As soon as the monomer supply was granted, suitable catalysts and conditions for the polymerization have to be found, which should not interfere with the principles of green chemistry.

The successful polymerization includes a complete characterization of the molecular structure of the obtained polymer. Since different diastereomeric configurations are possible due to the chiral nature of menthol and the menthene oxides, an investigation of the stereochemical orientation of the substituents at the cyclohexane ring is necessary. Thermal properties have to be checked as well to evaluate later processing methods.

Due to the experience with PLimC and the sterically demanding molecular structure indicating rather stiff menthol-based polymers, ways have to be found to obtain an impact-resistant polymer at room temperature. Therefore, plasticizers can be added internally or as an additive. Linear aliphatic epoxides such as butene oxide or undecene oxide must be tested in a terpolymerization to introduce more flexibility. Incorporation and thermal properties have to be evaluated for later applications.

Lower T_g samples should also be examined but might require crosslinking to maintain dimensional stability at room temperature or slightly above. Applicability as bulk materials has to be tested by preparing films or electrospun non-wovens. Suitable parameters have to be found to obtain nanometer-scale fibers.

5 Results and Discussion

5.1 Synthesis of Poly(menthene carbonate)

5.1.1 Monomer Synthesis

The major requirements which had to be fulfilled for the synthesis of the monomer were high selectivity, high yield, scalability and a low number of steps. The selectivity became interesting because a direct elimination of the hydroxyl moiety of menthol could result in two different olefins. 2-Menthene is the kinetically favored, while 3-methene is thermodynamically favored. Although the usage of a mixture of isomers might be feasible in the following steps, a study of each isomer is necessary to determine the specific influence. A separation of these two isomers might be possible by distillation but requires a further purification step and reduces the overall yield of the single compounds. Thus, an isomer-selective reaction would be the optimum. The yield of the reaction, keeping the scalability in mind, should be as high as possible and the number of steps should be kept to a necessary minimum to reduce waste, effort and to keep the overall yield high.

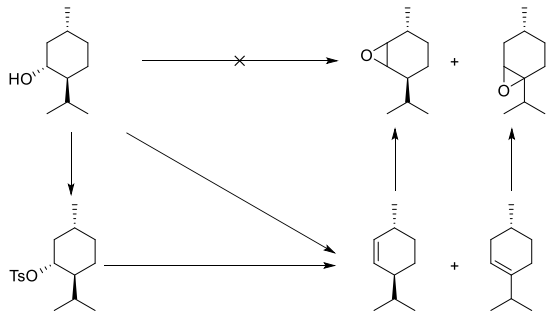

Scheme 8. Potential pathways for the synthesis of 2- and 3-menthene oxide.

In the literature, there are two primary routes known as depicted in Scheme 8. The direct elimination of the hydroxyl moiety using heterogeneous under harsh conditions and on the other hand, the modification and subsequent elimination of the modified group. The majority of the direct routes were published between 1955 and 1979 and showed only poor analytics for modern standards.[158–160] Due to the significant advantage of the lower number of steps and the apparent easier work-up, four procedures were investigated. An experiment with pyridine on an Al_2O_3 surface did not show any elimination products; eliminations with phosphoric, sulfuric or boric acid were successful but lacked a significant selectivity. Both menthenes were formed simultaneously with many other compounds, which had to be removed by the subsequent purification step. 3-Menthene was formed as the preferred isomer in all

successful eliminations, but the portion of 2-menthene was higher with boric acid (see Figure 9). Besides the low purity of the products, only 42% could be achieved in the reaction with sulfuric acid and 74% with boric acid. Due to the lack of selectivity towards a single isomer of menthene and the high amount of contaminations, these reactions were not pursued further. A more modern procedure seemed promising, but the use of expensive rhenium made the scalability unfavorable.[161]

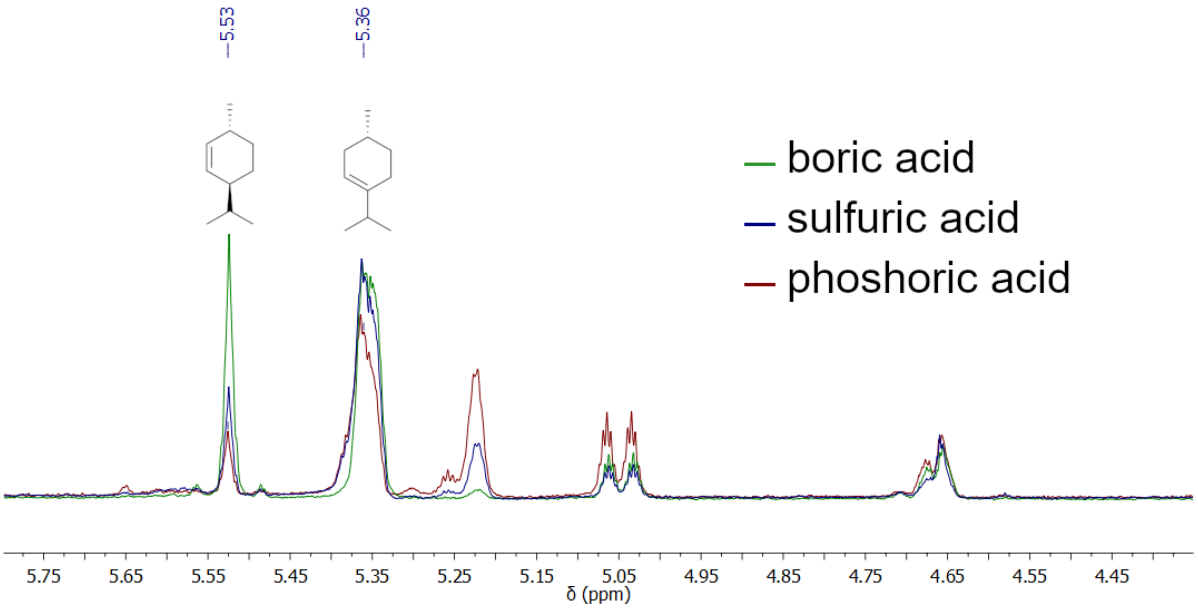

Figure 9. ^{1}H NMR spectra of obtained compounds after single step elimination with phosphoric, sulfuric or boric acid.

Since single-step eliminations did not meet the requirements, a literature study suggested a modification of the hydroxyl moiety to an easier cleavable functional group. Xanthates or urethanes seemed to have the same problems as the single-step procedures and were ignored for this reason.[162] The most promising functionalization was the synthesis of sulfonic acid esters like tosylates or methyl sulfonates.[163,164] According to the literature, both reactions were possible in almost quantitative yields. Due to the similar price per mole and scalability, the less toxic tosylic chloride was chosen over the methyl sulfonyl chloride. Since these reactions required pyridine as the solvent, experiments with trimethylamine as scavenger base were performed but lacked selectivity. Thus, further reactions were performed using pyridine as solvent. The tosylation gave the expected high yields up to 95%. The crude product could be isolated from the reaction mixture by precipitation from diluted hydrochloric acid, dissolving in diethyl ether and drying over $MgSO_4$, making it possible to perform this reaction in batches up to 180 g of menthol. After the functionalization, the actual

elimination step had to be completed by deprotonation of vincinal protons with a strong base. The elimination was even easier scalable and could be performed in 3 L DMSO with up to 700 g menthyl tosylate in a single batch (see Figure 10). The almost quantitative yield of the functionalization gave this elimination an overall yield of over 70%. Additionally, the elimination was performed selectively to menth-2-ene due to the usage of the sterically demanding base potassium *tert*-butoxide.

Figure 10. Elimination of menthyltosylate in a 10 L reactor.

Developing a direct and selective elimination of menthol could improve the sustainability aspect of this procedure and increase the feasibility of industrial processes. However, it was not investigated during this work due to the major focus on the resulting polymer.

After the successful synthesis of menthene, it had to be oxidized to the responding epoxide. Two reactions were investigated. The Prilezhaev reaction with *m*CPBA and the bromohydrine route using NBS. The first was performed in DCM at 0 °C for 8 h and stirring for another 16 h. Those long reaction times were necessary to ensure high conversions. A procedure with reduced reaction times was published but reached only yields of 30%.[163] After aqueous workup and fractional distillation, a mixture of the two possible diastereomers ((1*R*,2*S*,5*R*,6*S*)-2-isopropyl-5-methyl-7-oxabicyclo[4.1.0]-heptane and (1*S*,2*S*,5*R*,6*R*)-2-isopropyl-5-methyl-7-oxabicyclo[4.1.0]heptane) in a diastereomeric ratio of 3:7 was obtained as depicted in Scheme 9. These diastereomers could neither be separated by fractional distillation nor assigned to the major or minor product. This mixture is called MenO in the following thesis. Yields up to 78% could be achieved.

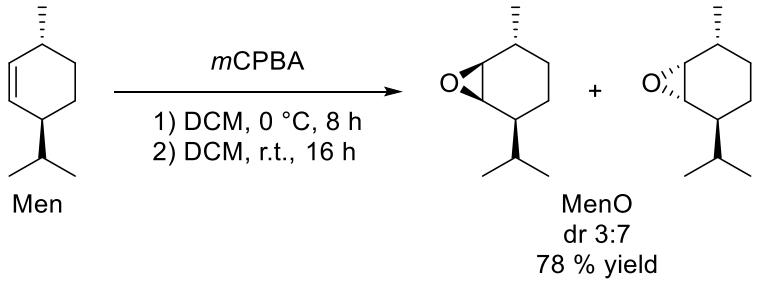

Scheme 9. Synthesis of menthene oxide.

The bromohydrine route worked as well but resulted in significantly lower yields of 31%. This reaction obtained a different diastereomeric ratio due to the varied reaction mechanism. Gas chromatography (GC) measurements revealed a percentage of 56:44. The proton nuclear magnetic resonance (^{1}H NMR) spectrum of the mixture changed accordingly (see Figure 11). The integral ratio of the two signal pairs 3.16, 2.80 pm and 3.01, 2.95 ppm changed from 7:3 to 57:43.

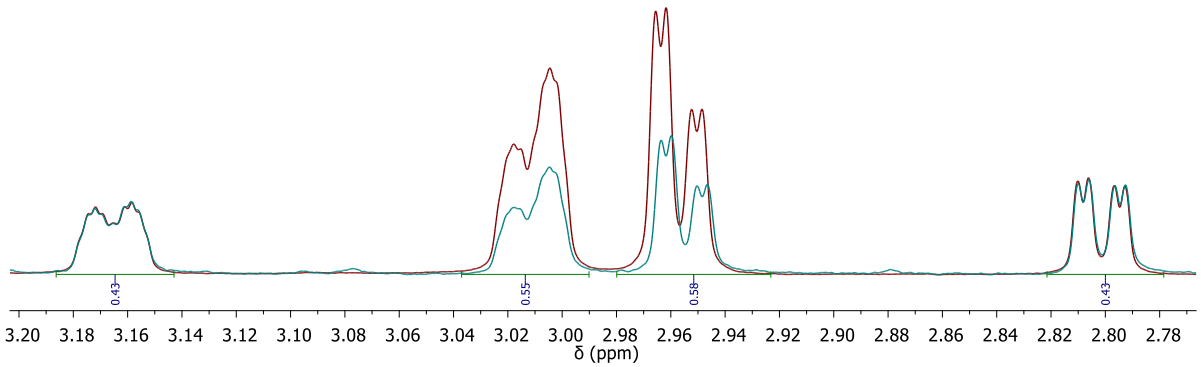

Figure 11. Differences in the ^{1}H NMR spectra of MenO synthesized with mCPBA (red) and NBS (cyan).

Only the 3:7 mixture was used for the polymerization due to the higher yields of the Prilezhaev reaction and the easier work-up.

5.1.2 Polymerization with [(bdi)Zn(OAc)]

The results presented here were already published in “ACS Sustainable Chemistry and Engineering”.[165] Since a route for a sufficient supply of MenO was established, initial experiments for the copolymerization of MenO with CO_2 were planned. The choice for a catalyst fell on a β-diketiminate zinc acetate complex ([(bdi)Zn(OAc)]), which already demonstrated its capability to copolymerize LimO and its high activity for CHO.[16] It was synthesized in a three-step synthesis according to a literature procedure.[82] The acetate ligand acts as the initiator for the controlled alternating copolymerization. Experiments were conducted in toluene at room temperature because these conditions successfully polymerized the structurally similar LimO. A white powder was obtained after precipitation from methanol (poly(menthene carbonate), PMenC).

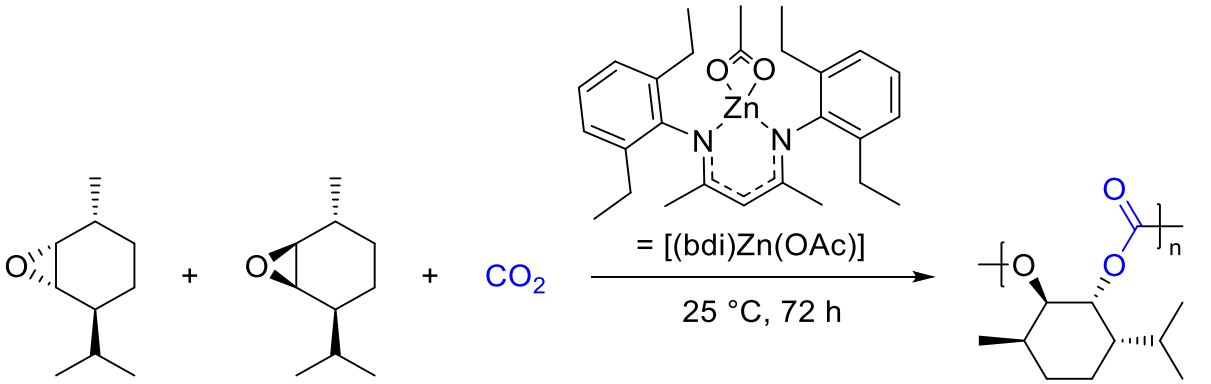

Scheme 10. Copolymerization of MenO with CO_2 catalyzed by [(bdi)Zn(OAc)].

A carbonyl stretch vibration at 1756 cm^{-1} in the infrared (IR) spectrum verified a successful formation of the carbonate linkages. This observation was confirmed by a threefold carbonyl signal at 154 ppm in the ^{13}C NMR spectrum, which also showed the expected number of signals. The two only positive signals beside the carbonyl in a ^{13}C APT experiment at 28.2 and 23.7 ppm additionally revealed only two methylene groups (3 and 4) per repeat unit. There are three prominent signals in the ^{1}H NMR spectrum (see Figure 12). The signals at 4.99 and 4.78 ppm correspond to the two protons geminal to the carbonyl moiety (8 and 9). The large pseudo singlet at 0.87 ppm can be assigned to the three methyl moieties per repeat unit (1 and 5). Ether linkages could not be observed. Cross peaks in a COSY NMR experiment allowed the assignment of protons 2 and 6. An HMQC experiment connected the insights of ^{1}H and ^{13}C NMR and thus allowed a complete assignment of all signals and a verification of the expected structure (Figure 12). The only unexplained signal remaining was splitting the carbonyl

signal in the ^{13}C NMR. Three separate signals at 154.08, 153.86 and 153.66 ppm in relative intensities of 1:2:1 were observed.

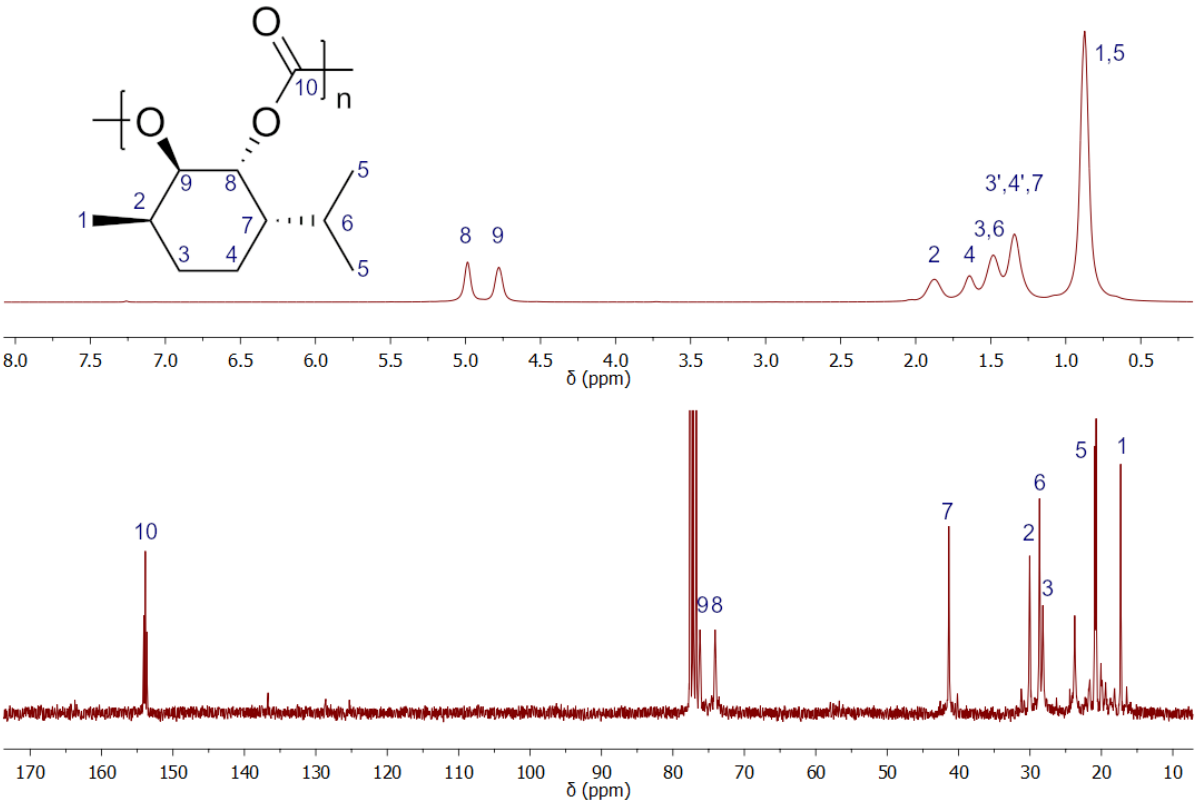

Figure 12. ^{1}H NMR (top) and ^{13}C NMR spectra (bottom) of PMenC with assignments.

The polymer was hydrolyzed to gain insights into the molecular structure of PMenC. Four diastereomers of menthanediol are possible in theory and two are likely to be formed during the ring opening step. The three carbonyl signals could either indicate a mixture of configurations at the cyclohexane ring or other linkages other than head-to-tail. Only a single diastereomer of the four potential diols was observed ((1*R*,2*R*,3*S*,6*R*)-3-isopropyl-6-methylcyclohexane-1,2-diol), thus indicating a random configuration of head-to-tail, head-to-head and tail-to-tail at the carbonate. GC analysis of the precipitated reaction mixture revealed that both diastereomers were consumed. A diastereomeric ratio of 2.4:7.6 could be observed. Since both diastereomers were consumed during the reaction, but only one configuration was found in the polymer, each diastereomer of the epoxide has to be attacked in a specific position to result in the observed configuration. The observation of substituents in an all-equatorial configuration of the hydroxyl/carbonyl moieties in the diol/PMenC at elevated reaction temperatures with another catalyst (see Chapter 5.1.3) suggest that the existence of the single diastereomer is the consequence of different kinetic rates for the formation

of each configuration during the ring-opening. A favored formation of the (1*R*,2*R*,3*S*,6*R*)-diastereomer is also reported for the hydrolysis of this mixture of epoxides at room temperature.[164]

Further experiments with varying monomer to initiator (*[M]/[I]*) ratios were performed and yields between 27 and 35% were achieved for *[M]/[I]* between 126 and 505. No correlation between the yields and the catalyst concentration could be observed. Due to the proposed chain-growth mechanism of this polymerization, the low yields also resulted in low molecular weights (see Table 1). A correlation can be observed for lower *[M]/[I]* ratios if a theoretical value including the reduced yield is calculated. No products of potential side reactions were observed in the reaction mixture after the reaction. A majority of the monomer remained unreacted. Apparently, the dilution was too high to proceed with the reaction after conversions of 35% were reached. Although the low yields in the range of the percentage of the minor diastereomer might imply a limitation by its low concentration, this explanation could be discarded due to the consumption of both diastereomers.

Table 1. Molecular weights and thermal properties of the copolymerizations of MenO and CO_2 with [(bdi)Zn(OAc)] as the catalyst.

Entry	Solvent	*[M]/[I]*	*Yield*[a]/ %	$\bar{M}_{theo}$[b]/10^3	$\bar{M}_n$[c]/10^3	M_p[c]/10^3	*Đ*[c]
1	toluene[d]	126	28	7.0	7.4	10.0	1.23
2	toluene[d]	253	30	15.0	14.8	18.7	1.18
3	toluene[d]	379	35	26.3	17.5	20.4	1.11
4	toluene[d]	505	27	27.0	23.1	26.6	1.11
5	bulk	126	67	16.7	-[e]	21.0	-[e]
6	bulk	253	60	30.1	-[e]	44.4	-[e]
7	bulk	379	52	39.1	-[e]	38.9	-[e]
8	bulk	505	52	52.1	-[e]	39.7	-[e]

a) determined by gravimetry, b) M_{theo}=198.26([M]/[cat.])(yield%), c) determined by $CHCl_3$ GPC with a polystyrene (PS) standard, d) 1 mL toluene/ 1mL monomer, e) as GPC showed bimodal distributions (for further information see Figure 36,Figure 37) M_n and molar mass dispersity could not be determined. Reprinted with permission from Wambach, A.; Agarwal, S.; Greiner, A. Synthesis of Biobased Polycarbonate by Copolymerization of Menth-2-ene Oxide and CO_2 with Exceptional Thermal Stability. ACS Sustainable Chem. Eng. ***2020****, 8 (39), 14690–14693. Copyright 2020 American Chemical Society.*

Experiments in bulk were performed to overcome these limitations by dilution. Yields increased up to 52% for high monomer to initiator ratios and up to 67% for lower ones. Here the yields were limited by the poor solubility of the polymer in the monomer, which resulted in precipitation of the product and a white solidified reaction mixture.

Significantly higher molecular weights up to M_p = 44400 were achieved, but broader and bimodal distributions were obtained. This might be attributed to the precipitation during the reaction, increased viscosity of the reaction mixture or the recombination of two reactive species at the dimer of the catalyst.

Thermal analysis by TGA and DSC revealed excellent thermal properties. Decomposition of 5% was observed at temperatures up to 308 °C, significantly higher than PLimC at 229 °C and PCHC at 283 °C (see Figure 13). No degradation could be observed for temperatures up to 225 °C if the temperature has been kept constant for 1 h. According to GC-MS measurements, the primary pyrolysis product seems to be 5-methyl-2 (1-methylethenyl)- cyclohexanol. These were promising results for later processing experiments. The glass transition temperature of 144 °C was also higher than the one of PLimC. No crystallinity could be observed, which was also verified by wide-angle X-ray scattering (WAXS). A processing window above 160 °C between softening and decomposition may be ideal for the utilization as an engineering plastic.

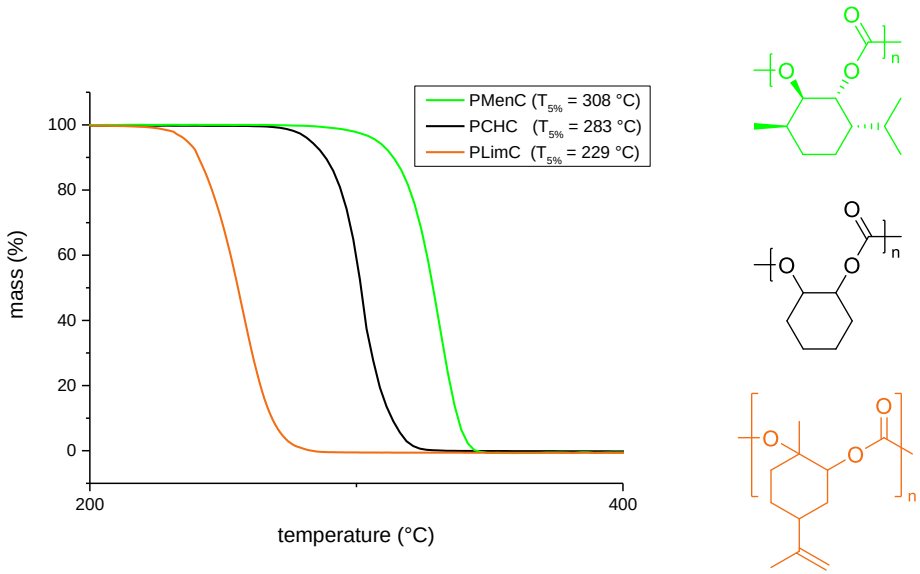

Figure 13. Thermal gravimetric analysis of PMenC (green), PCHC (black) and PLimC (Orange). 10 K/min, N_2. Adapted with permission from Wambach, A.; Agarwal, S.; Greiner, A. Synthesis of Biobased Polycarbonate by Copolymerization of Menth-2-ene Oxide and CO_2 with Exceptional Thermal Stability. ACS Sustainable Chem. Eng. ***2020****, 8 (39), 14690–14693. Copyright 2020 American Chemical Society.*

Polymer films were tried to be prepared by solvent casting from DCM and toluene, but the material was too brittle and films cracked during evaporation of the solvent. Even thicker films at slower evaporation rates in a saturated atmosphere were not stable. Melt pressing was investigated as an additional method to obtain specimen for rheology and tensile measurements, but the sample broke into shards during removal from the tool.

Due to the stiff backbone of the polymer with rigid cyclohexane rings, possible chain movement is inhibited, which results in a brittle nature of PMenC. The methyl and isopropyl substituents attached to it might further reduce mobility. Additives or more flexible monomers could increase flexibility. Stiffness and low intermolecular attraction can be cumbersome for the entanglement of these relatively short polymer chains, which is required for typical polymeric properties. Higher molecular weights might be the solution to this problem, but this catalytic system could not achieve these. Other catalysts might have a better performance with MenO.

Terpolymerizations of MenO and CO_2 with CHO or LimO were also tested using the [(bdi)Zn(OAc)] catalyst. MenO and the catalyst were mixed with the respective epoxide and reacted with CO_2. Molecular weight distributions were unimodal in the GPC, indicating a successful copolymerization. Observed molecular weights were with $\bar{M}_n$ = 35400 for the PCHC copolymer and $\bar{M}_n$ = 29100 for the PLimC copolymer significantly higher than common copolymerizations of MenO and CO_2. However, one must consider that GPC values are relative and the results of different polymers cannot be compared. ^{1}H NMR spectra revealed the expected signals for the contained polycarbonates. A difference could be observed in the ratio of the PMenC to the other polycarbonate. PCHC was 2.27 times more abundant in the copolymer than PMenC, while PLimC reached only 0.57 times the content of PMenC. The methyl group vicinal to the epoxide in LimO might increase the sterical demand of the monomer and should thus reduce its reactivity and reaction rate. ^{13}C NMR could indicate the formation of the different carbonate species. However, no additional signals of mixed carbonate moieties were detected, potentially indicating a block copolymer (see Figure 14). Further investigations on the kinetic of the terpolymerizations are necessary to determine the actual architecture of the polymers.

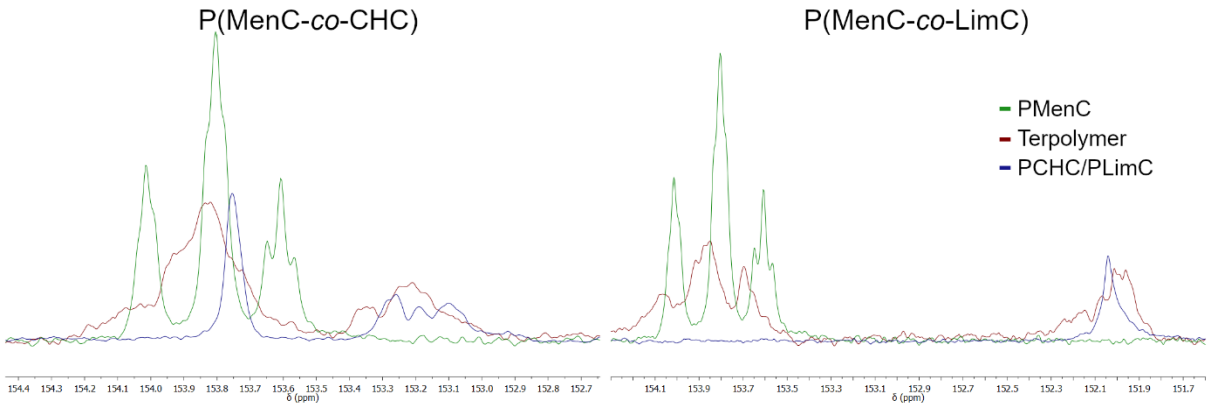

Figure 14. Comparison of the Carbonyl signals of P(MenC-co-CHC) and P(MenC-co-LimC) with the separated polycarbonates PMenC, PCHC and PLimC.

Both polymers showed a T_g of 128 - 129 °C, which matches the literature values of PLimC and PCHC.[17,166] No second T_g could be observed, which is in contradiction to the hypothesis of the existence of separated blocks. P(MenC-*co*-LimC) decomposition of 241 °C was lower than that of P(MenC-*co*-CHC) with 276 °C.

5.1.3 Borane catalyzed Copolymerization of MenO and CO_2

Inspired by the successful polymerization of PO and CHO with TEB as the catalyst by Zhang *et al.*, it enables the easy polymerization of alicyclic and aliphatic epoxides without elaborated ligand and catalyst synthesis was tried to implement this procedure for the biobased monomer MenO.[67] The reaction is initiated by the chloride ion of a salt with a low coordinating cation. Bis(triphenylphosphine)iminium chloride ([PPN]Cl) was chosen here due to its high yields and molecular weights for PO and CHO. The potential copolymerization with PO might help in a future copolymerization of MenO, biobased linear aliphatic epoxides and CO_2. TEB acts as the catalyst and the stabilizer of the growing chain end; thus, two equivalents regarding the initiator are necessary. Other publications showed that higher numbers of equivalents are required for electron-rich epoxides.[99] After the reaction, TEB is either hydrolyzed or oxidized to non-toxic colorless components, which invalidates the necessity of catalyst removal compared to potentially hazardous cobalt or chromium catalyst.

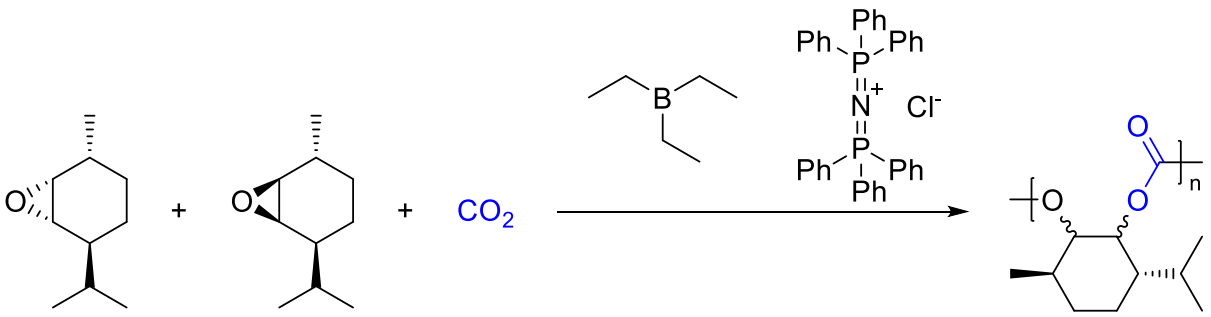

Scheme 11. Copolymerization of PMenC from MenO and CO_2 under the catalysis of TEB initiated by [PPN]Cl.

Initial experiments with this catalytic system resulted in a similar white powder with a matching ^{1}H NMR spectrum compared to the PMenC synthesized by the zinc catalyst. The reaction parameters were varied to increase yield and molecular weights in the following. Although a fractional factorial design of experiments might result in statistically more precise values, each parameter was varied independently of the other parameters due to the number of parameters and levels of these. First, the influence of the reaction temperature was investigated by varying it in a range from 60 to 120 °C, keeping the number of TEB equivalent at two, the reaction time at 17 h and the CO_2 pressure at 12 bar (Table 2, Entries 1-4). The maximum yields and molecular weights were reached between 80 and 100 °C. Reaction temperatures of 60 °C are not high enough to maintain a sufficient reaction, while temperatures of 120 °C reduced the activity of the catalyst drastically. Yields increased from 25% at reaction temperatures

of 60 °C to 59% at 100 °C. The yield dropped down to 26% with a further increase in temperature to 120 °C. Molecular weights and dispersities peaked at temperatures of 80 °C with 26400 and 1.15. The values at 100 °C were comparable, but with 19600 and 1.21, slightly lower. Due to lower yields, molecular weights almost halved at 60 or 120 °C. Under these conditions, 80 °C seems to be the local optimum (see Figure 15, a).

Table 2. Varied reaction conditions and resulting molecular weights of the copolymerization of MenO and with TEB as the catalyst.

Entry	TEB/ eq.	*t*/ h	*p*/ bar	*T*/ °C	solvent	*Yield*[a]/ %	$\bar{M}_n$[b]/ 10^3	*Đ*[b]
1	2	17	12	60	bulk	25	13.8	1.16
2	2	17	12	80	bulk	57	26.4	1.15
3	2	17	12	100	bulk	59	19.6	1.21
4	2	17	12	120	bulk	26	13.9	1.30
5	2	17	5	80	bulk	39	10.7	1.17
6	2	17	20	80	bulk	64	23.5	1.14
7	4	17	12	80	bulk	58	22.2	1.24
8	6	17	10	80	bulk	37	9.94	1.30
9	2	24	14	80	THFc	55	21.9	1.20
10	2	168	12	80	THFc	73	24.6	1.21

a) determined by gravimetry, b) determined by $CHCl_3$ GPC against a PS standard, c) 1 mL THF/ mL MenO.

Additionally to the differences in yields, molecular weights and dispersities, differences in the ^{1}H NMR spectra could be observed. A peak at 4.47 ppm rises with increasing temperature. This peak was not observed in PMenC synthesized with the zinc catalyst. No other peaks for potential ether-linkages were observed. Hydrolysis revealed that in this case, two diastereomers of the menthanediol are present in the polymer chain. If the reaction temperature was increased, the (1*S*,2*S*,3*S*,6*R*)-diastereomer was formed more frequently. Apparently, its all-equatorial configuration is favored at higher temperatures. While polymers with a T_g of 144 °C were obtained by catalysis with the zinc complex, glass transitions at temperatures up to 163 °C were observed here. Since this transition is connected with the movement of the polymer chain, the (1*S*,2*S*,3*S*,6*R*)-diastereomer could result in higher glass transition temperatures because, in contrast to the (1*R*,2*R*,3*S*,6*R*)-diastereomer, only one conformation at the cyclohexane ring is energetically favored. While in the (1*R*,2*R*,3*S*,6*R*)-diastereomer,

two substituents at the cyclohexane ring are axial and two equatorial, which should allow at least a small degree of movement in the ring, the substituents in the (1*S*,2*S*,3*S*,6*R*)-diastereomer are all-equatorial and prohibit any movement due to repulsion. A pure copolymer of the (1*S*,2*S*,3*S*,6*R*)-diastereomer and CO_2 could give an aliphatic polycarbonate with an extremely high T_g and other exciting properties but cannot be synthesized under these conditions. Another stereoselective catalyst, a reaction mechanism with a more expressed equilibrium or a polycondensation with a phosgene derivative could be a route for the direct synthesis of this polymer.

As mentioned above, the number of TEB equivalents might as well have an impact on the polymerization. Additionally to the two equivalents, four and six were tested. Although the yields with two and four equivalents were in the same range, the observed molecular weights were slightly lower and the dispersity higher. The yield in a reaction with six equivalents dropped down to 37%. Respectively, the apparent molecular weight of 9940 was lower and the dispersity went up to 1.30. Two equivalents seem to be optimal to achieve higher molecular weights, but four equivalents could be tolerated and showed even a slightly higher yield of 58 % at the cost of slightly reduced molecular weights (see Figure 15, b).

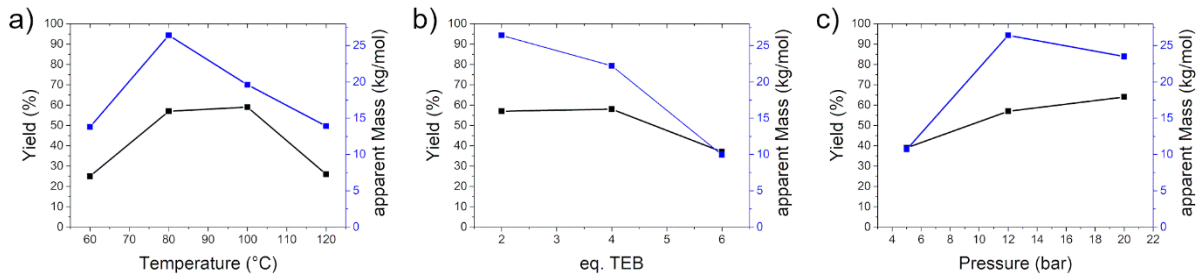

Figure 15. Dependencies for yield and apparent molecular mass number average for different a) temperatures, b) equivalents of TEB and c) pressures of CO_2.

Although the insertion of CO_2 into the growing polymer chain is usually not considered the rate-determining step and is used in an enormous excess, the influence of CO_2 pressure on the reaction was tested because different pressures might alter the reaction mechanism. 5 and 20 bar were chosen as additional pressure steps due to adjustability and technical limitations. All three experiments were successful and PMenC could be obtained. Interestingly, 5 bar was sufficient to maintain a reaction at acceptable yields of 39%, but due to the low conversion $\bar{M}_n$ reached only 10700. A reaction at 20 bar CO_2 pressure could accomplish high yields of 64%. Although the yields were slightly higher, molecular weights number average of 23500 were lower

than at 12 bar. Since the mechanical properties of PMenC are limited by molecular weights and the differences in yield were insignificant, an alternation of the CO_2 pressure away from 12 bar is not beneficial.

Another factor, which had to be investigated, is the dilution. If this procedure is successful in yield and molecular weights, a scale-up might be interesting. The high glass transition temperature of PMenC makes a bulk polymerization unfavorable in a more voluminous reactor because the mixture solidifies under reaction conditions. Removal of the polymer might cause problems without a working stirrer, resulting in a reaction in solution almost a technical necessity. A potential synthesis of block copolymers might also require a polymerization in solution. THF was used in the original publication and the author reported only limited results with other solvents.[67] Anyway, reactions with DCM and a mixture of THF and DCM were conducted but were unsuccessful in the first case or resulted in meager yields of 19% in the second. Reactions in THF were comparable with those in bulk. Yields and molecular weights remained in the same range. Longer reaction times could increase the yield but did not significantly increase the molecular weights.

Table 3. Variation of [M]/[I] for the TEB-catalyzed copolymerization of MenO and CO_2.

Entry	*[M]/[I]*	*t* /h	*T* / °C	Solvent	*Yield*[a]/%	$\bar{M}_n$[b]/10^3	*Đ*[b]
1	80	22	80	THF	71	10.4	1.14
2	274	64	80	THF	58	28.5	1.12
3	504	64	80	Bulk	60	18.3	1.16
4	504	235	60	Bulk	58	27.5	1.36

General parameters: 2 eq. TEB, dilution 1 mL of THF per mL of MenO, 12 bar CO_2, a) determined by gravimetry, b) determined by $CHCl_3$ GPC against a PS standard, c) 1 mL THF/ mL MenO.

Experiments with different *[M]/[I]* were also performed to evaluate a dependency of the molecular weights (see Table 3). At a low ratio of 80 (Entry 1), a yield of 71% could be achieved, which was only slightly outperformed by Entry 10 of Table 2 at over seven times longer reaction times. Entry 2, as a thirteenfold scaled-up reaction with a slightly increased ratio of 274 compared to Table 2, reached a yield of only 58%. Still, its apparent molecular weight reached almost the theoretical weight of 31507 for the proposed chain growth reaction. Samples taken during this reaction also show the limitation of this reaction by the decreasing reaction rate. A conversion of 25% was achieved in the first 18 h of the reaction. It increased to 54% after another 24 h and to 67% after 64 h of total reaction time. Reactions at higher *[M]/[I]* were only possible in

bulk (Entries 3 and 4), indicating an inhibition by the low TEB concentrations. Entry 3 achieved a yield of 60% at 80 °C but only an $\bar{M}_n$ of 18300, while an $\bar{M}_n$ of 27500 was reached with a similar yield at 60 °C and longer reaction times (Entry 4). The introduction of impurities, which act as chain transfer agents, is the most probable explanation. However, a chain scission due to higher temperatures combined with higher shear forces in bulk might also occur. Furthermore, these reactions show a limitation of the reactions in bulk. Solidification of the reaction mixture hinders a complete conversion of the monomer to the polymer.

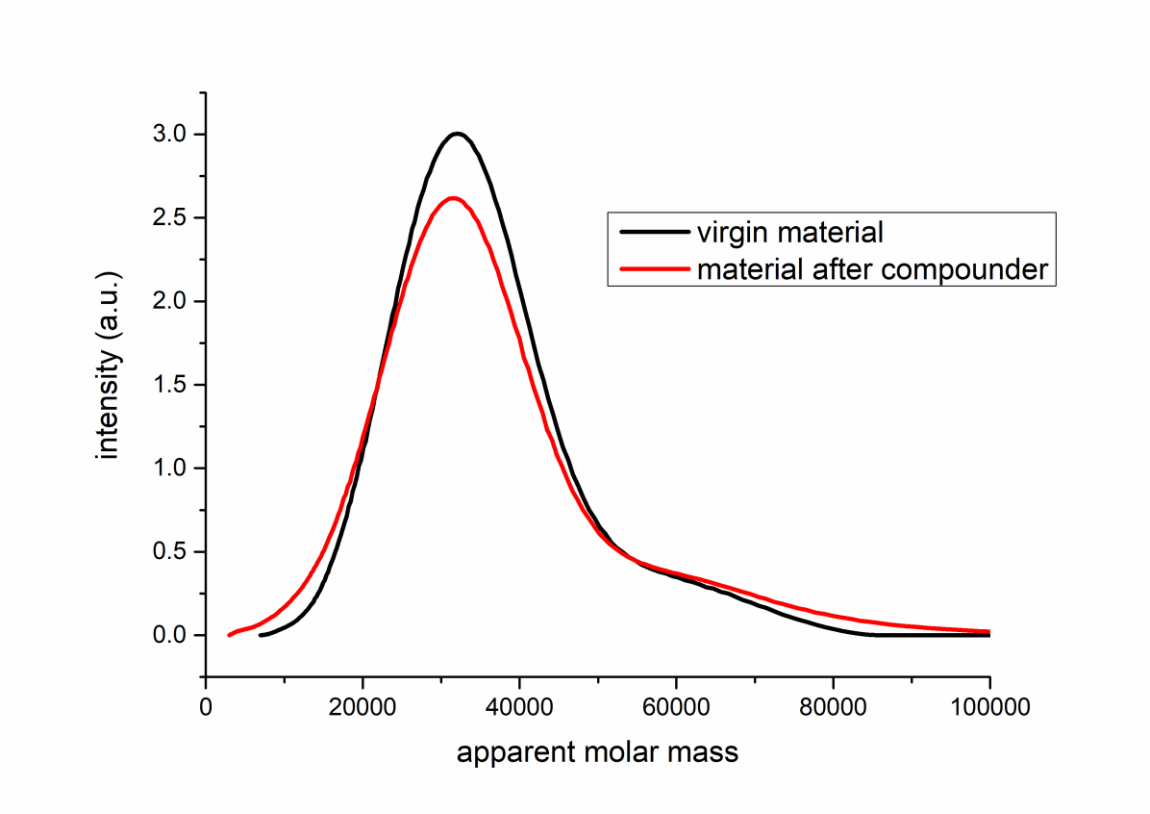

Figure 16. Comparison of apparent molar mass distributions of virgin PMenC and after 20 min in the compounder.

TGA showed thermal stability under N_2 of PMenC up to 300 °C, but these measurements do not represent the conditions under continuous lower temperatures and shearing during the processing. Thus, PMenC was processed in a small-scale double screw compounder at 200 °C. Compared to commercial polymers, *e.g.,* polystyrene or polylactide, the addition of PMenC was much more challenging due to the low softening of the material, which also resulted in much higher forces in the compounder due to increased melt viscosities. Although a slight yellow discoloration could be observed, $\bar{M}_n$ was only reduced from 28500 to 25900, expanding the dispersity from 1.12 to 1.20 (see Figure 16). Both numbers indicate that chain scission

occurs, but only in minimal amounts. The extended time for adding the polymer into the compounder over 20 min caused an inhomogeneous residence time. Other set-ups might allow shorter processing times with less degradation.

The combination of two equivalents of TEB, 12 bar CO_2 and a reaction in bulk at 80 °C achieved the highest molecular weights in the chosen range of experiments. Reactions in bulk showed similar yields compared to the zinc catalyst, but molecular weight remained lower. Long reactions in THF could reach higher yields, which is especially interesting for potential upscaling experiments or block copolymers. Increasing the yields is promising since the synthesis of the monomer is still a labor-intensive multi-step process. The low molecular weights remain as a drawback hampering an application. These could be a result of chain transfer or premature interruption of the chain growth. In the meantime, more advanced borane catalysts were developed, allowing a more precise stoichiometry and an additional electrostatic attraction between the catalyst and the anionic polymer chain. The use of one of these multifunctional boranes might be a viable solution for the challenges which were identified here.

5.1.4 Plasticizing Additives for PMenC

Both catalytic systems produced a highly brittle, high T_g polymer, which could not be cast into films. None of these synthetic pathways allowed the synthesis of higher molecular weight distributions and thus stronger entanglement. Increased chain mobility by adding a plasticizing additive could be a viable way to obtain a less brittle material. The following six potential plasticizers were tested: ethyl oleate, trioline, methyl-10-undecanoate, isosorbide dimethyl ether, methyl cinnamate and citronellal. Additionally, dimethyl phthalate (DMP) and dibutyl phthalate (DBP) were used to compare known commercially applied plasticizers. One polymer synthesized with the zinc catalyst and one with TEB were each dissolved together with one of the plasticizers before the solvent was slowly evaporated to dryness.

Table 4. Used polymers for plasticizer tests.

Entry	Catalyst	$\bar{M}_n$[a] / 10^3	$Đ$[a]	$T_{5\%}$[b] / °C	T_g[c] / °C
1	[(bdi)Zn(OAc)]	23.1	1.11	304	144
2	TEB	27.5	1.36	258	152

a) determined by $CHCl_3$ GPC against a PS standard, b) determined by TGA at 10 K/min under N_2 atmosphere, c) determined by DSC at 10 K/min under N_2 atmosphere.

TGA revealed a significant drawback of the selection. All small chosen organic molecules, except for trioline, either evaporated or decomposed earlier than the polymer itself. A considerable mass loss was observable for samples with methyl-10-undecanoate or citronellal under 200 °C, which prevents a measurement up to the T_g of the polymer in the DSC due to the interfering heats of evaporation or decomposition. No conclusions about complete miscibility or slightly reduced transitions are possible here. Even if the T_g might be reduced, these compounds are not suitable as an additive for a polymer, whose significant advantage is a high decomposition temperature. Phthalates and fatty acid esters were at least sufficiently stable at 200 °C, but fatty acid esters as trioline or ethyl oleate showed another drawback. These compounds crystallized just under 0 °C.

25 $mg_{ethyl\ oleate}/g_{PMenC}$ resulted in a slight reduction of the T_g of both polymers. No T_g could be observed for 0.25 $g_{ethyl\ oleate}/g_{PMenC}$. Additionally, prominent melting peaks could be observed in the heating curves of Entry 1, Table 4. A difference between the two polymers was observed for trioline. Entry 1, Table 4 did not show a T_g when mixed with trioline. A reduction of the T_g of a mixture with 0.25 $g_{trioline}/g_{PMenC}$ additive from 144 °C to 32 °C was measured for combinations of Entry 2, Table 4. The other values

followed a trend described by the Fox equation (Equation 5). DMP successfully lowered T_gs for both polymers to 56 °C or 69 °C. Samples with lower loading of DBP showed curves with a single lowered T_g compared to the virgin polymer. This T_g continued to decrease to 28 °C at 0.25 g_{DBP}/g_{PMenC} loading, but another transition became more visible starting at 0.10 g/g_{PMenC}. This indicates that the polymer might not be fully miscible with the plasticizer.

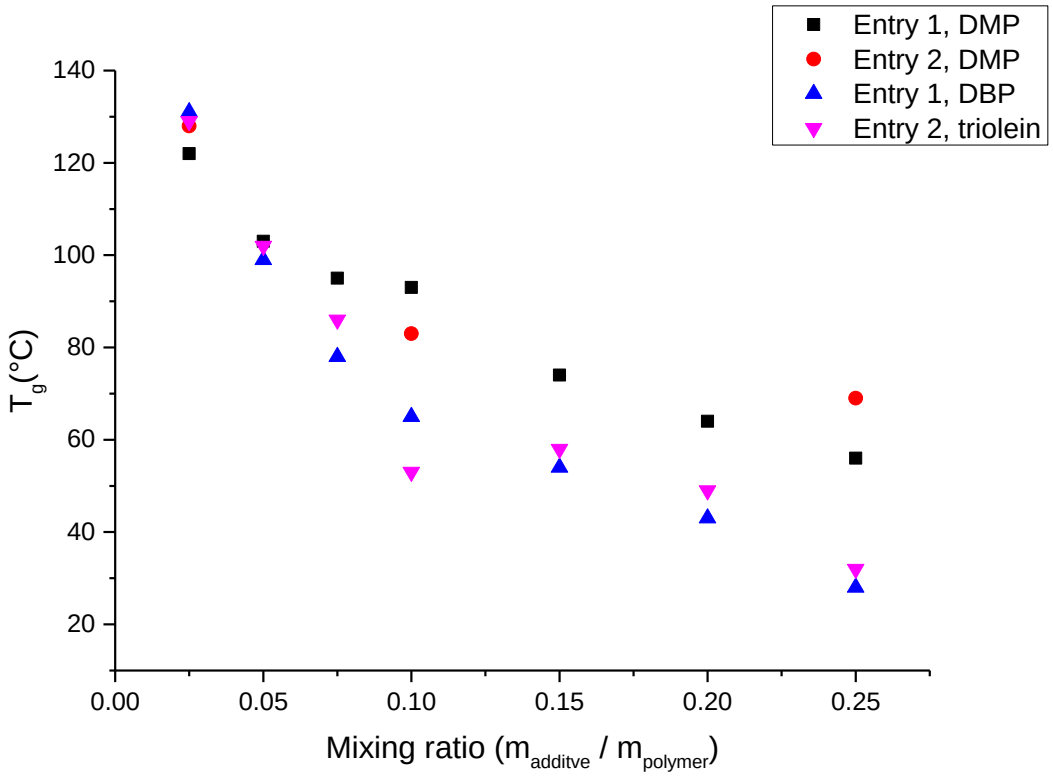

Figure 17. Dependency of the T_g to the mixing ratio for PMenC with different additives.

Poor mechanical properties also accompanied problems with the thermal stability of the potential plasticizers. Samples were prepared by mixing polymer and additive in solution and subsequent evaporation and should thus give films if a successful softening was achieved. It was not possible to obtain films from the prepared polymer mixtures. Hence, additives are not the appropriate way to improve the film-forming properties of PMenC. Apparently, the mobility of the backbone is too low and has to be increased.

5.2 Borane catalyzed Terpolymerization of MenO, BO and CO_2

The primary objective of the copolymerization of MenO and CO_2 is to synthesize a polycarbonate that could be used as an engineering plastic. Experiments with the zinc catalysts showed that the raw material was brittle, which might result from low entanglements by the stiff and short polymer chains. Two major synthetic approaches were postulated to solve this problem. Increasing the average molecular weight could be realized with neither the zinc nor the borane catalyst. The other approach might be to increase chain mobility. It has already been shown that a terpolymerization with aliphatic monocyclic epoxides is a viable route to increase the chain mobility and thus decrease the glass transition temperature.[40,167,168] Here, butene oxide was chosen. It has a higher boiling point than propylene oxide, is hence better to handle than PO and can additionally, at least theoretically, be derived from butanol, which is produced as biofuel, or from 1-butene, which is a potential product of controlled dimerization of bio ethylene and thus a biobased monomer.[32,169,170] A T_g of 6°C was reported for a poly(butene carbonate) (PBC) with 92% carbonate linkage, an $\bar{M}_n$ of 24600 and dispersity of 4.6.[38]

Successful incorporation requires an understanding of the ideal conditions for both monomers. Therefore, these had to be studied for BO with the TEB system despite its similarity to PO. The CO_2 pressure, TEB equivalents, reaction time and temperature are the prime parameters, which can be adjusted and influenced. Preliminary experiments showed a favored reaction to cyclic butene carbonate (cBC) as a side-product at temperatures above 80 °C. Reaction temperatures thus were kept at 60 °C to minimize the formation of the side-product but also be high enough to polymerize MenO in a later terpolymerization.

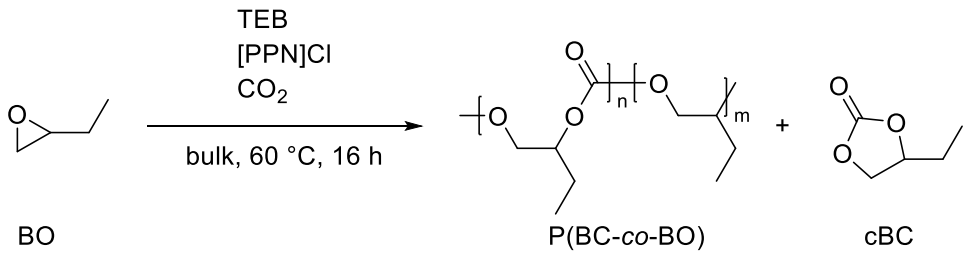

Scheme 12. Copolymerization of BO and CO_2 and the potential side-product cBC.

TEB stabilizes the growing chain end and activates the epoxide. Increasing the equivalents of TEB to the initiator suppressed backbiting and thus the formation of cBC. Yields increased with the reduction of side-products, but higher portions of

poly(butene oxide) (PBO) were observed due to the stronger activated epoxide and the resulting higher rate of homopolymerization. These findings are in accordance with other studies.[99,171] Pure PBC could be produced with two equivalents of TEB at pressures of 25 bar, but this procedure was limited by its selectivity towards the polymer (see Table 5).

Table 5. Conditions, resulting molecular weights and thermal properties of the copolymerization of BO and CO_2.

Entry	TEB/ eq.	*p*/ bar	*Yield*[a]/ %	F_{CO2}[b]/ %	$\bar{M}_n$[c]/ 10^3	*Đ*[c]	T_g[d]/ °C
1	2	20	65	>99	36.2	1.06	14
2	2	12	56	90	37.7	1.10	9
3	4	12	58	82	29.7	1.18	3
4	6	12	76	78	44.7	1.15	5

General parameters: 60 °C, 20 h, bulk, a) determined by gravimetry m(obtained polymer)/m(complete conversion to polycarbonate), b) numerical carbonate content according to ^1H NMR, c) $CHCl_3$ GPC relative to PS standard, d) DSC at 10 K/min under N_2 atmosphere

Glass transition temperatures between 5 and 14 °C could be observed, showing its potential as a softer component of the terpolymer. Entry 1 shows the T_g of pure PBC, which is higher than the one reported in the literature.[38] The reported polymer had a lower $\bar{M}_n$ with a significantly higher dispersity. Chains with a lower degree of polymerization could act there as a plasticizer. The T_gs presented here were mainly dependent on the ether content and the molecular weight. Although an increased ether content adds another component to the mixture and increases the complexity of characterization, its low T_g of approximately -60 °C and high flexibility are more beneficial than cumbersome for applications in the future. It is only essential to keep the content low and reproducible due to its strong influence on thermal properties.

The preferred reaction conditions of this reaction are too low with 60 °C and too high with six equivalents of TEB for the terpolymerization with MenO. Since the tolerance of both systems towards the ideal number of equivalents of catalyst is relatively high, four equivalents were chosen for initial tests of terpolymerization. The temperature was kept at 60 °C due to the otherwise rapid formation of cBC.

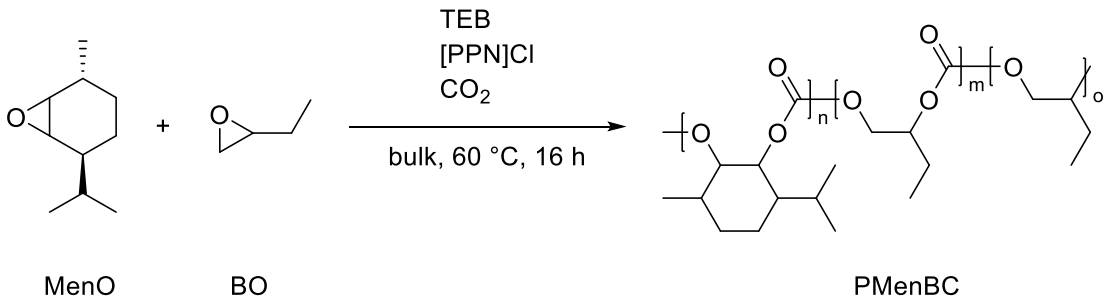

Scheme 13. Terpolymerization of MenO and BO with CO_2.

Three compositions with 50, 20 and 10 mol% of BO in the feedstock were tested. The ^{1}H NMR spectra of the reaction mixtures showed complete conversion of BO to either cBC, PBC or PBO after the reaction. A complete conversion of MenO could not be achieved and the majority remained unreacted. The composition of the obtained polymers was thus richer in PBC or PBO than the feedstock, which was confirmed by ^{1}H NMR as well. An exact ratio of the incorporated monomers could not directly be determined by the proportions of separated signals in the ^{1}H NMR but had to be calculated by comparing the signals of the methyl, ether and carbonyl moieties according to equations 1-4 (see Appendix 10.3). Hydrolysis was tested as an alternative. Although it showed the same trends as NMR analysis, hydrolysis with KOH was not suitable to determine the composition of these polymers. The aqueous work-up reduced the observed ratio of PBC/PBO to PMenC drastically because 1,2-butanediol is easily soluble in water.

Table 6. Terpolymerization of MenO, BO and CO_2 with different molar ratios of the epoxides.

Entry	*Feedstock*/ % BO	*Yield*[a] / %	$\bar{M}_n$[b]/ 10^3	*Đ*[b]	*Content* (mol%)[c]			T_g exp[d] / °C	T_g Fox[e] / °C
					PMenC	PBC	PBO		
1	50	63	35.5	1.09	0.30	0.67	0.028	31	60
2[f]	50	40	40.5[g]	1.21[g]	0.24	0.73	0.031	28	51
3[f]	50	51	46.1[g]	1.16[g]	0.21	0.72	0.066	21	44
4[f]	50	48	45.3[g]	1.21[g]	0.23	0.69	0.080	26	46
5	20	30	11.6	1.20	0.53	0.44	0.036	70	93
6	10	23	14.2	1.23	0.70	0.23	0.069	97	116

General parameters: 12 bar CO_2, 4 eq. TEB, [M]/[I] = 317, 60 °C, 17 h, reaction in bulk, a) determined by gravimetry m(obtained polymer)/m(full conversion to polycarbonate), b) $CHCl_3$ GPC relative to PS standard, c) determined according to equations 1-4 and Figure 47, d) DSC at 10 K/min under N_2 atmosphere, e) determined according to equation 5, f) [M]/[I] = 634, g) bimodal distributions

Thermogravimetric analysis of the terpolymer (PMenBC) showed decreased decompositions temperatures for all three compositions. This is the result of the lower thermal stability of PBC. The mass loss followed a homogeneous curve, which might be explained by PBC distribution along the chain and chain scission as the first step. Lower molecular weight parts then might unravel starting from the chain ends. DSC measurement revealed only a single T_g for all compositions, indicating either miscible blocks or a random copolymer. The DSC curve of a blend, obtained after mixing PMenC and PBC in solution with subsequent precipitation, showed two separated T_gs at the temperatures of the virgin materials, thus falsifying the possibility of miscible block copolymers. Estimations according to the Fox equation calculated with the determined polymer weight ratios ($T_{g.Fox}$, Table 6) followed the same trend but overestimated the glass transitions temperatures by 20 – 30 °C in every case.

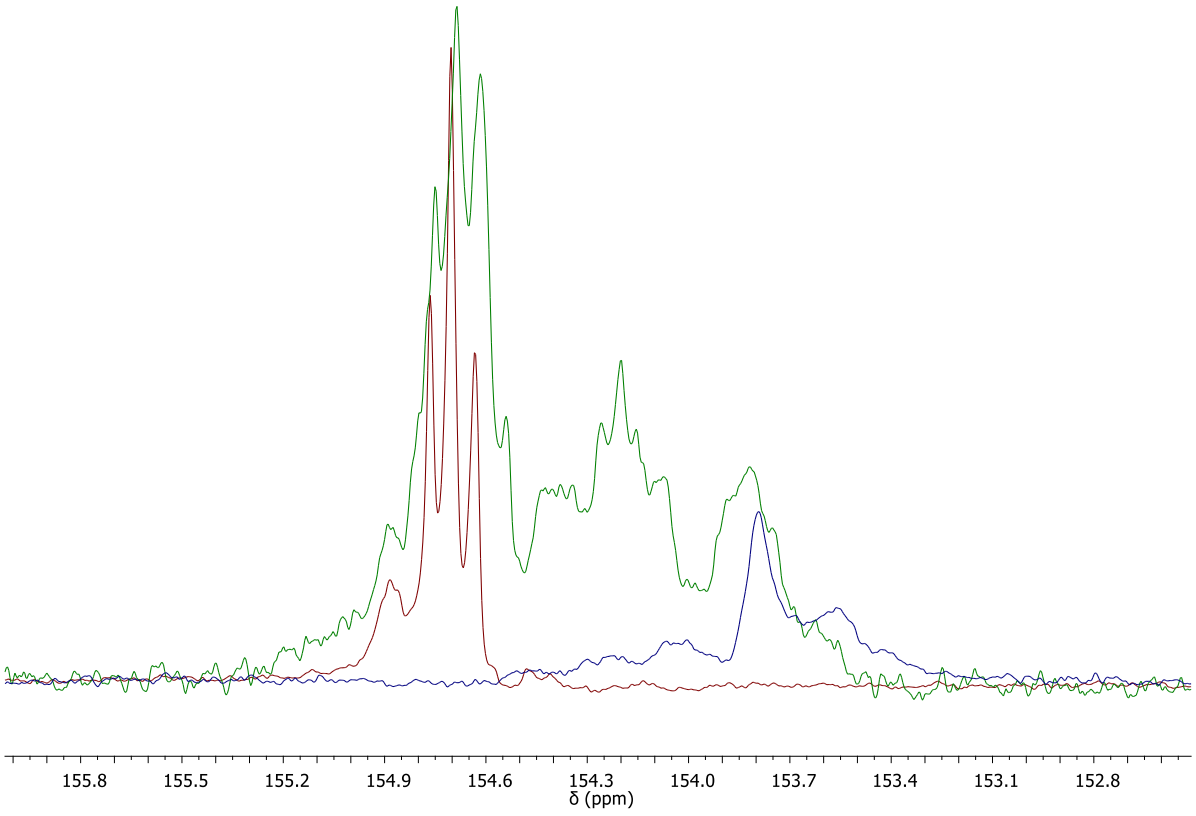

Figure 18. Comparison of the carbonyl signals in the ^{13}C spectra of PMenC (red), PBC (blue), and PMenBC (green).

If the carbonate signals in ^{13}C NMR of PBC, PMenC and PMenBC are compared, carbonate signals of PBC and PMenC can be assigned to the spectrum of PMenBC. At 154.2 ppm, another carbonate peak arises, which could be explained by a significant fraction of carbonates linked to one menthane ring and one butane moiety. A clear

assignment of single peaks to specific configurations and an estimation of the fractions was impossible due to the small range of chemical shifts and thus overlapping of the individual signals. Although the much higher reaction rate of BO compared to MenO suggests the formation of a block copolymer or gradient polymer, these findings indicate at least partial random copolymer with still existing blocky fractions of PMenC and PBC. Reactions with low conversions support the assumption of random copolymerization by showing the formation of PMenC while BO was still present. Further kinetic investigations of this copolymerization will be necessary in the future to understand the architecture of these specific terpolymers completely.

Since the objective of the terpolymerization of MenO, BO and CO_2 was the search for a menthol-based copolymer, which might be suitable as an engineering plastic, the film formation properties of the three terpolymers were checked. A feedstock of 1:1 (Table 6, Entry 1) resulted in a soft material, which was easily solvent cast into a film. The films were transparent and crack-free but could not be removed from the glass sheets used as substrates. Contact angles of 108 ° indicate a highly hydrophobic nature of PMenBC. A significant drawback is the low T_g of 31 °C, which is way too low for coating or packaging applications at room temperature. Terpolymers with higher PMenC content (Table 6, Entry 2-3) showed higher glass transition temperatures but could not be used for film formation. Both terpolymers were tried to be cast into films by solvent casting but cracked during evaporation of the solvent. The attempted films of Entry 3 showed a behavior similar to pure PMenC, while Entry 2 showed slightly fewer cracks at lower solvent content. Apparently, the working hypothesis of introducing PBC to PMenC to reduce stiffness of the chains and thus increase the entanglement could be backed up by these results but was only successful for Entry 1. Another difference was the molecular weights, which were significantly higher for Entry 1 than the others. Entry 2 gave a good tradeoff in T_g and improved film formation but needed to be used in higher molecular weights.

Since the reaction conditions might not be optimal for the terpolymerization of this particular molar feedstock ratio of MenO and BO, reaction conditions were varied to increase molecular weights. Other numbers of equivalents of TEB were tested and six equivalents resulted in almost doubled molecular weights. The maximum $\bar{M}_n$ 33100 was reached with a doubled monomer to initiator ratio and six equivalents of TEB per initiator over 3 days in bulk. Neither even higher monomer to initiator ratios nor a reaction in solution were beneficial for higher molecular weights. In addition, the

pressure was increased due to the higher molecular weights in the experiments with pure MenO but did not contribute to higher molecular weights. Unfortunately, these improved reaction conditions could not produce terpolymers, which could be cast into films.

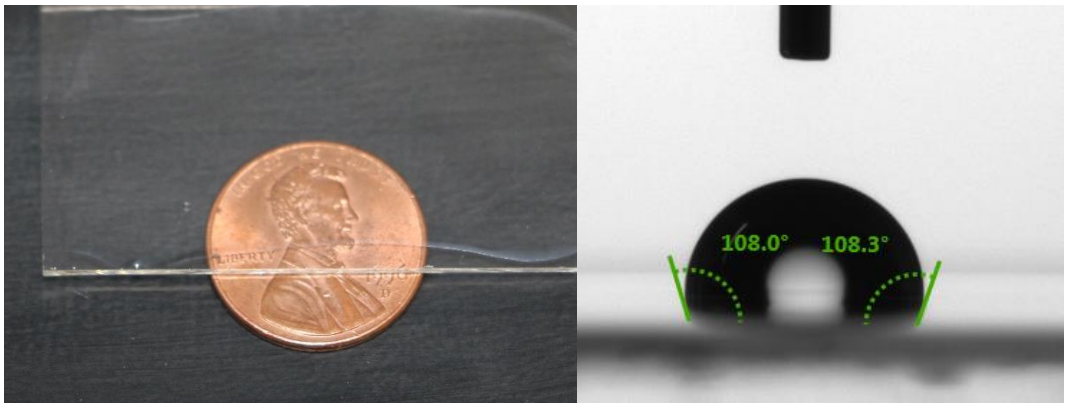

Figure 19. Film of PMenBC with a feedstock ratio of 1:1 on a glass plate (left) and a contact angle measurement on its surface (right).

Table 7. Varied reaction conditions for the terpolymerization with 80% MenO in the feedstock and the resulting yields, molecular weights and disperities.

Entry	*[M]/[TEB]/[I]*	*t*/ h	*p*/ bar	Solvent	*Yield*[a]/ %	$\bar{M}_n$[b]/ 10^3	*Đ*[b]
1	317/2/1	16 h	12	bulk	30	7.31	1.12
2	317/4/1	16 h	12	bulk	30	11.6	1.20
3	317/6/1	16 h	12	bulk	41	20.0	1.29
4	634/4/1	3 d	12	bulk	30	10.4	1.17
5	634/6/1	3 d	12	bulk	51	33.1	1.29
6	634/6/1	3 d	20	bulk	49	19.2	1.33
7	634/4/1	3 d	12	THF	34	23.9	1.23
8	634/6/1	3 d	12	THF	38	19.3	1.29
9	1268/4/1	3 d	12	bulk	0.8	9.98	1.14
10	1268/6/1	3 d	12	bulk	19	11.5	1.20

a) determined by gravimetry m(obtained polymer)/m(full conversion to polycarbonate), b) $CHCl_3$ GPC relative to PS standard

It could be shown that incorporating PBC into PMenC is possible by terpolymerization of the two monomers BO and MenO with CO_2. In theory, the T_g can be adjusted in a range between the two T_gs of PBC and PMenC. Film formation could be observed for a feedstock of 1:1. Higher fractions of PMenC resulted in brittle materials, which tend to crack under the conditions of solvent casting. Although this might result from low molecular weights, a synthesis of higher molecular weight samples was not possible

with this catalytic system. More modern bifunctional borane catalysts might work under the more dilute reaction conditions of higher monomer to initiator ratios and thus increase molar masses.

Higher average molecular weights could be achieved for a feedstock with 50 mol% BO if *[M]/[I]* was doubled (Table 6, Entries 2-4). Entries 2 and 3 followed the same procedure and were a twofold scale-up of Entry 1 and Entry 4 was a fourfold scale-up. Apparent $\bar{M}_n$ up to 46100 could be detected by GPC, although an increasingly significant shoulder in the distribution rises from Entry 2 to Entry 4 at the twofold mass of the main peak. The position of the main peak remains in a range between 50900 and 53400 and shows a certain reproducibility of the method as well as a dependency of the molar mass and *[M]/[I]*. Since these experiments were performed in temporal order as listed in Table 6 and all monomers were freshly dried, masked and distilled, a slow degradation or contamination of the catalyst might be an explanation for the increasingly bimodal distribution. Very low quantities of water could act as an additional bifunctional initiator, explaining the doubled molecular weight.

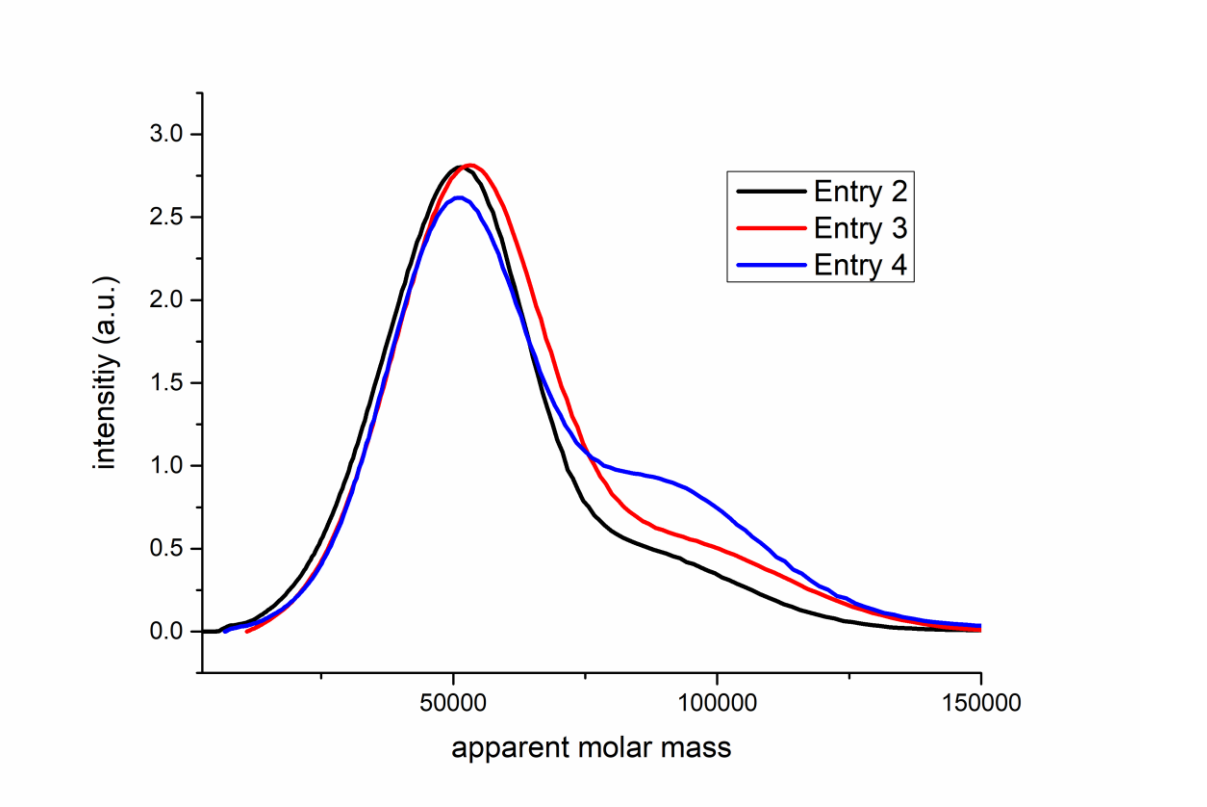

Figure 20. Comparison of the apparent molar masses and distributions according to GPC of Entries 2-4 of Table 6.

Although various terpolymers of MenO, BO and CO_2 were synthesized, the objective to find a suitable bulk material has not been fulfilled yet. PMenBC synthesized with a

feedstock ratio of 8/2 had a T_g of around 80 °C, which was still high enough to be used at average ambient temperatures, but was still way too brittle to form films or to be used in a bulk application.

A broad range of monomers was published for the catalytic system consisting of TEB and [PPN]Cl.[99] Hence, modifications of PMenC by terpolymerization with further epoxides with other functionalities were considered. After the terpolymerization with BO, dodecene oxide ($C_{12}O$) was tested as aliphatic epoxide with a much longer side chain. For the poly(dodecene carbonate) ($PC_{12}C$), a T_g of -38 °C was reported.[38] Drying and masking procedures remained the same as for BO. The copolymerization of $C_{12}O$ with CO_2 was successful and could be proven by the characteristic signals of the protons geminal to the carbonate in the ^{1}H NMR spectrum at 4.88 ppm and 4.40 - 3.93 ppm. A significant portion of $C_{12}O$ was converted to cyclic carbonate. Separation of monomer and side-product revealed itself as challenging as the highly nonpolar cyclic carbonate could not be separated by precipitation from methanol. Less polar solvents as pentane were unsuitable for precipitation due to the high solubility of the polymer.

Terpolymerizations with MenO were carried out with fractions of 20 and 5 mol% $C_{12}O$ in the feedstock. Other reaction parameters remained the same as in the terpolymerization of PMenBC, except for 2 equivalents of TEB. The reactions were successful but lacked high yields or molecular weights. ^{1}H NMR spectra showed drastically lower contents of the corresponding polycarbonate and polyethers of $C_{12}O$ than expected from experiments with BO. Spectra of the reaction mixture revealed high contents of the cyclic carbonate of $C_{12}O$, which is formed favorably under these conditions. The most elevated $\bar{M}_n$ reached were 12800, heavily limited by the low incorporation of $C_{12}O$ and the overall low reactivity of MenO. Purification was successful here and samples could be used for thermal studies. T_gs up to 105 °C were observed for 80% MenO in the feedstock and 144 °C for 95%. This new monomer might enable a significant lowering of the T_g, but the chosen reaction conditions are not favorable. A considerable excess of $C_{12}O$ or other reaction conditions, including other catalytic systems, is necessary to achieve sufficiently high incorporation. A higher number of TEB might reduce the cyclic carbonate formation but was not tested due to the already functional BO system.

In summary, linear aliphatic epoxides are a viable way to introduce intrinsic plasticizers into PMenC. Lowered T_gs in comparison to the PMenC homopolymer were realized with two different comonomers. Applications of PMenBC were hampered either by the low T_g of the terpolymers with high PBC contents or the low molecular weights of the ones with low PBC content. Crosslinking low T_g PMenBC is tackled in the following chapters. Higher molecular weights might require an advanced catalyst. $C_{12}O$ is also a promising candidate but requires even more refinements in reaction conditions and catalyst selection.

5.3 Crosslinking of PMenBC

Although various terpolymers of MenO, BO and CO_2 were synthesized, the objective to find a suitable bulk material has not been fulfilled yet. PMenBC with high PBC content formed transparent films, but a T_g between 25 and 30 °C would result in softening even at ambient temperatures. Hence, this PMenBC had to be stabilized against higher temperatures by crosslinking to suppress macroscopic deformation. Unfortunately, the only functional groups of the polymer are in its backbone, and attacking these would result in chain scission.

Other monomers were tested to introduce double bonds as potential linking positions into the polymer. Glycidyl methacrylate (GMA) contains both an epoxide and a double bond. The epoxide part of the molecule could be deduced from epichlorohydrin, making it partially biobased.[42] After the reaction of GMA with TEB and [PPN]Cl under a 12 bar CO_2, a white solid was obtained. This solid could not be dissolved in DCM or other organic solvents, indicating crosslinking during the reaction. Apparently, a Michael-type reaction occurred at the α,β-unsaturated ester of the methacrylate moiety, making GMA a bifunctional monomer. The bifunctional behavior was also observed in the synthesis of the GMA polyether.[172] Another experiment with BO to dilute the GMA was conducted. Although the product was softer than before, no solubility could be achieved. The solid residue had to be partially hydrolyzed in the pressure vessel with methanol at 100 °C and then removed by brute force. No experiments with MenO were performed since these initial tests already reveal that these reaction conditions are unsuitable for GMA.

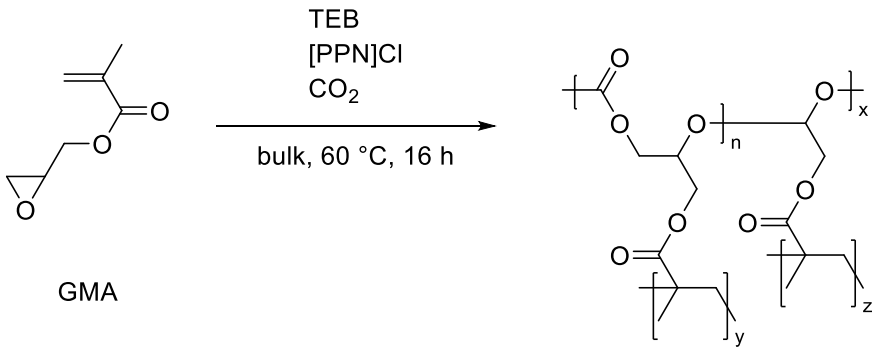

Scheme 14. Attempted copolymerization of GMA and CO_2.

Another biobased molecule with an epoxide and a double bond is isoprene oxide. Its double bond is linked to the epoxide, which should reduce the electron density in the double bond and might enable 1,4-additions additional to the traditional 1,2-additions.

Isoprene oxide was synthesized according to procedures published by Gramlich *et al.* with the one-pot approach of Satake *et al.* [173,174] The necessity of pure monomers resulted in significant losses during isolation and purification. After the TEB-catalyzed reaction with CO_2, a deeply red and liquid reaction mixture was obtained. Signals in the ^{1}NMR remained narrow but were shifted. This indicated that isoprene oxide was transformed into the cyclic carbonate and not the desired polymer.

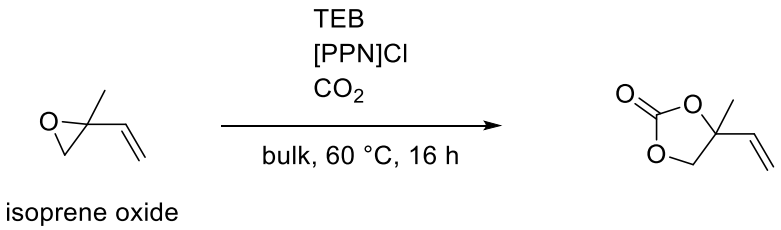

Scheme 15. The reaction of isoprene oxide and CO_2 forming the cyclic carbonate.

Neither GMA nor isoprene oxide seemed to be suitable for the polymerization with TEB and consequently the copolymerization with MenO, BO and CO_2 under the before investigated conditions. Limonene oxide is another epoxide with an additional double bond but could not be copolymerized with BO with this catalytic system. Catalysts with a more specific affinity towards epoxides might be necessary for these reactions or monomers with protected functionality, as seen in Chapter 2.4.

Another approach of crosslinking PMenBC could not introduce functional groups into the molecular structure as alternative radicals had to be introduced. A preliminary test with a plasma oven reduced the contact angle of the surface from 108° down to 68°, but the polymer was still easily soluble in DCM. Apparently, radicals reacted with oxygen but did not sufficiently recombine to crosslink the polymer.

Benzophenone derivates are often used as photosensitizers. Benzophenone is elevated to an excited state under UV irradiation, which decays to a biradical. One can abstract a hydrogen atom from a polymer chain, while the other forms a semi-stable ketyl radical, which can recombine with one of the radicals formed by hydrogen abstraction. The addition of pure benzophenone and exposure to UV light could not crosslink PMenBC11. Benzophenone does not seem to have the potential to fuse two chains, although it was shown for PE.[175] Under the assumption that each benzophenone binds to a single chain, a diester of 4-hydroxy benzophenone and adipic acid (bisBP) was synthesized as a bifunctional crosslinker. It followed a similar route published by Mukherjee.[176] Solutions of low T_g PMenBC with different amounts

of bisBP were prepared, cast on glass slides, dried and exposed to UV radiation for different time intervals. Concentrations of 1 wt% bisBP per gram PMenBC were insufficient to crosslink the polymer even after 20 min of high irradiation. Although most of the polymer with 5 wt.% bisBP was not soluble anymore after 5 min, 10 min were necessary to crosslink thicker films. Although all films did not dissolve in the solvent, significant swelling of the crosslinked polymer could be observed.

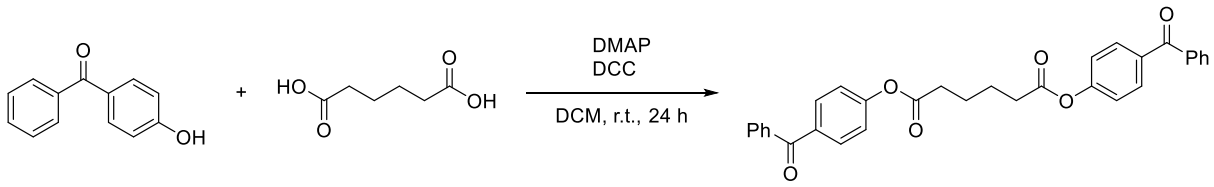

Figure 21. Steglich esterification of 4-hydroxylbenzophenone with adipic acid to form bisBP.

Larger transparent and freestanding films were prepared for a characterization of the material properties. Contact angles were slightly reduced to 95° compared to the virgin material. Tensile testing showed a 320% elongation at break and a Young's modulus of 350 MPa. Specimens, which were deformed and curled after tensile testing, were submerged in water at 70 °C for 1 min. Afterward, a noticeable decrease in curvature was observed and length was observed.

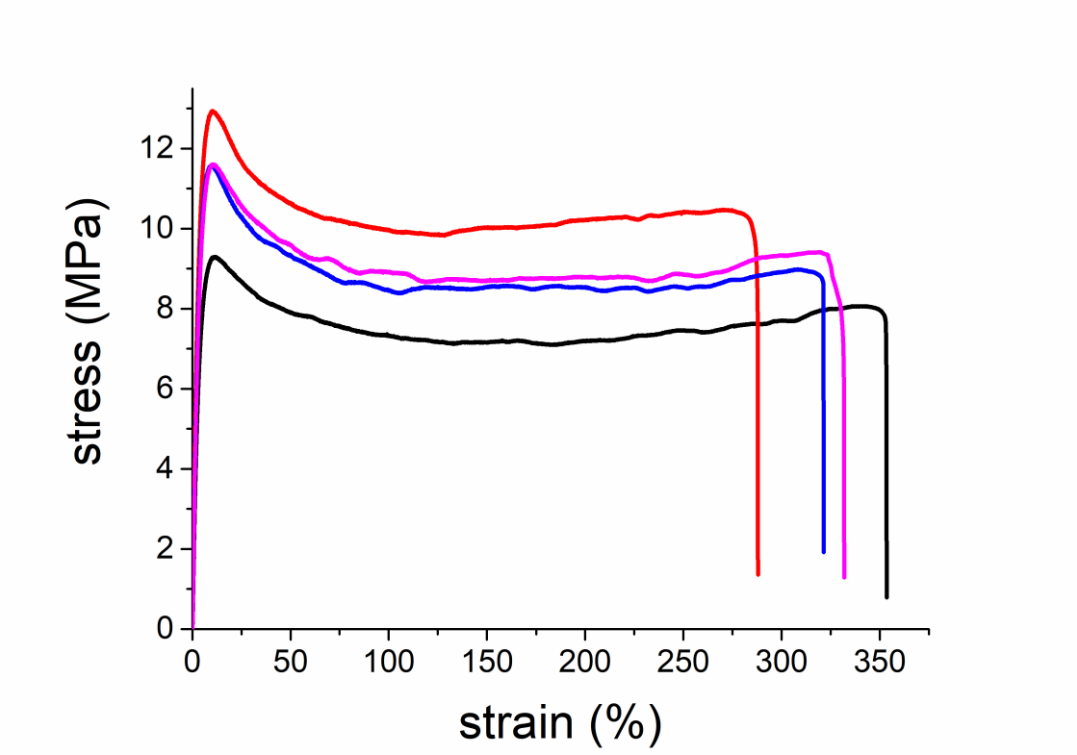

Figure 22. Tensile tests of five samples of low T_g terpolymer of MenO, BO and CO_2 crosslinked with 50 mg/$g_{polymer}$.

Hydrolysis showed another advantage of this system. Although the polymer chains were crosslinked, the film swelled significantly in THF and thus allowed the transport of methanol and potassium hydroxide to the whole network. No delay or deceleration of the reaction could be observed. Since the ester moieties of bisBP can be saponified under the same basic conditions, the network can be broken down in a single step. No polymer was observed after the hydrolysis. The products of this reaction, potassium adipate, 1,2-butanediol and the menthanediols, could in principle be separated and utilized as a building block of new polymeric structures.

In summary, a crosslinking of low T_g PMenBC by introducing additional double bonds during the reaction was not successful. GMA formed an insoluble polymeric network under the current reaction conditions and isoprene oxide formed the cyclic carbonate. Crosslinking was achieved with bisBP as an additive under UV irradiation. This polymer showed high elongations at break and a humble shape-memory effect. Certain recyclability was also shown by complete hydrolysis of the crosslinked polymer to valuable diols and potassium adipate.

5.4 Electrospinning of PMenBC

Electrospinning is a well-established processing method for producing fibers down to the nanometer scale from a wide variety of polymers tolerating a large scale of additives and fillers. The fine structure of the obtained non-wovens facilitates many applications such as filter material, tissue engineering or templates.[177–179] According to Wenzel-equation, a structured surface shows increased hydrophobicity.[180] PMenBC already showed a high contact angle and a structured surface might enable super-hydrophobic behavior. Furthermore, processing at ambient temperatures is beneficial to avoid early thermal degradation of PMenBC compared to melt-spinning.

First, different solvents were tested to dissolve PMenBC and spin these solutions. THF and DCM were chosen due to the excellent solubility of the polymer in these solvents. DMF, as the preferred solvent for spinning applications, was able to produce solutions up to 2 g of polymer per gram of solvent. Loadings between 0.50 and 0.30 wt.% were chosen for THF and DMF to achieve the necessary viscoelastic properties of the solutions. 0.30 wt.%was enough for DCM.

Table 8. Conditions for the electrospinning of PMenBC and resulting morphology.

Entry	Solvent	*w* / wt.%	V_{Needle} /kV	Flow[a]/ mL/h	Morphology[b]	Diameter[b]/ µm	σ[b]/ µm
1	DMF	0.50	14	1.95	uniform	1.8	0.46
2	DMF	0.50	18	1.95	uniform	1.4	0.43
3	DMF	0.50	22	1.95	uniform	1.5	0.35
4	DMF	0.50	26	1.95	uniform	1.4	0.34
5	DMF	0.45	24	1.95	beads	-[c]	-[c]
6	DMF	0.45	28	1.95	beads	-[c]	-[c]
7	DMF	0.30	25	1.30	only droplets	-[c]	-[c]
8	THF	0.50	25	1.00	thick and sticky	-[c]	-[c]
9	THF	0.40	29	1.00	uniform	1.9	0.30
10	THF	0.30	16	0.65	many droplets	2.9	3.3
11	THF	0.30	20	0.65	uniform	2.2	0.76
12	THF	0.30	24	0.65	uniform	1.1	0.28

13	DCM	0.30	25	0.65	uniform	2.7	1.36
14	DCM	0.30	29	0.65	not continuous	3.1	1.09
15	DCM	0.20	12	0.65	beads	- [c]	- [c]
16	DCM	0.20	16	0.65	less beads	1.6	0.37
17	DCM	0.20	20	0.65	less beads	1.7	0.35
18	DCM	0.20	24	0.65	uniform	1.7	0.35
19	DCM	0.20	28	0.65	uniform	1.5	0.38
20	DCM	0.15	20	0.65	beads	- [c]	- [c]
21	DCM	0.15	24	0.65	beads	- [c]	- [c]
22	DCM	0.15	28	0.65	beads	- [c]	- [c]

a) determined by the calibration curve for the machine, b) estimated by optical microscopy, c) sample to inhomogeneous, no direct measurement possible

0.50 wt.% solutions of DMF resulted in a perfectly shaped spinning cone and produced uniform fibers. Optical microscopy revealed that fibers diameters reduced from 1.8 to 1.4 µm by increasing the applied voltage to 26 kV. SEM imaging showed even lower diameters of 279 nm at 26 kV, indicating that SEM should be the preferred method to determine these small diameters (Figure 23, a). Reducing the polymer concentration resulted in bead formation at 0.45 wt.%. No fibers and droplets were observed for spinning experiments with 0.30 wt.%.

Solutions with a concentration of 0.40 wt.% in THF could be spun into homogeneous fibers, but the average diameters of 1.9 µm, even at 29 kV, were higher than those spun from DMF. Smaller diameters were achieved by reducing the concentration to 0.30 wt.% at 24 kV. Measuring the average diameter of single fibers in SEM images resulted in an average of 500 nm (Figure 23, b). Lower voltages caused either the formation of beads/ droplets or drastically wider distribution.

It was possible to spin a solution of 0.30 wt.% of PMenBC in DCM, but rather big average diameters of 2.7 µm were obtained at 25 kV. Higher voltages of 29 kV were also tested to reduce diameters, but the high viscosity did not allow a constant fiber formation. Lower contents of 0.20 wt.% PMenBC allowed the formation of uniform fibers by spinning at high voltages. According to SEM, average diameters of 472 nm at 24 kV and 585 nm at 28 kV were achieved (Figure 23, c and d). A 0.15 wt.% copolymer solution resulted only in beads connected by tiny fibers.

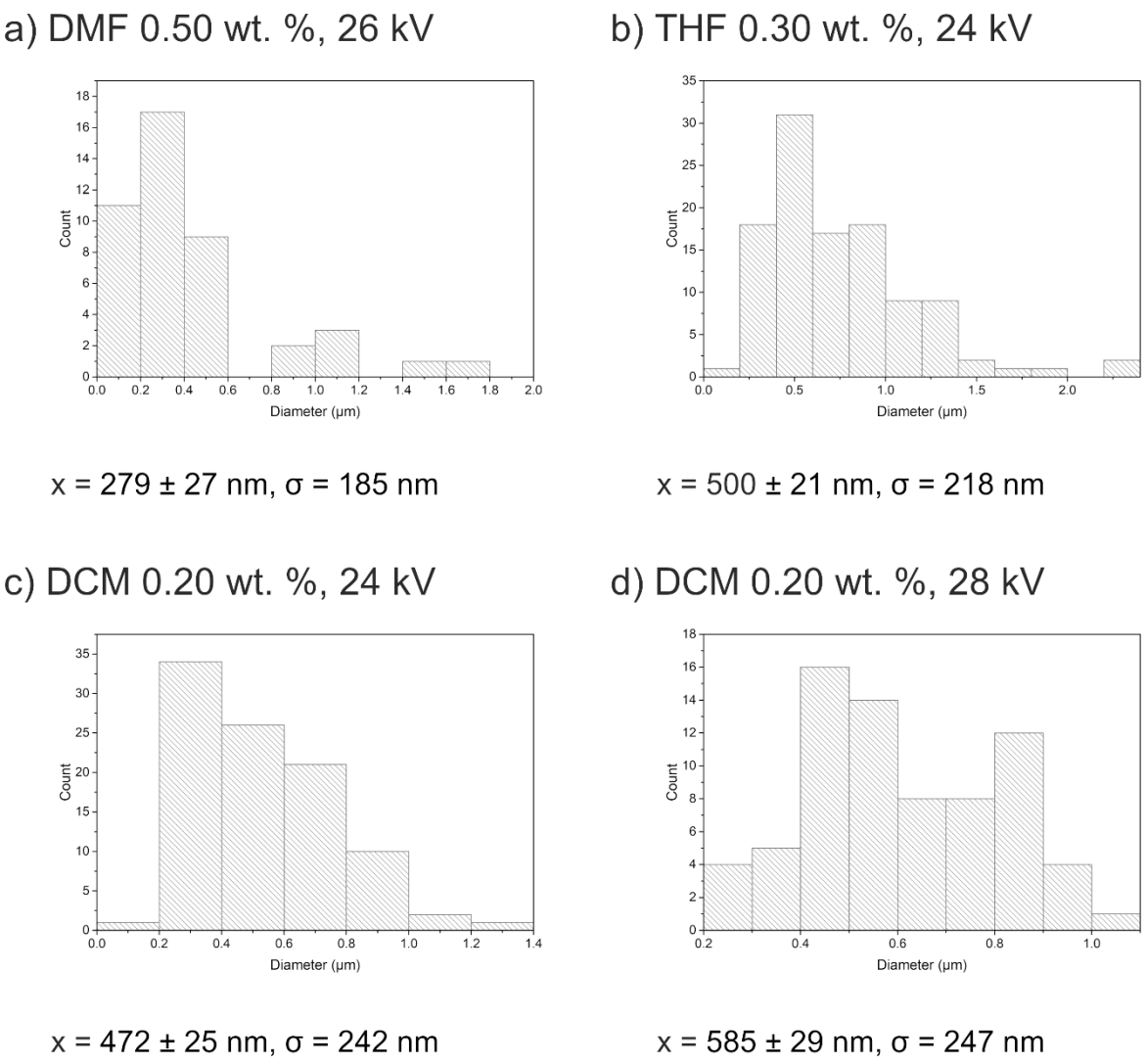

Figure 23. Diameter distribution for electrospun fibers of PMenBC in the SEM images from solutions of a) DMF n = 44, b) THF n = 109, c) DCM at 24 kV n = 95 and d) DCM at 28 kV n = 72.

Drop shape analysis of the surface of these fiber mats also revealed that the contact angles increased from 108 ° of the bulk material up to 141 ° for fibers spun from DMF (Figure 24). These high hydrophobicities resulted from the introduced structured surface and were reported for many electrospun polymers.[180–182] The combination of this strong repulsion of water with the high solubility of the polymer in a wide range of solvents could be interesting for an application in the separation of water and organic solvents.

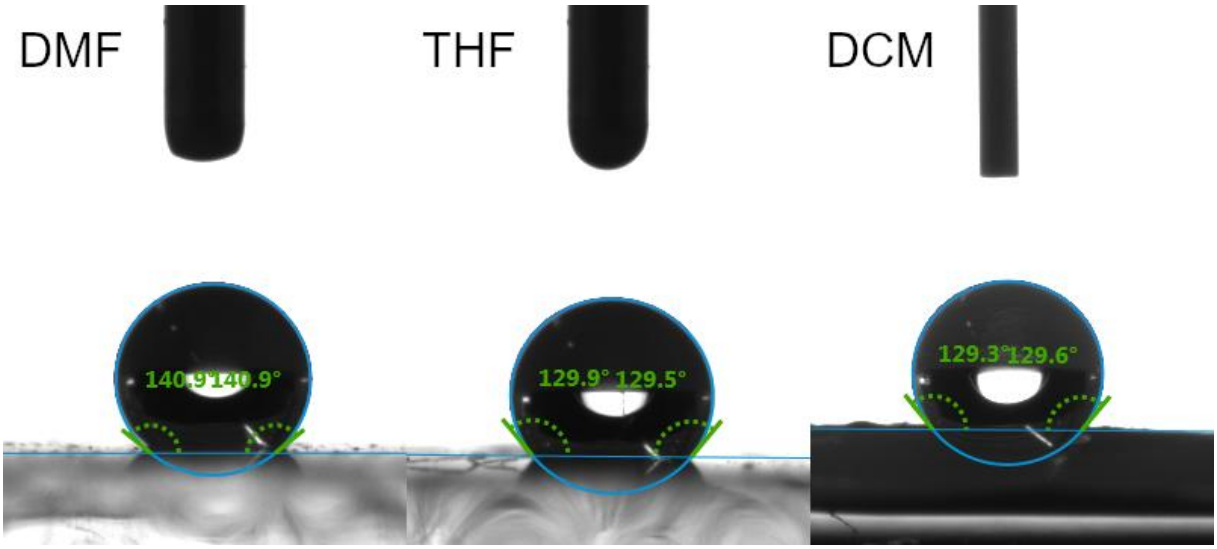

Figure 24. Contact angle measurements for non-woven spun from DMF (left), THF (middle) and DCM (right).

Although the hydrophobicity suggested an application for this purpose, two other properties had to be altered to obtain a suitable material. Successful and continuous separation requires remaining the fibrous microstructure in the presence of organic solvents and thus, solubility has to be reduced. The other challenge is that only PMenBC with a T_g of 31 °C could be processed. This low transition temperature might have negative effects on the performance in the summer or hotter regions. Hence, bisBP as UV-crosslinker was added to the spinning solution. 5 wt.% of the polymer weight is substituted by bisBP resulting in 0.053 $g_{bisBP}/g_{polymer}$. Analog to the previous electrospinning experiments without crosslinker, DMF, DCM and THF were used as solvents. Spinnable weight contents were adopted from the preliminary tests as well.

All used solutions resulted in the significant formation of beads. Contrary to the results of the solutions before, the 0.50 wt.% DMF solution gave as many beads as the 0.45 wt.% solution while producing higher diameters. Only the conditions of the 0.45 wt.% solution thus were varied to decrease beads formation, which was possible due to a combined increase in the applied voltage to 38 kV and a reduction in the flow rate to 1.25 mL/h. If the flow rate was further decreased, beads again became more frequent.

Similarly, bead formation could be reduced for DCM solution by increasing the voltage up to 34 kV and reducing the flow rate to 0.55 mL/h. A complete suppression was not possible for any tested solvent, voltage, and flow rate combination.

Table 9. Conditions for electrospinning of PMenBC with bisBP and the resulting fiber morphology.

Entry	Solvent	*w*(PMenBC+bisBP)/ wt.%	V_{Needle} /kV	Flow[a]/ mL/h	Morphology[b]
1	DMF	0.50	26	1.95	beads
2	DMF	0.50	29	1.95	beads
3	DMF	0.45	28	1.95	beads
4	DMF	0.45	28	1.25	beads
5	DMF	0.45	34	1.25	beads
6	DMF	0.45	34	1.0	beads
7	DMF	0.45	34	1.95	beads
8	DMF	0.45	38	1.95	beads
9	DMF	0.45	38	1.8	less beads
10	DMF	0.45	38	1.5	less beads
11	DMF	0.45	38	1.25	sporadic beads
12	DMF	0.45	38	1.0	beads
13	DMF	0.45	38	0.75	beads
14	DCM	0.20	24	0.65	beads
15	DCM	0.20	28	0.65	beads
16	DCM	0.20	30	0.65	less beads
17	DCM	0.20	34	0.65	less beads
18	DCM	0.20	34	0.55	almost no beads
19	THF	0.30	24	0.65	beads
20	THF	0.30	28	0.65	mainly beads

a) set at the machine, b) determined by optical microscopy.

The aim of adding bisBP was to crosslink the fibers after fabrication. Two different intensity levels and exposure times between 1 and 20 min were tested to find viable conditions. Since light source gives off a particular heat and the thin fibers might be faster heated above the T_g of 31 °C of the used PMenBC than the bulk material, not only the complete insolubility in suitable solvents but also the retention of the fibrous morphology had to be taken into account of the evaluation. 5 min of irradiation with 60 mW/cm² of UV light was the fastest way to crosslink the fibers completely. Lower irradiation times were not sufficient to introduce insolubility to the fibers. Total stability against solvents was only achieved for reduced intensities of 33 mW/cm² in the 20 min sample. All crosslinked samples showed significant swelling in DCM and various other

organic solvents. Fibrillary structures could be observed in optical microscopy and SEM, proving that UV-crosslinking provides a stable non-woven even at elevated temperatures. Fibers were also stable at prolonged irradiation times. Thicker fiber mats might need longer exposure times and were kept in the following under UV light for one hour to guarantee a complete fixation. Mats, which were used to test potential applications (*vide infra*), were all produced following the presented procedure of spinning with bisBP from a single solvent and subsequent crosslinking over one hour.

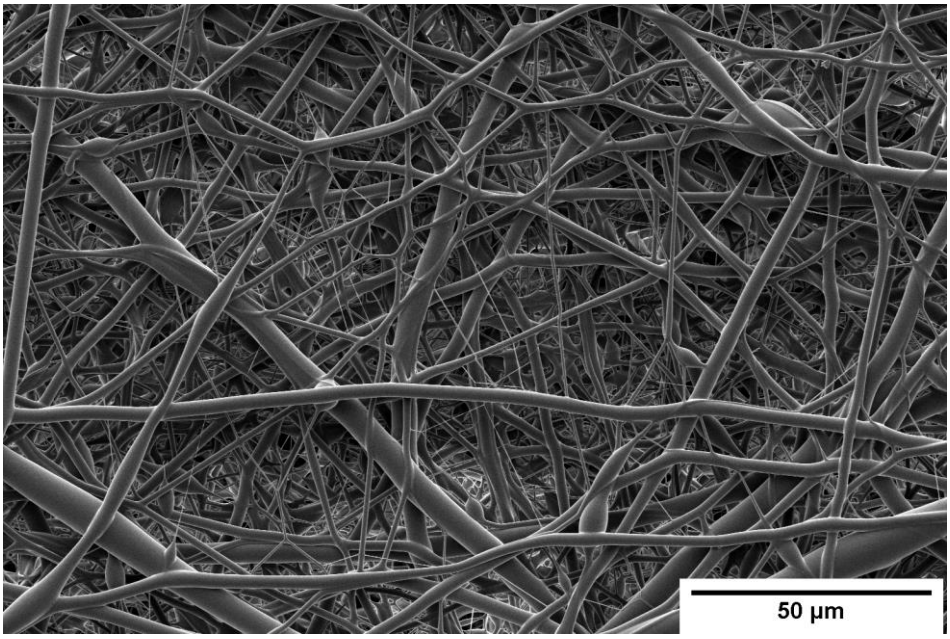

Figure 25. PMenBC fiber mat after irradiation with 60 mW/cm^2 for 20 min.

This procedure also allowed the fabrication of yarns. Therefore, two syringes were loaded with a 20 wt.% PMenBC/bisBP solution in DCM and placed on opposing sides of a rotation cone at a distance of 20 cm as established in the group.[183] Voltages of -17 and 17 kV were applied to the needles at a relative humidity of 25% at 20 °C room temperature. The yarn is then extracted from the cone with an auxiliary yarn. The single nanofibers are twisted together during this process. Yarn spinning with PMenBC was possible but not stable over longer periods of time and only a few centimeters of yarn could be obtained.

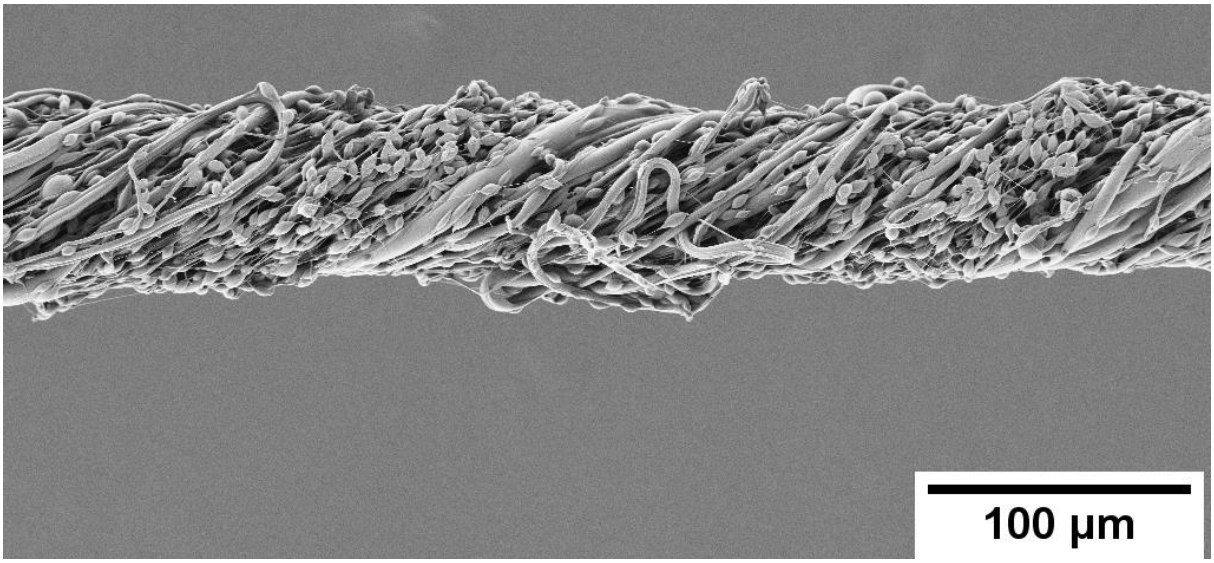

Figure 26. Yarn obtained by electrospinning of PMenBC with notable beads and varying fiber diameters.

The procedure had to be altered to produce fibers without beads. Mixtures of solvents with smaller parts of non-solvents present a viable solution to this problem. Solutions for these experiments were prepared as the 0.45 wt.% solution in DMF and the 0.20 wt.% solution in DCM, but 10 or 20% of the solvent was substituted by methanol. All components were still soluble in these mixtures except the 80/20 weight/weight mixture with DMF. This solution was turbid and minor crystals might indicate the precipitation of bisBP. While spinning, the same voltages were applied, but the flow rates had to be reduced. Both mixtures of DMF with methanol were not ideal for this approach. Spinning with the 80/20 mixture was not as continuous as before and gave beadless thick fibers at flow rates of 1.25 mL/h. A flow rate reduction reduced the average diameter to 553 nm with a low standard deviation. Further variations in concentration, flow rate and applied voltage might lower the diameter (Table 8, Entry 1). These options have to be investigated in the future. The 90/10 mixture was an improvement to pure DMF regarding the number of beads but was not able to suppress the formation of beads entirely.

Fibers without beads could be produced by electrospinning of the 80/20 mixture of DCM with methanol at flow rates between 0.20 – 0.45 mL/h. Fiber mats spun at 0.45 mL/h showed the lowest diameters at first inspection under the light microscope (Table 10, Entry 3). The average diameter of 528 nm determined by SEM imaging was in a close range as the uniform fibers obtained by Table 8 Entries 18 and 19. The 90/10 mixture of DCM and methanol (Table 10, Entry 4) produced fibers in the same regime but slightly higher diameters and standard deviation than Entry 3.

Table 10. Optimized electrospinning of PMenBC with bisBP with solvent/non-solvent mixtures and the resulting formation of beads.

Entry	Solvent	*w*(PMenBC+bisBP)/ wt.%	V_{Needle} /kV	*Flow*/ mL/h	*Diameter*[a] /nm	σ^a / nm
1	DMF/MeOH (80/20)	0.45	38	0.60	553	181
2	DMF/MeOH (90/10)	0.45	38	0.30	Beads	-
3	DCM/MeOH (80/20)	0.20	34	0.45	528	195
4	DCM/MeOH (90/10)	0.20	34	0.20	569	298

a) determined by evaluation of SEM images.

The fabrication of nanofibers is another labor-intensive step; specialized high-demand applications could make this process break even. Here investigations on two different fields were conducted. The first is air filtration. Due to the ongoing Corona crisis during this work, it is an attractive and urgent research topic.[184–186] Out of this aim, several objectives have to be fulfilled, the permeability of air, stability in an air stream and porosity. The process of electrospinning itself achieves porosity. Overlapping fibers in the non-woven create hollow spaces, which hold back particles depending on the size of the pores as well as the particles. All non-wovens were spun on aluminium foil or baking paper up to this point and either not or hardly removable from the surfaces. Additionally, none of these substrates was air permeable. A PE mesh (50 µm fiber diameter, 0,1 mm mesh size), a metal mesh (30 µm fiber diameter, 45 µm mesh size and a PET non-woven (17 µm fiber diameter) thus were tested as permeable substrate. It was possible to spin on every surface, but the fiber mats obtained from the PET non-woven were not homogeneous enough. Fibers did not cover parts of the substrate. The two meshes showed a much more even distribution of fibers.

Samples were prepared by spinning from DCM or DMF on the metal or PE mesh, resulting in four samples. After drying and crosslinking under UV light, the samples were tested in an air filtration test bench with a di(2-ethylhexyl) sebacate (DEHS) aerosol in a size range from 0.2-5 µm.

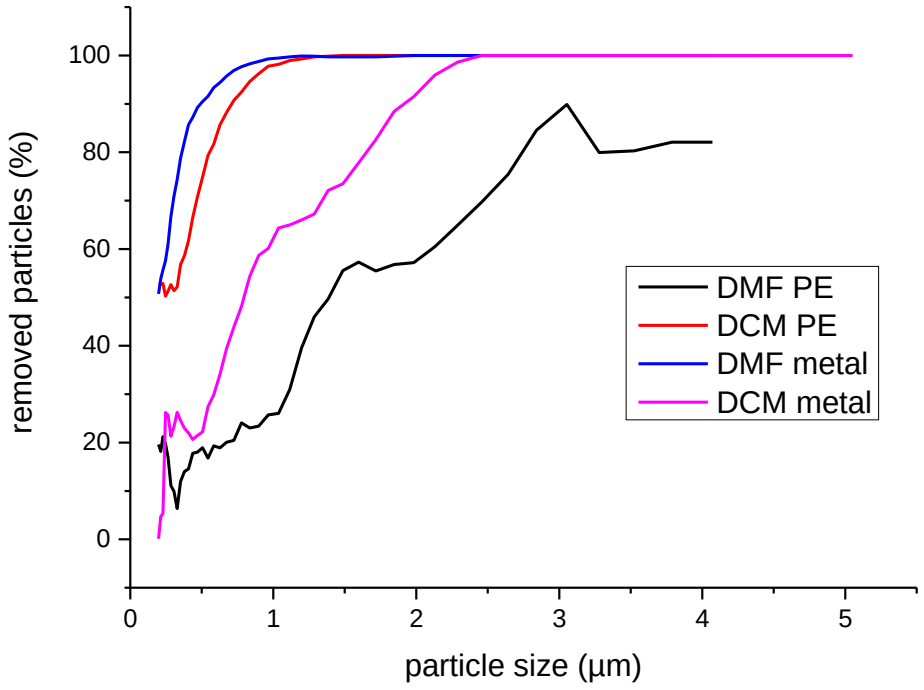

Figure 27. Removal of particles depending on their size for samples produced by electrospinning from DCM or DMF on a PE or metal mesh.

All samples performed better than the virgin meshes themselves (not shown here), showing potential as filter material. A non-woven spun on a metal mesh from DMF achieved the highest removal (Figure 27, blue curve). Surprisingly, although spun under the same conditions, the non-woven on the PE mesh was the sample with the lowest performance (Figure 27, black curve). Bubble point measurements resulted in a pore size of 12.9 µm on the metal mesh and one of 3.56 µm on the PE mesh, but the comparison of microscopy pictures revealed a much higher coverage of the metal mesh. Further inspection showed much higher radial differences for the PE mesh due to the rotating collector and electrostatic charges on the surface, which could not be removed on the non-conductive mesh. From samples spun from DCM, it was vice versa (Figure 27, red and pink curve). Although no difference in coverage was observable in SEM images, this trend could be attributed to the shorter time used to prepare the sample on the metal mesh (Figure 27, pink curve). If both high-performing samples (DMF metal mesh, DCM PE mesh) are compared, DMF on metal mesh shows better performance for particles below 1.20 µm, but particles smaller than 1.98 µm are not removed entirely. DCM on PE mesh removed all particles with diameters bigger than 1.49 µm. Further investigations are necessary to increase overall filtration

performance. Still, they might be realized by prolonged spinning times of DCM solutions on PE meshes to match the deposition of spinning with DMF solutions.

As mentioned above, oil-water separation is another application where electrospun non-wovens could be used.[187] Oil-water separation is essential in the chemical industry. Furthermore, Water-oil mixtures are skimmed from the surface of contaminated water bodies after oil spills and require further separation before possible disposal. A membrane was spun from a 0.45 wt.% DMF solution of PMenBC over 8 h and consequently crosslinked. Although removal of the entire non-woven from the substrate was not possible, undamaged pieces could be used for preliminary tests. These revealed an applicability for separating biphasic mixtures of water with DCM, pentane, limonene, anisole and methyl-10-undecanoate. All led to significant swelling of the membrane without dissolving it, which allowed the permeation of the organic solvent. The solvents almost instantaneous form drops on the lower side of the membrane, which can be removed easily. The high hydrophobicity of the dry membrane prevents the permeation of pure water. Pure isopropanol could also penetrate the membrane, but a homogeneous solution with water could not be separated through the membrane. *n*-butanol was able to swell the membrane and formed a biphasic system with water and it was still impossible to separate with this membrane.

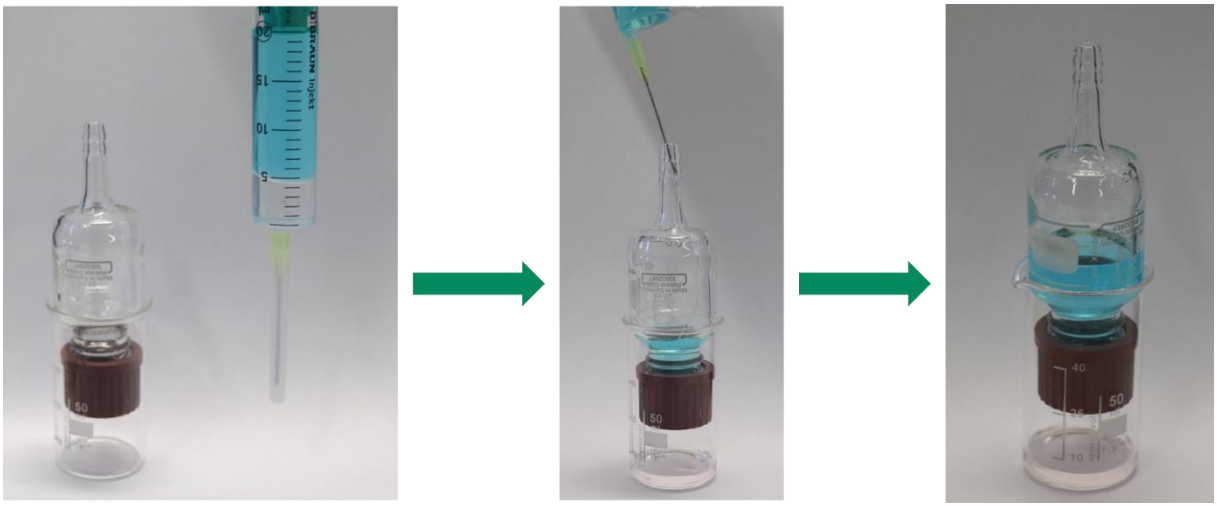

Figure 28. Separation of a DCM-water mixture (upper phase water colorized with copper(II) nitrate, lower phase DCM) by an electrospun PMenBC membrane.

More quantitative tests were performed to determine phase contamination. The water content in DCM was determined with an aqueous copper(II) nitrate solution and DCM. Clear and colorless DCM dropped directly through the membrane. ICP-OES showed

copper contents in the solution below the calibrated concentration range, which suggests a neglectable water content in DCM. The opposite test was performed with water and a solution of Sudan red in DCM. The red DCM dropped out of the bottom of the apparatus, while the aqueous phase remained on top. Red stains remained on the walls. These could be removed by washing with DCM and were only on the wall. A clear and colorless solution was obtained if the water was removed from the middle. A more cylindrical device and a more homogenized biphasic mixture might circumvent these staining problems. The colorant concentration was relatively high with 1 mg/mL, which increases visibility, but might be another cause of the staining issues.

It could be shown that fibers of PMenBC can be produced by electrospinning. Low average diameters down to 279 nm were achieved, but the addition of bisBP as a crosslinker resulted in a significant formation of beads. The partial substitution of the solvent could suppress this behavior by methanol as a non-solvent. Fiber mats with bisBP could be crosslinked successfully without losing the fibrous structure. These were then used in experiments investigating their ability to filter air or separate mixtures of organic solvents and water. These investigations only touched the surface and provided a proof of concept. Further experiments are needed to decrease fiber diameters of solvent mixture solutions and to show the full potential of this fully biobased fibrous material.

6 Summary

Here a successful synthesis of a fully biobased polycarbonate starting from menthol was established. Therefore, an upscalable route for the synthesis of menthene oxide was installed. Direct elimination of the hydroxyl moiety of menthol was not possible; thus, a tosylation and subsequent elimination had to be performed. Epoxidation using *m*CPBA resulted in the necessary monomer for the polymerization.

Two catalytic systems were tested for the copolymerization of MenO and CO_2. The first was a β-diketiminate complex of zinc. A controlled reaction was possible and the polycarbonate PMenC was obtained without ether defects. However, the reaction lacked sufficient monomer conversion, limiting its molecular weight to an M_p of 44400. Thermal properties exceeded that of PLimC and PCHC. Its T_g of 145 °C and $T_{5\%}$ of 308 °C were both extraordinarily high and provided a reasonable processing window of over 160 °C for potential melt processing applications. Hydrolysis of the polymer showed a stereoselectivity towards a single configuration at the cyclohexane ring. The second catalytic system relied on the combination of the Lewis acid TEB and an initiating Lewis base. Here a full screening of the reaction parameters was performed to establish a metal-free route for the synthesis of PMenC. Conversions up to 70% were achieved, but molecular weight could not be raised above an $\bar{M}_n$ of 28500. ^{1}H-NMR spectroscopy revealed differences in the polymers obtained with the zinc catalyst depending on the reaction temperature. Hydrolysis identified these differences as the incorporation of the two different diastereomers at the cyclohexane ring.

Furthermore, terpolymers of MenO and CO_2 with BO or undecene oxide were synthesized to increase chain mobility. Although the reaction was successful and the T_g could be varied from 6 °C to 165 °C, it was only possible to prepare films with polymers, which contained a high content of PBC. After crosslinking with a bifunctional UV-crosslinker, these films were even stable at temperatures above room temperature.

These terpolymers were then electrospun to fibers in the nanometer scale. The formation of beads, which occurred upon the addition of the crosslinker, could be suppressed by the use of a solvent mixture with methanol as a non-solvent. Yarns and fiber mats were obtained, which were applied as air filtration membrane or for the separation of water and apolar solvents.

7 Zusammenfassung

In dieser Arbeit wurde die erfolgreiche Synthese eines vollkommen biobasiertem Polycarbonates ausgehende von L-Menthol gezeigt. Dafür wurde zuerst eine skalierbare Syntheseroute für Menthenoxid etabliert. Eine direkte Eliminierung der Hydroxylgruppe des Menthols war nicht möglich, weshalb Menthol zuerst tosyliert werden musste, gefolgt von einer Eliminierung des neu gebildeten Esters. Eine ausreichende Versorgung mit dem Epoxid konnte mittels Epoxiderung mit *m*CPBA sichergestellt werden.

Für die Copolymerisation von MenO und CO_2 wurde zwei katalytische Systeme untersucht. Das erste was ein β-diketiminat Komplex des Zinks. Eine kontrollierte Reaktion war möglich und das Polycarbonat PMenC konnte ohne Defekte in Form von Etherbrücken hergestellt werden, allerdings wurden keine hohen Umsätze erreicht, was zu einer Begrenzung der molekularen Masse auf maximal M_p = 44400 führte. Thermische Eigenschaften übertrafen die von PLimC und PCHC. Der T_g mit 145 °C und $T_{5\%}$ mit 308 °C liegen beide über dem der beiden anderen alicyclischen Polycarbonaten und waren außerordentlich hoch, was ein ausreichend großes Fenster von über 160 °C für die thermische Verarbeitung aufspannt. Die Hydrolyse des Polymers zeigte eine Stereoselektivität für nur eine Konfiguration der Substituenden am Cyclohexanring. Das zweite katalytische System setzte sich aus der Lewissäure TEB und einer initiierenden Lewisbase zusammen. Für diese metallfreie Route wurde ein Screening aller Reaktionsparamter durchgeführt und Umsätze von bis zu 70% erreicht, wobei die mittlere molekulare Masse $\bar{M}_n$ 28500 nicht übertrafen. Temperaturabhängige Unterschiede zur Synthese mit dem Zinkkatalysator wurden mittels ^{1}H NMR Spektroskopie festgestellt, welche durch Hydrolyse als der Einbau zweier unterschiedlicher Diastereomere am Cyclohexanring identifiziert werden konnte.

Außerdem wurden Terpolymere von MenO und CO_2 mit entweder BO oder Undeceneoxid hergestellt, um die Kettenbeweglichkeit zu erhöhen. Obwohl Polymere mit T_gs zwischen 6 und 165 °C nach erfolgreicher Reaktion erhalten werden konnten, war es nur mit Polymeren, deren PBC-Anteil hoch war, möglich Filme zu ziehen. Durch das quervernetzen mit einem bifunktionalen UV-Vernetzer konnte sogar eine räumliche Stabilität oberhalb der Raumtemperatur erreicht werden.

Diese Polymere konnten zudem mittels Elektrospinnen zu Fasern im Nanometerbereich verarbeitet werden. Zwar resultierte die Zugabe des Vernetzers in der Bildung von Kügelchen, jedoch konnte dies durch die Verwendung einer Beimischung von Methanol als Nicht-Lösemittels zur Spinnlösung unterdrückt werden. Garne und Vliese wurden erhalten. Letztere konnten ihre Anwendbarkeit als Membranen für die Luftfiltration sowie die Trennung von Wasser und unpolaren Lösungsmitteln zeigen.

8 Outlook

This work presents only a start in the research of menthol-based polycarbonates. There are still several unresolved questions that could not be tackled during the period of this work, starting from the synthesis of the monomer. Here was a focus on the menthene-2-oxide, while the monomer with the epoxide in the last remaining position was neglected. More sophisticated catalysts for the elimination step could show another selectivity and/ or reduce the number of steps necessary. Besides the obvious different approaches involving menthol, there is still a wide variety of terpenes and other biobased molecules (e.g., pinenes) that could be utilized as a monomer in the copolymerization with CO_2.

There are also more elaborated metal and metal-free catalysts for the synthesis of polycarbonates published, which might overcome the problem of the low conversion and the slow rates of MenO. Higher conversions while retaining the living and controlled character of the polymerization should result in higher molecular weights, which again should increase the entanglement of the chains, making even pure PMenC or at least a copolymer with higher PMenC content usable for film formation. Multifunctional catalysts, in particular, could be a massive improvement of the presented systems. Stereoselective catalysts might also increase the portion of the all-equatorial diastereomer and thus the T_g even more.

Other applications could be made accessible by block copolymers. These could be synthesized either by sequential addition of monomers or by a controlled functionalization of the end-groups with potential initiating groups. Block copolymers then could act as compatibilizers for blends with commercial polymers to increase their sustainable character.

The presented electrospinning experiments only scratched the surface, which is possible with this single material. Higher molecular weight PMenC, other compositions of PMenBC or combinations with other (functional) monomers might result in fibers with exciting properties. It was also shown that the spinning of yarn is possible, but a continuous procedure could not be established.

9 Experimental Section

9.1 Materials

Menthol, potassium *tert*-butoxide, *m*CPBA (77%), *p*-toluenesulfonyl chloride, isoprene, 4-hydroxybenzophenone, NaH (60% in mineral oil), MeI, TEB (1 M solution in THF in septum bottle), KOH, NaOH, NBS, pyridine, DMSO, DMF and limonene were used as received. Adipic acid was recrystallized in ethyl acetate before usage. Technical grade DCM, diethyl ether, THF and methanol were purified by distillation under reduced pressure. DCM was further dried over CaH_2 and distilled afterward for polymerizations. THF was refluxed over CaH_2 for 3 d and further 3 d over potassium chunks before being used for polymerizations. Butene oxide, undecene oxide, limonene oxide, menthene oxide and cyclohexene oxide were dried over NaH and masked with MeI according to a procedure of Hauenstein *et al.* and subsequently reduced under reduced pressure if necessary.[50] [PPN]Cl was purified by repeated dissolving in DCM and precipitation from diethyl ether. The solid was collected by filtration, dried in a vacuum for 3 d at 100 °C and transferred into the glovebox. Carbon dioxide (5.0, Linde Gase) was dried by passing through a column packed with molecular sieves (pore size 3 Å) and a Vici P600-2 gas purifier column. Zinc catalyst prepared according to a literature procedure from acetyl acetone, diethyl aniline, diethyl zinc and acetic acid.[188] All reactions were performed under protective gas (N_2 or Ar).

9.2 Methods

NMR spectra were recorded on a Bruker AMX-300 operating at 300 MHz (^{1}H) or 75 MHz (^{13}C). Chemical shifts δ are indicated in parts per million (ppm) with respect to residual solvent signals.[2]

TGA measurements were performed on a Netzsch TGA 209 F1 Libra at a heating rate of 10 K/min under N_2 in a range from 20 to 600 °C. Samples of 6 to 10 mg were prepared in aluminum crucibles with a pierced lid.

DSC measurements were performed on a Netzsch DSC 204 F1 Phoenix at a heating rate of 10 K/min under N_2 in a range of -80 to 180 °C. Samples of 6 to 14 mg were prepared in aluminum crucibles with a pierced lid. The second heating curve was used to determine the glass transition temperature.

IR spectra of solids were obtained with a Digilab Excalibur FTS-3000 equipped with an ATR unit.

Gas chromatograms were recorded on a Shimadzu QP-5050 with N_2 as the carrier gas with a FID detector.

GPC measurements were performed on a 1200 Series/1260 Infinity by Agilent Technologies equipped with a SDV 5µm precolumn, a SDV linear XL 5µm column, and a refractive index detector at a flow rate of 0.5 mL/min at room temperature. Chloroform (HPLC Grade) was used as eluent and toluene as an internal standard. The system is calibrated to a polystyrene standard in $\bar{M}_n$ range from 630 Da to 2580 kDa.

WAXS measurements were performed on a Bruker D8 ADVANCE operating at 40 kV/40mA with a Cu-Kα radiation (λ = 0.154 nm). The samples were covered in polyimide insulating tape and fixed in the instrument stage. XRD Profiles were recorded with a transmittance program in the 2θ angle range from 5° to 45 ° at a scanning speed of 0.05 °/min at 25 °C. The background was measured to the pure polyimide insulating tape.

GC-MS data were collected on a GC 8790B coupled to a MSD5977A quadrupole mass spectrometer both by Agilient equipped with a MPS 2 XL multi-purpose sampler by Gerstel GmbH and a pyrolysis module by Gerstel GmbH.

Specific rotation was determined in a JASCO P1020 polarimeter.

Crosslinking was performed under a UV-F400 by Dr. Hönle AG with a metal halide light source of the type MHL/ ES 450. It operates between 325-380 nm.

Electrospun fibers were produced with an ELSA 2015 electrospinning machine built by the workshop of the University Bayreuth. It is capable of voltages between +60 KV and -30 kV.

Samples for SEM images were sputtered with a 2 nm platinium layer quantified by QCM in a Cressington Platin-Sputter Coater 208HR with planetary stage. Measurements were performed either on a Zeiss Leo 1530 or a FEI Quanta FEG 250 at an acceleration voltage of 3 kV and detected with a Everhart-Thornley detector.

Optical microscopic images were obtained with a Zeiss Smartzoom 5 equipped with a Zeiss PlanApo D 5c/0.3 FWD 30 mm objective.

Air filtration of filters with an area of 28.3 cm^2 were investigated at a Palas MFP 2000 test bench. DEHS particles in a size range from 0.2-40 µm were counted at a volume flow of 1.65 L/min and a flow rate of 25 cm/s.

Copper contents were determined on a PerkinElmer Avio200 ICP-OES against a copper standard. Both absorptions at 327.393 nm and 324.752 nm were considered.

Contact angles were determined with a DSA25 Drop Shape Analyzer manufactured by Krüss with a 4 µL droplet of deionized water.

A Zwick/Roell Z0.5 tensile tester with testXpert II software was employed for the tensile testing. The tests were performed at 23 °C and relative humidity of 25%. The strain rate was set to 10 mm min^{-1}, to test the tensile properties of cast polymer films that were cut into specimen having a width of 3 mm, a length of 30 mm and a thickness of 100–200 µm.

9.3 Procedures

9.3.1 Synthesis of Menthyl Tosylate

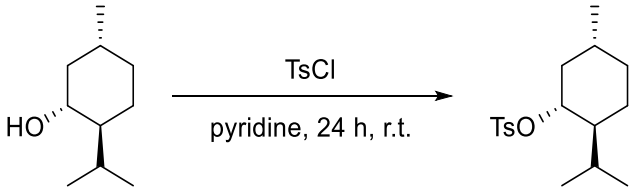

Scheme 16. Tosylation of L-menthol.

Menthyltosylate was synthesized according to a literature procedure by Erker *et al*.[189] Menthol (89.4 g, 572 mmol) was dissolved in pyridine at 0 °C and *p*-toluenesulfonyl chloride (120 g, 630 mmol) was added over a period of 30 min. After stirring for 24 h at room temperature, the mixture was precipitated from ice-cold 4 M hydrochloric acid. The formed precipitate was separated by filtration, dissolved in diethylether and dried over $MgSO_4$. The solvent was removed under reduced pressure to obtain a colorless crystalline solid. (169 g, 545 mmol, 95%)

^{1}H NMR (300 MHz, $CDCl_3$) δ = 7.80 (*app* d, *J*=8.3, 2H), 7.32 (*app* d, *J*=8.0, 2H), 4.39 (td, *J*=10.8, 4.6, 1H), 2.44 (s, 3H), 2.18 – 2.09 (m, 1H), 1.95 – 1.82 (m, 1H), 1.71 – 1.55 (m, 2H), 1.50 – 1.30 (m, 2H), 1.25 – 1.10 (m, 2H), 1.05 – 0.92 (m, 1H), 0.90 – 0.77 (m, 6H), 0.51 (d, *J*=6.9, 3H).

Data are in accordance with the literature.[189]

9.3.2 Synthesis of Menthene

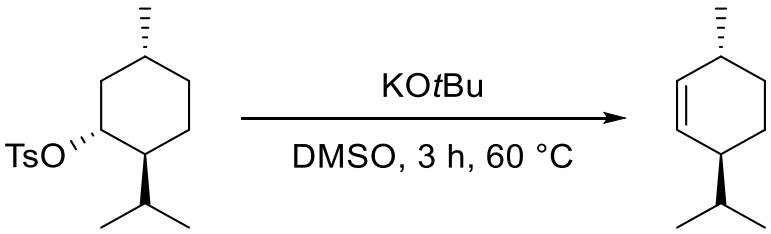

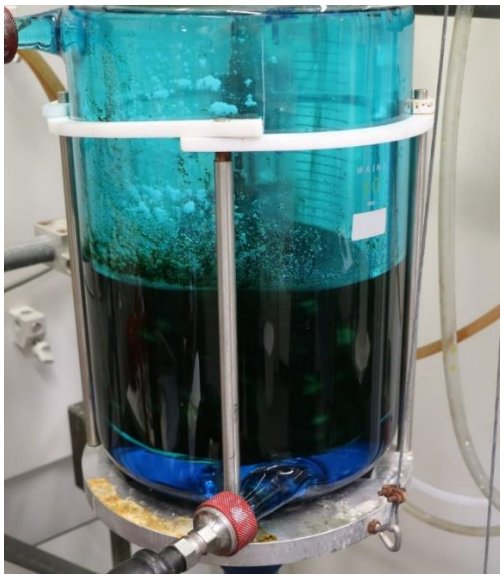

Scheme 17. Synthesis of menth-2-ene (top), 10 L reactor and green reaction mixture (bottom).

The elimination of the tosylate followed a procedure of Fiorani *et al.* for the corresponding mesylate.[163] Menthyltosylate (700 g, 2.25 mol) was suspended in DMSO (3 L) under vigorous stirring and cooled to 20 °C. Potassium *tert*-butanolate (380 g, 3.38 mol) was added in portions over 30 min to the reactor. During heating to 60 °C for 3 h all reactants dissolved and formed a deep green solution. Afterward, water (3 L) was slowly added, which resulted in phase separation of the product and the aqueous DMSO. Hexane (3 L) was added to extract the crude product. A clear oil was obtained after removal of the solvent under reduced pressure and distillation under dynamic vacuum (240 g, 1.75 mol, 77%).

^{1}H NMR (300 MHz, $CDCl_3$) δ = 5.59 – 5.44 (m, 2H), 2.20 – 2.03 (m, 1H), 1.98 – 1.87 (m, 1H), 1.88 – 1.77 (m, 1H), 1.76 – 1.64 (m, 1H), 1.64 – 1.45 (m, 1H), 1.34 – 1.02 (m, 2H), 1.00 – 0.78 (m, 9H).

^{13}C NMR (75 MHz, $CDCl_3$) δ = 134.12, 130.05, 42.10, 32.36, 32.17, 31.14, 25.79, 22.16, 19.74, 19.41.

Data are in accordance with the literature.[163]

9.3.3 Synthesis of Menthene Oxide

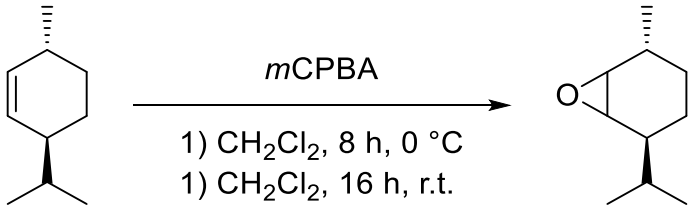

Scheme 18. Epoxidation of menth-2-ene.

Menth-2-ene (20 g, 144 mmol, 24.7 mL) and dichloromethane (370 mL) were mixed and cooled with an ice bath. *m*CPBA (164 mmol) was slowly added over 30 min and stirring was continued for 8 h. Afterwards, the reaction mixture was allowed to warm to room temperature and stirred for a further 16 h. The formed precipitate was removed via filtration and the filtrate was washed once with aqueous 1 M NaOH, sat. $NaHCO_3$ and sat. NaCl solution. The organic phase was dried over $MgSO_4$, the solvent was removed under reduced pressure and the crude product was distilled at 55 °C under dynamic vacuum to obtain a clear liquid with a strong odor (17.3 g, 112 mmol, 78%).

The crude product was further dried with NaH (0.16 eq.). After a completed reaction (no more hydrogen formation visible), iodomethane (0.08 eq) was added according to a procedure of Hauenstein *et al*.[17] The mixture was stirred overnight and fractionally distilled at 55 °C under dynamic vacuum.

^{1}H NMR (300 MHz, $CDCl_3$) δ = 3.20 – 2.76 (m, 2H), 1.95 – 1.13 (m, 7H), 1.11 – 0.70 (m, 9H).

^{13}C NMR (75 MHz, $CDCl_3$) δ = 58.08, 57.56, 56.82, 56.72, 42.64, 40.24, 31.31, 30.97, 26.35, 24.50, 22.06, 20.69, 20.15, 19.46, 18.79.

Data are in accordance with the literature.[163]

9.3.4 General procedure of the synthesis of PMenC with Zn-Catalyst

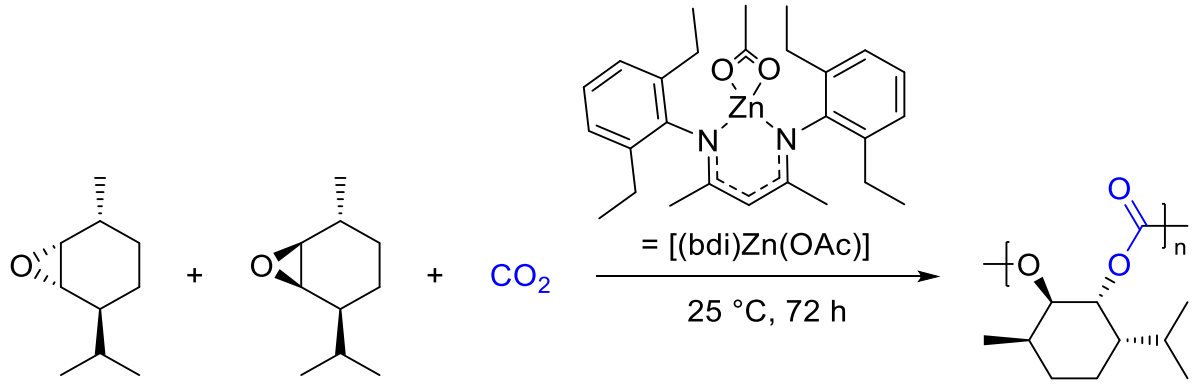

Scheme 19. Copolymerization of menth-2-ene oxide with CO_2.

An in vacuo at 75 °C predried 200 mL steel autoclave was charged in the glovebox with [(bdi)Zn(OAc)] (37.8 mg, 0.0778 mmol). Toluene (5 mL) and menth-2-ene oxide (5 mL, 4.53 g, 29.4 mmol) were added in a stream of nitrogen before the autoclave was pressurized with 25 bar CO_2 and the mixture was stirred for three days. The obtained viscous mixture was diluted with toluene (5 mL) before 20 wt.% of maleic anhydride were added. After 1 h the solution was precipitated in methanol, dissolved in DCM and reprecipitated and the product dried in vacuo.

^{1}H NMR (300 MHz, $CDCl_3$) δ 4.99 (s, 1H), 4.79 (s, 1H), 1.88 (s, 1H), 1.65 (s, 1H), 1.49 (s, 2H), 1.35 (s, 3H), 0.88 (s, 9H).

^{13}C NMR (75 MHz, $CDCl_3$) δ 154.08, 153.86, 153.66, 76.22, 74.10, 41.37, 30.06, 28.68, 28.20, 23.74, 20.92, 20.73, 17.29.

IR Characteristic peaks [cm^{-1}]: 2960, 2934, 2873, 1756, 1456, 1231, 1128, 927

[α] = -29.176 ± 0.993 (c 0.1, DCM)

9.3.5 General procedure of the terpolymerisation of MenO, CO_2 and other cyclohexene oxide derivatives

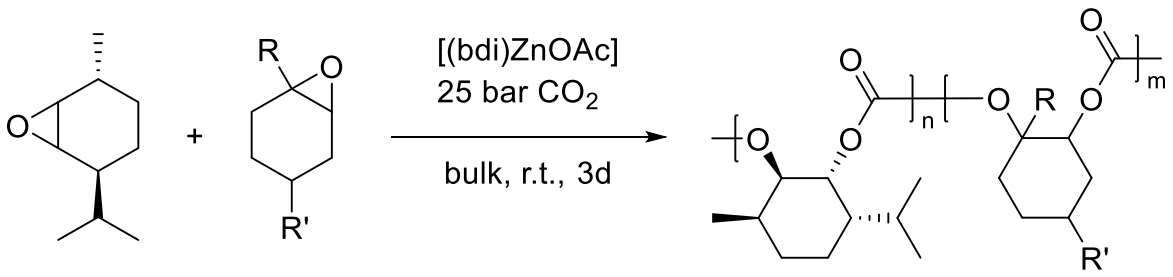

Scheme 20. Terpolymerization of MenO, CO_2 and cyclohexene oxide derivatives.

A steel autoclave was dried overnight at 75 °C in vacuo and then directly transferred into the glovebox. As soon as the reactor was cooled down, [(bdi)Zn(OAc)] (75.2 mg, 0.155 mmol) was placed into the vessel. The vessel was closed, removed from the glovebox, and connected to a schlenk line. The epoxides are freshly distilled. First, the cyclohexene oxide (2.4 mL, 2.31 g, 23.5 mmol) or limonene oxide (3.9 mL, 3.58 g, 23.5 mmol) is injected through a septum under positive nitrogen pressure, followed by menthene oxide (4 mL, 3.63 g, 23.5 mmol). 25 bar of CO_2 are added, the vessel is closed and placed on a magnetic stirrer for 3 d. After the release of the pressure, the solidified reaction mixture is dissolved in DCM and precipitated from methanol.

P(MenC-*co*-CHC):

Yield: 5.35 g

^{1}H NMR (300 MHz, $CDCl_3$) δ = 4.97 (s), 4.79 (s), 4.63 (s), 2.09 (s), 1.86 (s), 1.68 (s), 1.44 (s), 1.33 (s), 0.86 (s).

Ratio PMenC/PCHC (^{1}H NMR): 1/2.27

^{13}C NMR (75 MHz, $CDCl_3$) δ = 153.82, 153.21, 76.12, 74.02, 41.31, 30.38 – 28.94, 28.62, 28.09, 23.72, 23.36 – 21.37, 20.79, 17.16.

$T_{5\%}$ 276°C, T_g 128 °C

GPC: $\bar{M}_n$ 35400, $\bar{M}_w$ 40300, Đ 1.14

P(MenC-*co*-LimC):

Yield: 5.00 g

^{1}H NMR (300 MHz, $CDCl_3$) δ = 5.00 (s), 4.79 (s), 4.69 (s), 2.45 (s), 2.22 (s), 1.84 (s), 1.67 (s), 1.45 (s), 1.35 (s), 0.89 (s).

Ratio PMenC/PLimC (^{1}H NMR): 1/0.54

^{13}C NMR (75 MHz, $CDCl_3$) δ = 153.85, 152.01 148.77, 109.37 81.86 76.29 75.40 74.13 41.35 37.62 30.78, 30.04 28.69 28.17 25.80 23.76 21.61 20.91 20.75, 17.29, 17.22.

$T_{5\%}$ 241°C, T_g 129 °C

GPC: $\bar{M}_n$ 29100, $\bar{M}_w$ 31900, Đ 1.09

9.3.6 General procedure of the synthesis of PMenC with TEB and [PPN]Cl

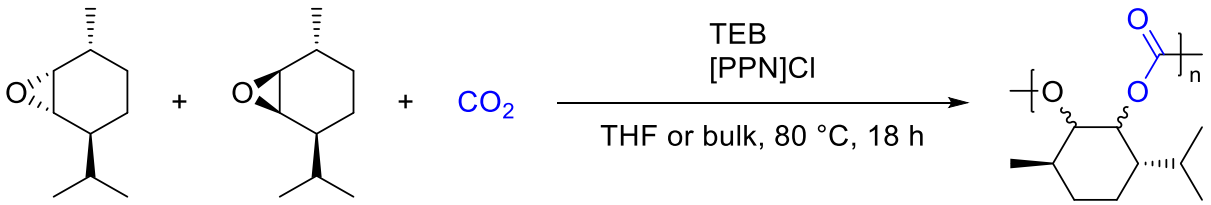

Scheme 21. Copolymerization of menth-2-ene oxide with CO_2.

A pressure vessel was dried overnight at 75 °C in vacuo and then directly transferred into the glovebox. As soon as the reactor was cooled down, PPNCl (67.0 mg, 0.117 mmol) was placed into the vessel. The vessel was closed, removed from the glovebox, and connected to a schlenk line. Freshly distilled MenO (5 mL, 4.53 g, 29.4 mmol) and, if desired, THF (5 mL) are injected through a septum under positive nitrogen pressure. TEB (0.23 mL, 0.23 µmol) is added just before the CO_2. The vessel is then directly placed into a preheated oil bath and stirred for the desired time. After completion of the reaction, the reaction mixture is diluted with the same amount of solvent or with the same volume of DCM. Next, maleic anhydride (20 wt% of MenO) is added and stirred for 1 h. The mixture was then precipitated from methanol until no more impurities could be detected.

^{1}H NMR (300 MHz, $CDCl_3$) δ = 5.30 – 4.12 (m, 2H), 2.00 – 1.14 (m, 7H), 1.13 – 0.45 (m, 9H).

^{13}C NMR (75 MHz, $CDCl_3$) δ = 153.89, 76.32, 73.99, 41.41, 30.05, 28.70, 28.21, 23.74, 20.95, 20.77, 17.34.

9.3.7 General procedure of the synthesis of PBC

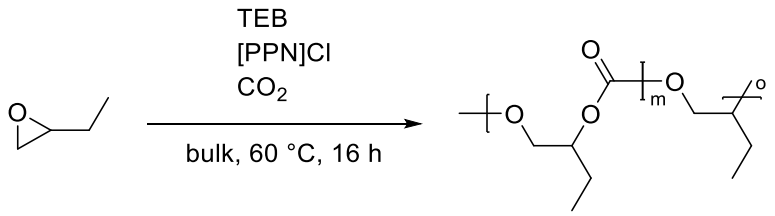

Scheme 22. TEB-catalyzed copolymerization of PMenC and CO_2.

A pressure vessel was dried overnight at 75 °C in vacuo and then directly transferred into the glovebox. As soon as the reactor was cooled down, PPNCl (76.8 mg, 134 µmol) was placed into the vessel. The vessel was closed, removed from the glovebox, and connected to a schlenk line. Freshly distilled BO (5 mL, 4.15 g, 57.6 mmol) is injected through a septum under positive nitrogen pressure. TEB (0.54 mL, 0.536 mmol) is added just before the CO_2. The vessel is then directly placed into a preheated oil bath and stirred for the desired time. After completion of the reaction, the reaction mixture is diluted with the same amount of solvent or with the same volume of DCM. Next, maleic anhydride (20 wt% of BO) is added and stirred for 1 h. The mixture was then precipitated from methanol until no more impurities could be detected.

^{1}H NMR (300 MHz, CDCl3) δ = 4.83 (s), 4.73 (s), 4.45 – 4.00 (m), 3.69 – 3.21 (m), 1.79 – 1.55 (m), 0.94 (t, J=7.2).

^{13}C NMR (75 MHz, CDCl3) δ = 155.00 – 154.54, 77.07, 67.84, 23.69, 9.41.

9.3.8 General procedure of the terpolymerization of MenO, CO_2 and linear aliphatic epoxides

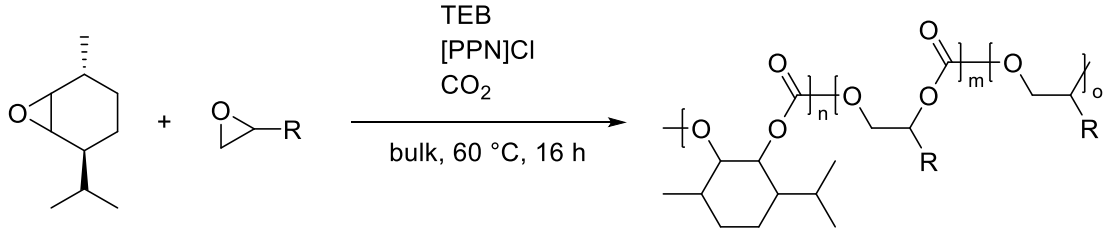

Scheme 23. Terpolymerization of MenO, CO_2 and linear aliphatic epoxides.

A pressure vessel was dried overnight at 75 °C in vacuo and then directly transferred into the glovebox. As soon as the reactor was cooled down, PPNCl (53.0mg, 92.6 µmol) was placed into the vessel. The vessel was closed, removed from the glovebox, and connected to a schlenk line. Freshly distilled MenO (4 mL, 3.63 g, 23.5 mmol), BO (0.5 mL, 415 mg, 5.76 mmol), and, if desired, THF (5 mL) are injected through a

septum under positive nitrogen pressure. TEB (0.37 mL, 0.37 mmol) is added just before the CO_2. The vessel is then directly placed into a preheated oil bath and stirred for the desired time. After completion of the reaction, the reaction mixture is diluted with the same amount of solvent or with the same volume of DCM. Next, maleic anhydride (20 wt% of MenO) is added and stirred for 1 h. The mixture was then precipitated from methanol until no more impurities could be detected.

^{1}H NMR (300 MHz, $CDCl_3$) δ = 5.18 – 4.60 (m), 4.54 – 4.00 (m), 3.82 – 3.38 (m), 1.88 (s), 1.77 – 1.58 (m), 1.48 (s), 1.33 (s), 1.16 – 0.58 (m).

^{13}C NMR (75 MHz, $CDCl_3$) δ = 155.33 – 153.20 (m), 76.36 (s), 74.08 (s), 67.82 (s), 41.34 (s), 30.01 (s), 28.89 – 28.29 (m), 28.06 (s), 23.80 (s), 20.78 (s), 17.51 – 16.82 (m), 9.95 – 9.01 (m).

9.3.9 Synthesis of Isoprene Oxide

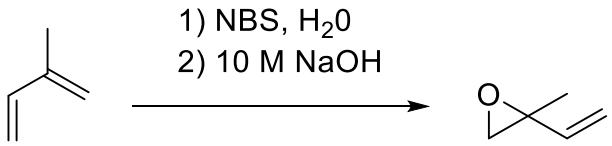

Scheme 24. Epoxidation of isoprene.

Isoprene (25 mL, 0.25 mmol, 1 eq.) was mixed under vigorous stirring with water (100 mL) at 0 °C. NBS (43.3 g, 0.243 mmol, 0.975 eq.) was added in portions over a period of 15 min. Stirring was continued for 3.5 h at 0 °C, allowed to shortly reach 10 °C, again cooled to 0 °C and slowly mixed with a 10 *M* aqueous NaOH solution (50 mL, 2 eq). After 20 min of stirring, the organic phase was separated, washed with brine and distilled at 80 °C.

Yield: 5.61 g, 27%

^{1}H NMR (300 MHz, $CDCl_3$) δ = 5.64 (dd, *J*=17.4, 10.7, 1H), 5.36 (dd, *J*=17.4, 1.1, 1H), 5.23 (dd, *J*=10.7, 1.1, 1H), 2.82 (d, *J*=5.2, 1H), 2.74 (dd, *J*=5.2, 0.6, 1H), 1.46 (d, *J*=0.6, 3H).

^{13}C NMR (75 MHz, $CDCl_3$) δ = 139.40, 116.96, 55.59, 53.44, 18.92.

9.3.10 Reaction of Isoprene Oxide with CO_2

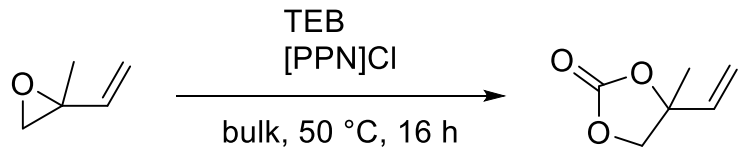

Scheme 25. Reaction of isoprene oxide with CO_2.

A pressure vessel was loaded with [PPN]Cl (66.9 mg, 117 mmol, 1 eq.) in the glovebox before it was removed. Isoprene oxide (1.4 mL, 1.20 g, 14.3 mmol, 122 eq.) was injected against a positive pressure of N_2, followed by TEB (0.5 mL, 0.5 mmol, 4 eq.). The vessel was set under a pressure of 10 bar of CO_2, closed and placed in an oil bath at 50 °C for 16 h. After the reaction, a bright red liquid was obtained.

^{1}H NMR (300 MHz, $CDCl_3$) δ = 5.94 (dd, *J*=17.3, 10.9, 1H), 5.44 (d, *J*=17.3, 1H), 5.33 (d, *J*=10.9, 1H), 4.27 (d, *J*=8.4, 1H), 4.18 (d, *J*=8.3, 1H), 1.60 (s, 3H).

9.3.11 Synthesis of bisBP

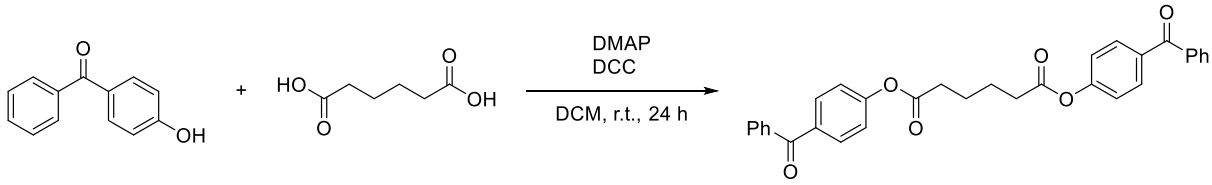

Scheme 26. Synthesis of bisBP by esterification of adipic acid with 4-hydroxybenzophenone.

Adipic acid (0.737 g, 5.04 mmol, 1 eq.), DCC (2.29 g, 11.1 mmol, 2.2 eq) and DMAP (0.308 g, 2.52 mmol, 0.5 eq.) were mixed in DCM (50 ml). 4-Hydroxy benzophenone (2.00 g, 10.0 mmol, 2 eq.) was added, and the reaction mixture was stirred under the exclusion of light for 24 h. Afterward, the formed urea is removed by filtration. The filtrate is washed with 1 *M* HCl, sat. $NaHCO_3$ and dried over $MgSO_4$ before the solvent was removed to obtain an off-white solid. The solid is first recrystallized from isopropanol and then from THF.

Yield: 1.30 g, 2.56 mmol, 51%

^{1}H NMR (300 MHz, $CDCl_3$) δ = 7.90 – 7.83 (m, 4H), 7.83 – 7.75 (m, 4H), 7.64 – 7.55 (m, 2H), 7.53 – 7.44 (m, 4H), 7.25 – 7.16 (m, 4H), 2.76 – 2.64 (m, 4H), 1.99 – 1.82 (m, 4H).

^{13}C NMR (75 MHz, $CDCl_3$) δ = 195.7, 171.4, 154.0, 137.6, 135.2, 132.7, 131.9, 130.1, 128.5, 121.7, 34.1, 24.3.

9.3.12 Crosslinking of PMenBC

Low T_g PMenBC (1 g) was dissolved in chloroform (3 mL), and the crosslinker (50 mg) was added. The mixture was vigorously stirred and transferred to a glass plate. The film was dried for 24 h at room temperature, 24 h at 40 °C, and 24 h at 40 °C under reduced pressure. After complete removal of the solvent, the film was irradiated for 10 min with UV light.

9.3.13 Hydrolysis of PMenC in Methanol

A sample of the polycarbonate (200 mg) was dissolved in THF (5 mL), mixed with KOH (2 eq. per repeating unit), and heated to reflux. Next, methanol (4 eq. per repeating unit) was added and stirred for 1 h, before 2 M aqueous HCl (2 mL) was added to quench the reaction. Finally, the products were extracted with ethyl acetate (2 mL), dried over $MgSO_4$, and isolated by evaporation of the solvent.

9.3.14 Homogeneous Hydrolysis of PMenC, PMenBC and Crosslinked PMenBC

The hydrolysis of PMen2C followed a procedure for the hydrolysis of PLimC.[16] PMen2C (502 mg) was suspended in methanol (50 mL), sodium hydroxide (520 mg) was added and the reaction mixture was heated to reflux for 24 h. Afterwards the cooled mixture was neutralized with hydrochloric acid, the solvent removed under reduced pressure. Diethylether(30 mL) was added and the organic phase was washed twice with sat. NaCl solution, before the solvent was removed and a highly viscous oil was obtained.

9.3.15 Electrospinning

Spinning solutions were prepared by adding the required solid compound (PMenBC and bisBP) in a glass vial and dissolving them in a volumetric measured amount of solvent (DCM, DMF, THF, DCM/methanol, DMF/methanol). The vial is closed, covered with aluminium foil and placed in a shaker overnight. Solutions were bubble-less transferred into syringes just before spinning.

The needle of the syringe was adjusted to 22 – 25 cm above and 12 – 14 cm beside the collector. Aluminium foil was used as a static collector for the checks of parameters. A collector rotating parallel to the ground was used for screening of substrates as well as for the samples of air filtration to increase homogeneity. A rotating drum collector

covered with baking paper was used for solvent/water separation membranes. Electrospun fiber mats were dried under vacuum at room temperature. Mats with bisBP were crosslinked under UV irradiation for one hour.

10 Appendix

10.1 Supplementary Data for Chapter 5.1.2

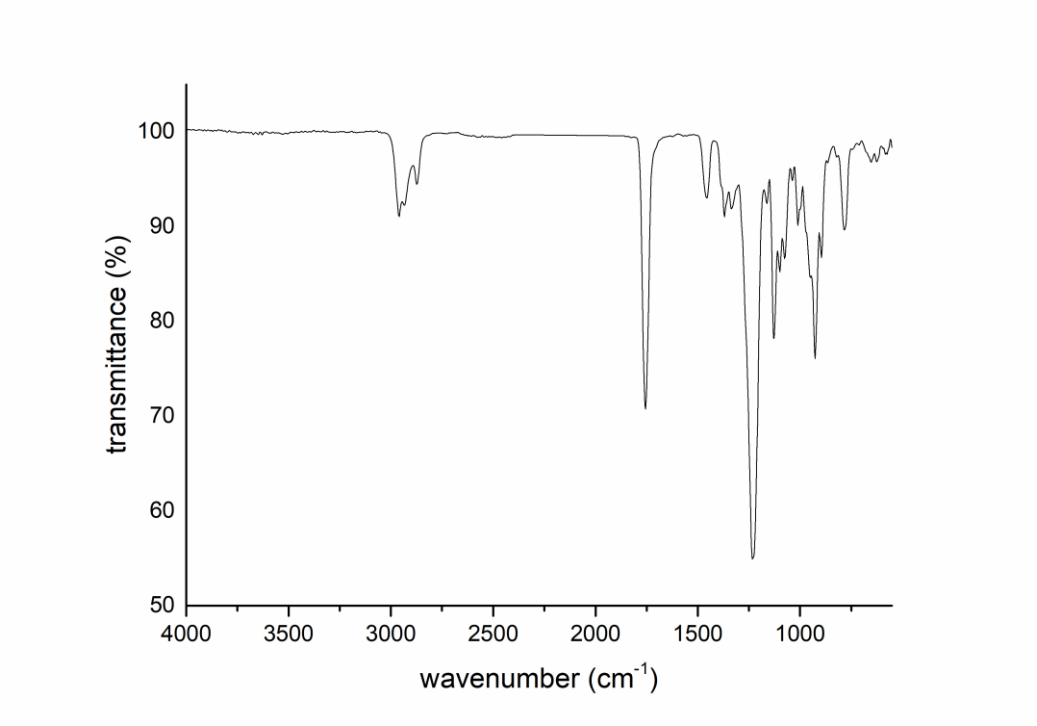

Figure 29. IR spectrum of PMenC. Reprinted with permission from Wambach, A.; Agarwal, S.; Greiner, A. Synthesis of Biobased Polycarbonate by Copolymerization of Menth-2-ene Oxide and CO_2 with Exceptional Thermal Stability. ACS Sustainable Chem. Eng. ***2020****, 8 (39), 14690–14693. Copyright 2020 American Chemical Society.*

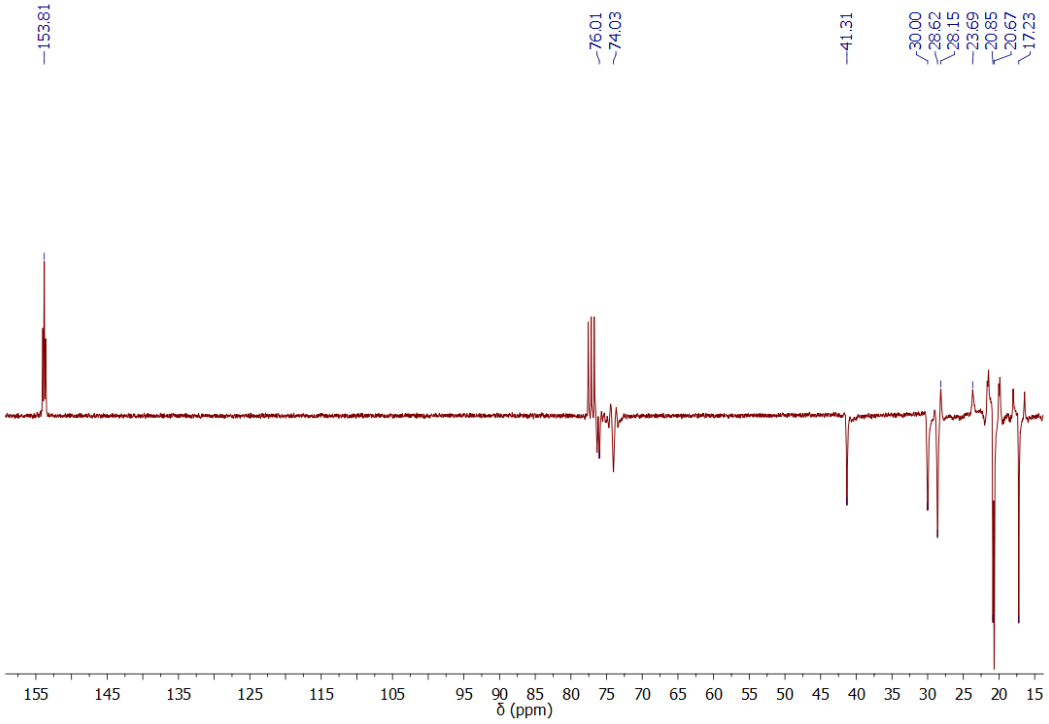

Figure 30. APT-^{13}C NMR spectrum of PMenC.

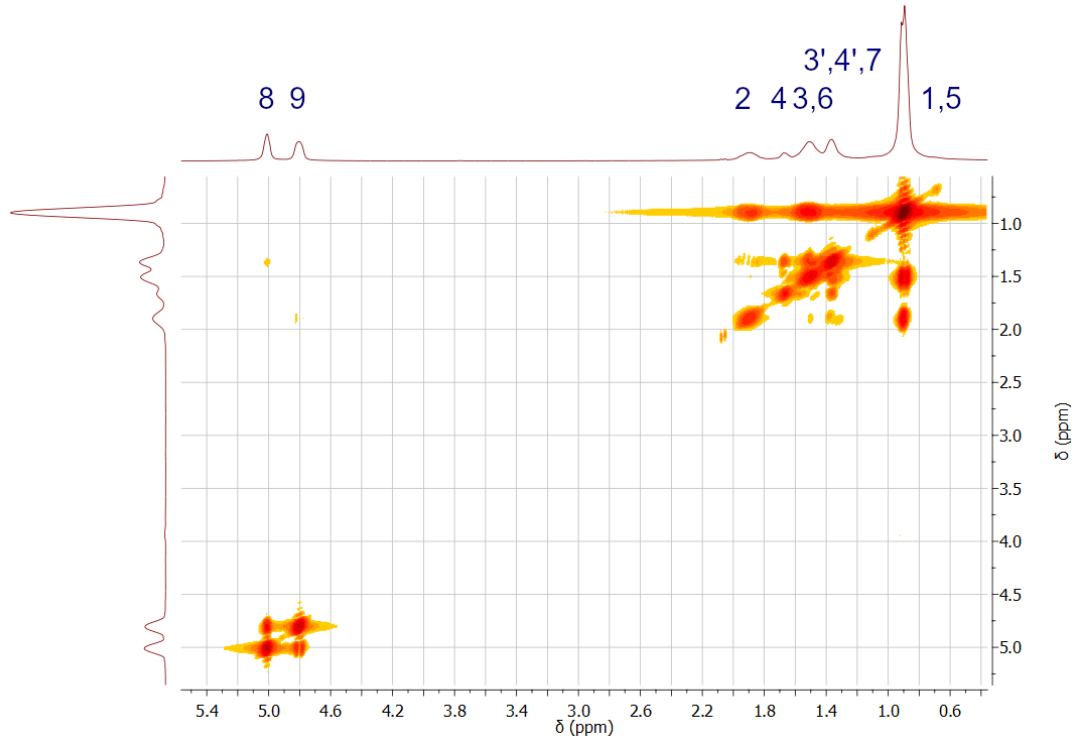

Figure 31. COSY NMR spectrum of PMenC.

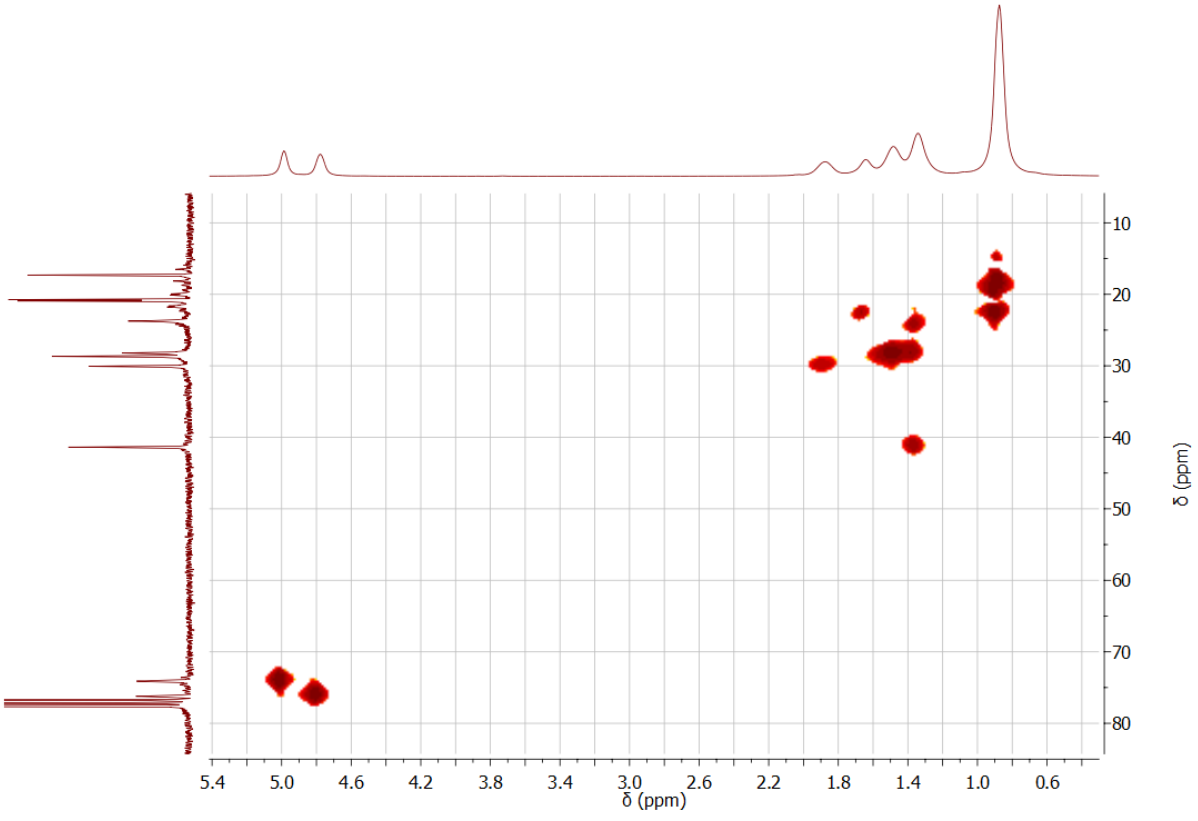

Figure 32. HMQC NMR spectrum of PMenC.

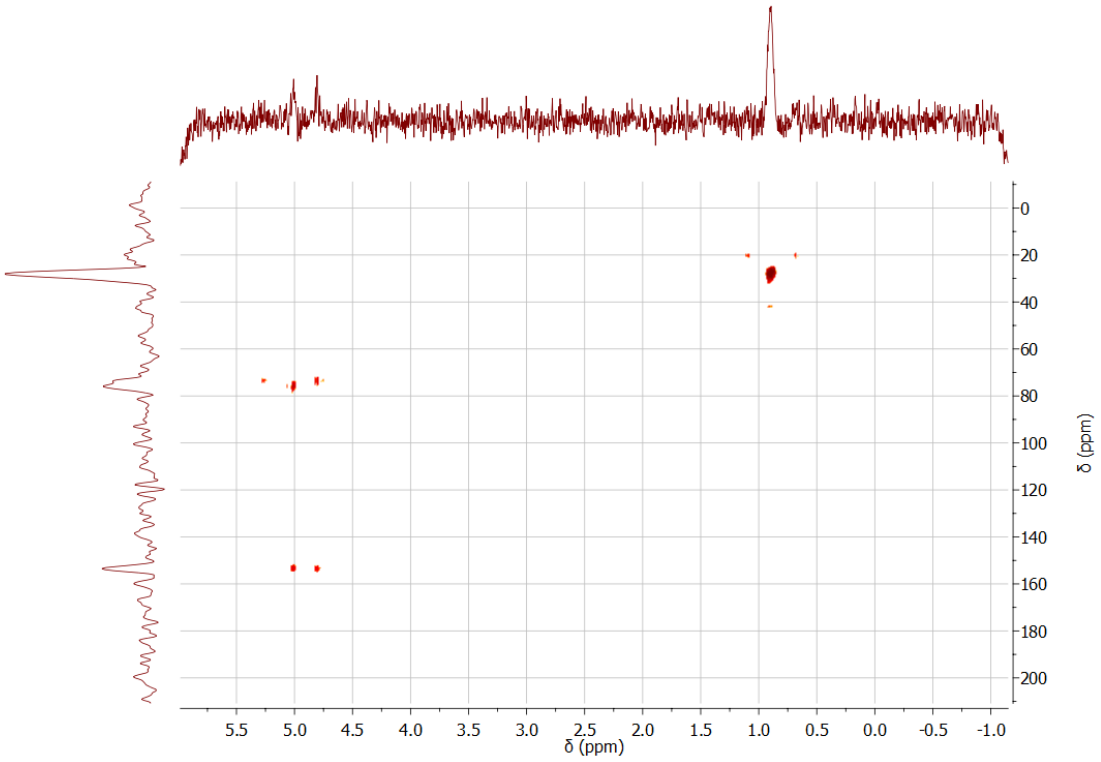

Figure 33. HMBC NMR spectrum of PMenC.

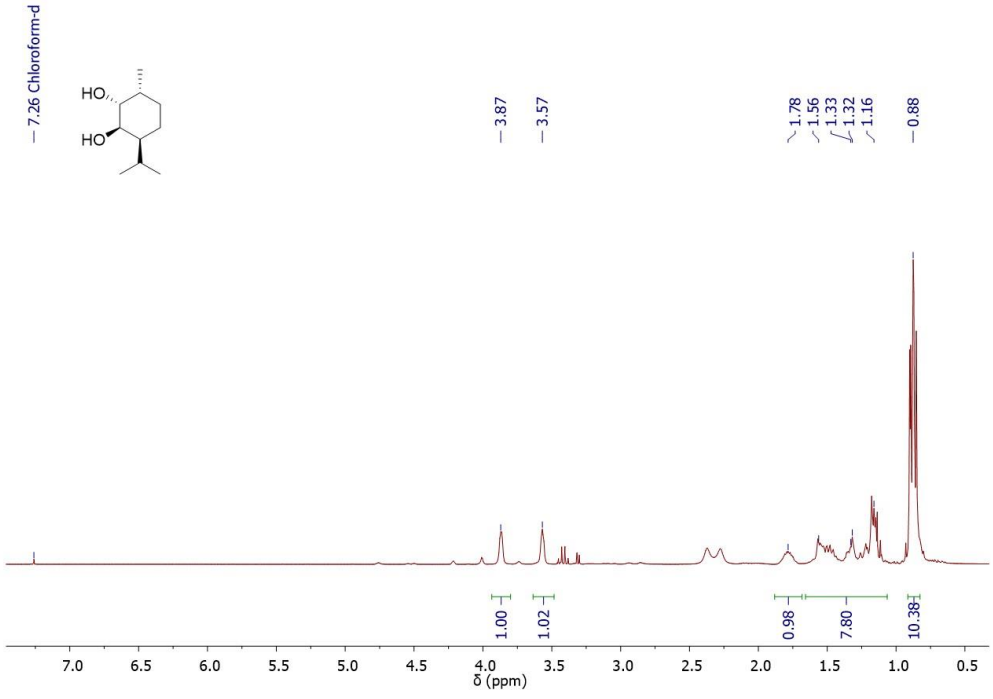

Figure 34. Crude reaction mixture of the hydrolysis marked with the signals of the (1R,2R,3S,6R)-diastereomer of menthandiol. Reprinted with permission from Wambach, A.; Agarwal, S.; Greiner, A. Synthesis of Biobased Polycarbonate by Copolymerization of Menth-2-ene Oxide and CO_2 with Exceptional Thermal Stability. ACS Sustainable Chem. Eng. ***2020****, 8 (39), 14690–14693. Copyright 2020 American Chemical Society.*

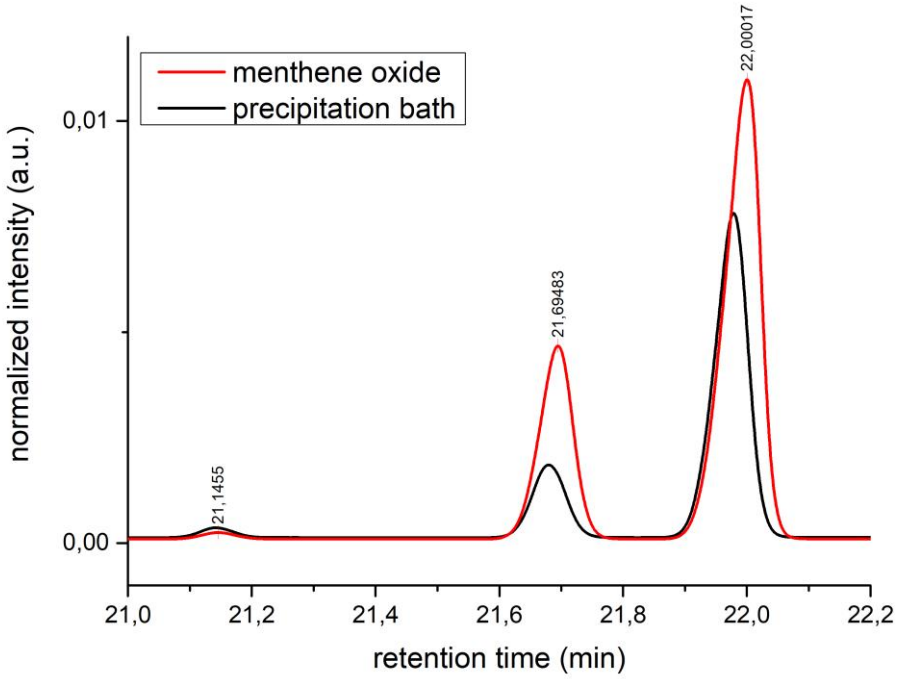

Figure 35. Gas chromatograms of menthene oxide and the precipitation bath after the reaction. Reprinted with permission from Wambach, A.; Agarwal, S.; Greiner, A. Synthesis of Biobased Polycarbonate by Copolymerization of Menth-2-ene Oxide and CO_2 with Exceptional Thermal Stability. ACS Sustainable Chem. Eng. ***2020****, 8 (39), 14690–14693. Copyright 2020 American Chemical Society.*

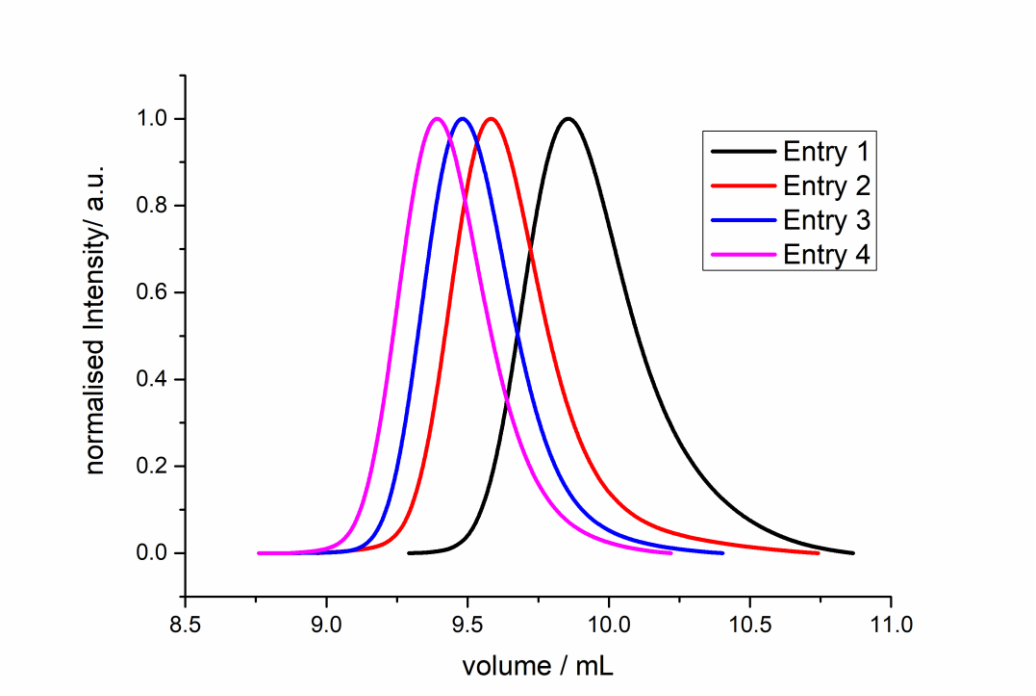

Figure 36. Chromatograms of Table 1, Entries 1-4. Adapted with permission from Wambach, A.; Agarwal, S.; Greiner, A. Synthesis of Biobased Polycarbonate by Copolymerization of Menth-2-ene Oxide and CO_2 with Exceptional Thermal Stability. ACS Sustainable Chem. Eng. ***2020****, 8 (39), 14690–14693. Copyright 2020 American Chemical Society.*

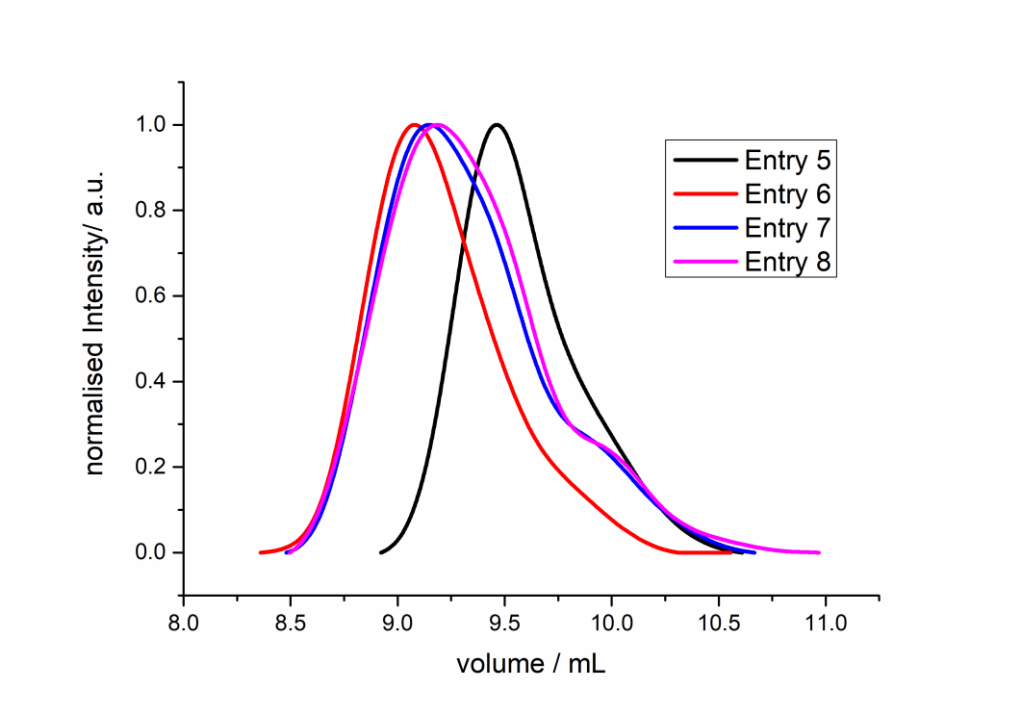

Figure 37. Chromatograms of Table 1, Entries 5-8. Adapted with permission from Wambach, A.; Agarwal, S.; Greiner, A. Synthesis of Biobased Polycarbonate by Copolymerization of Menth-2-ene Oxide and CO_2 with Exceptional Thermal Stability. ACS Sustainable Chem. Eng. ***2020****, 8 (39), 14690–14693. Copyright 2020 American Chemical Society.*

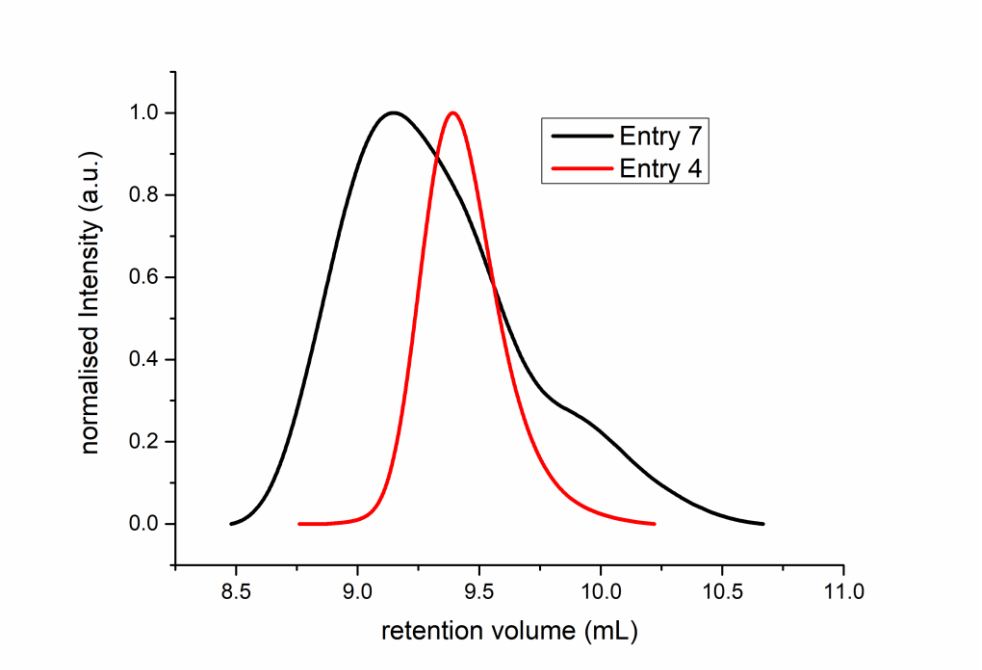

Figure 38. Comparison of the GPC traces obtained from the PMenC synthesis in bulk (black) and in solution (red). Adapted with permission from Wambach, A.; Agarwal, S.; Greiner, A. Synthesis of Biobased Polycarbonate by Copolymerization of Menth-2-ene Oxide and CO_2 with Exceptional Thermal Stability. ACS Sustainable Chem. Eng. ***2020****, 8 (39), 14690–14693. Copyright 2020 American Chemical Society.*

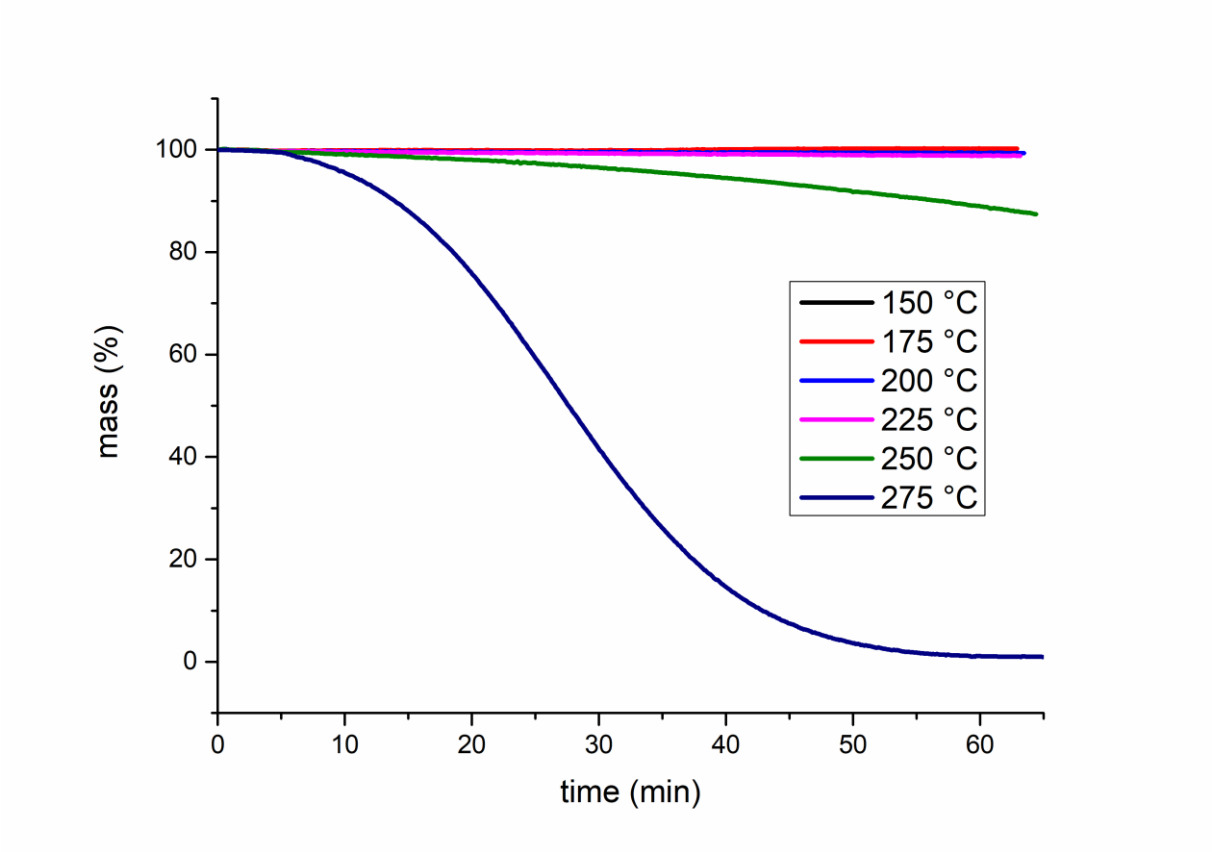

Figure 39. Isotherms of PMenC at temperatures between 150 °C and 275 °C.

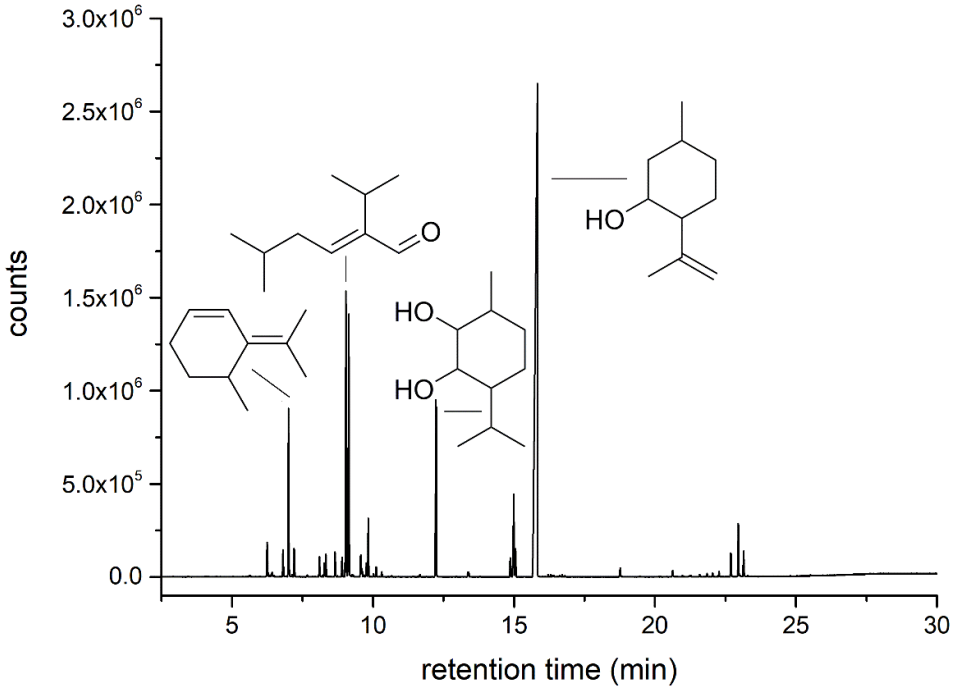

Figure 40. Gas chromatogram of the pyrolysis product of PMenC labeled with the compounds found by MS.

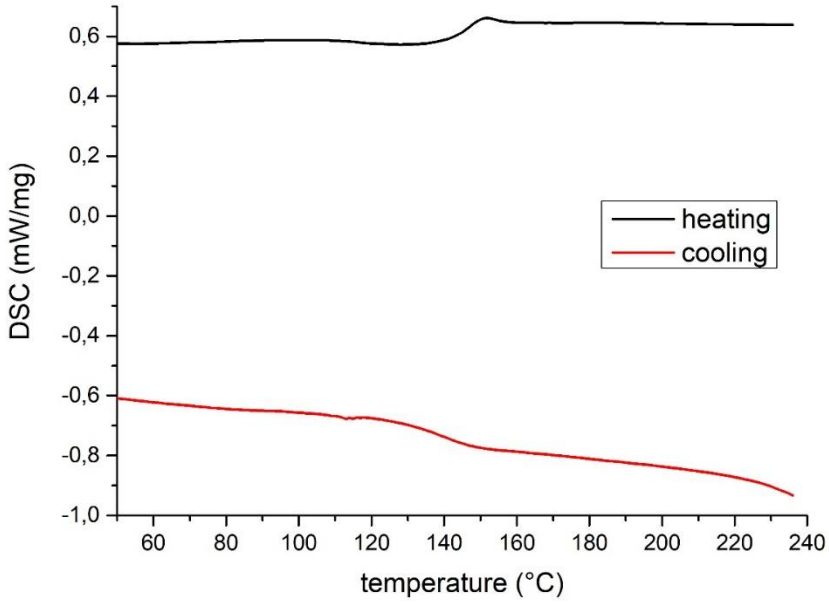

Figure 41. DSC curve of PMenC (endo up). Reprinted with permission from Wambach, A.; Agarwal, S.; Greiner, A. Synthesis of Biobased Polycarbonate by Copolymerization of Menth-2-ene Oxide and CO_2 with Exceptional Thermal Stability. ACS Sustainable Chem. Eng. ***2020****, 8 (39), 14690–14693. Copyright 2020 American Chemical Society.*

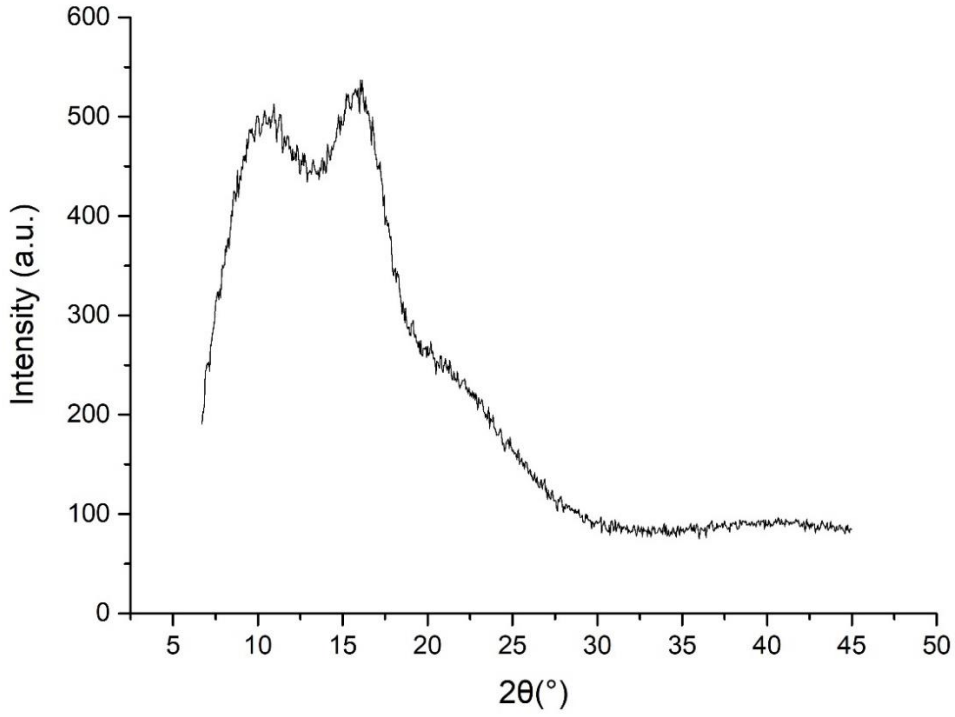

Figure 42. WAXS diffractogram of PMenC. Reprinted with permission from Wambach, A.; Agarwal, S.; Greiner, A. Synthesis of Biobased Polycarbonate by Copolymerization of Menth-2-ene Oxide and CO_2 with Exceptional Thermal Stability. ACS Sustainable Chem. Eng. ***2020****, 8 (39), 14690–14693. Copyright 2020 American Chemical Society.*

Figure 43. Scattered specimen obtained from melt pressing of PMenC.

10.2 Supplementary Data for Chapter 5.1.3

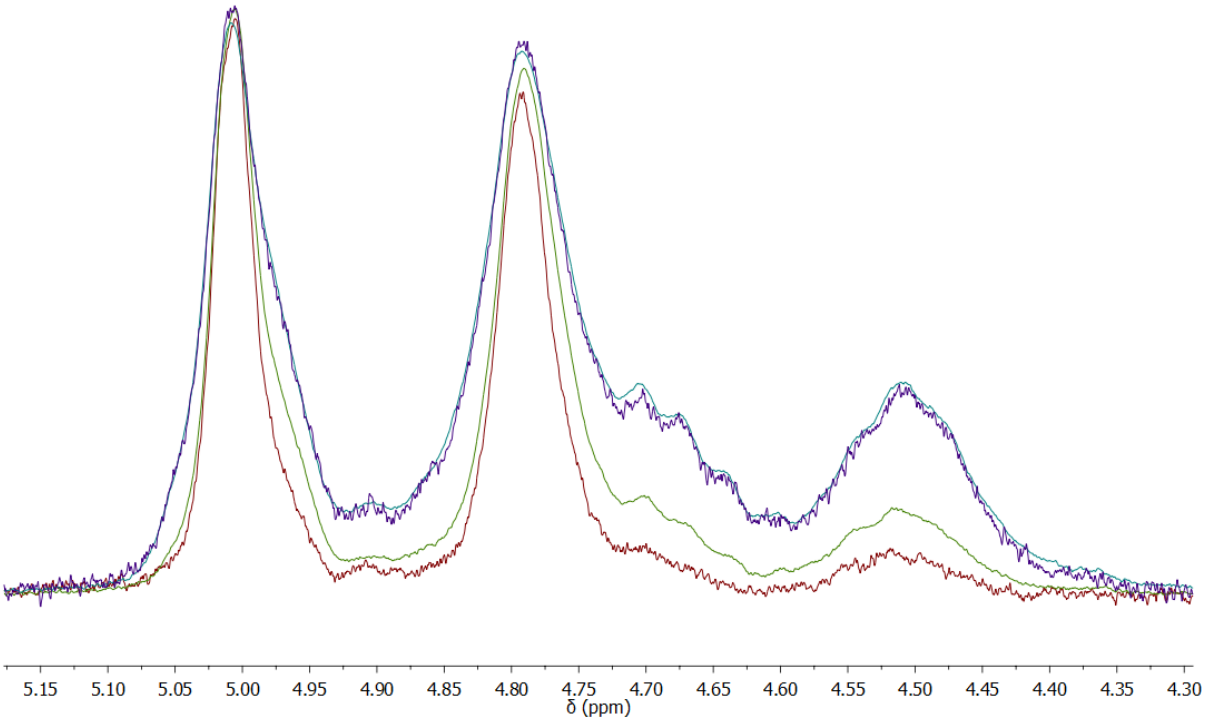

Figure 44. Differences in the ^{1}H NMR of PMenC synthesized with TEB at 60 (red), 80 (green), 100 (cyan) and 120 °C (blue).

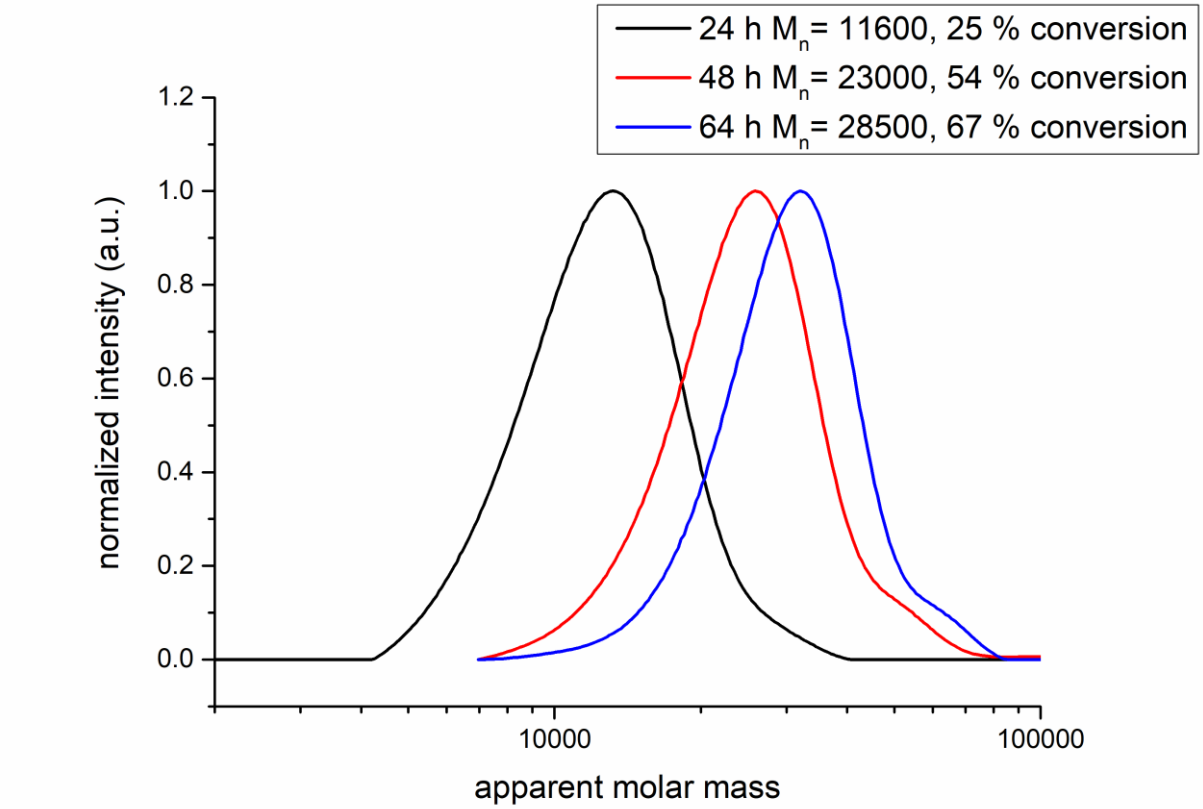

Figure 45. Apparent molar mass distributions during a copolymerization of MenO and CO_2 catalyzed by TEB. Samples were taken at 24 h (black), 48 h (red) and 64 h (blue).

10.3 Supplementary Data for Chapter 5.2

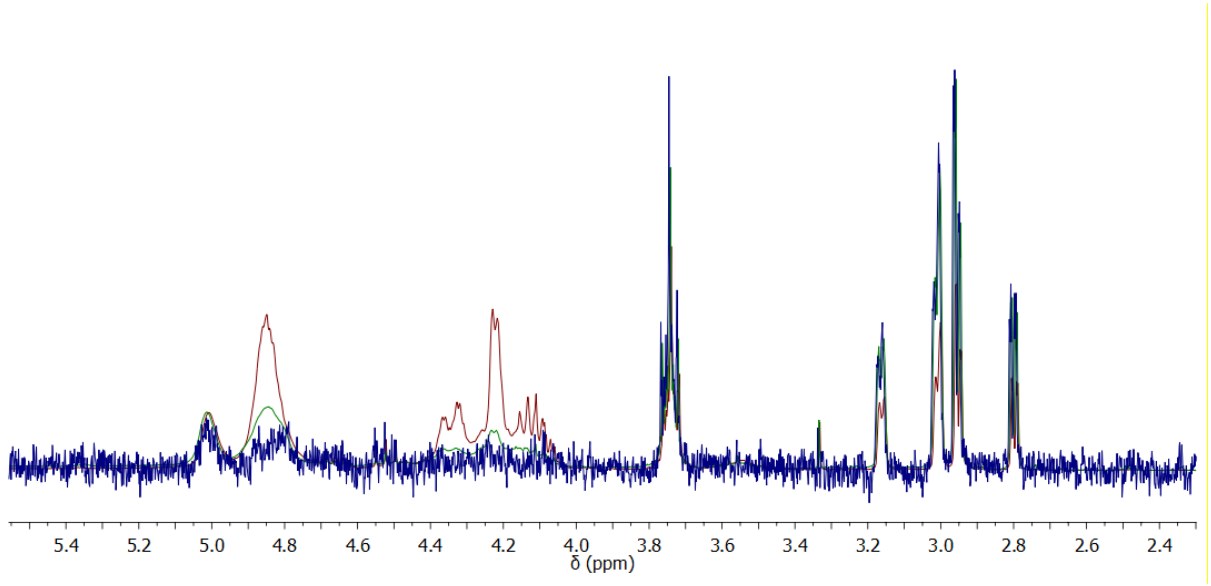

Figure 46. ^1H NMR spectra of the reaction mixtures of PMenBC with 50 (red), 20 (green) or 10% (blue) BO in the feedstock.

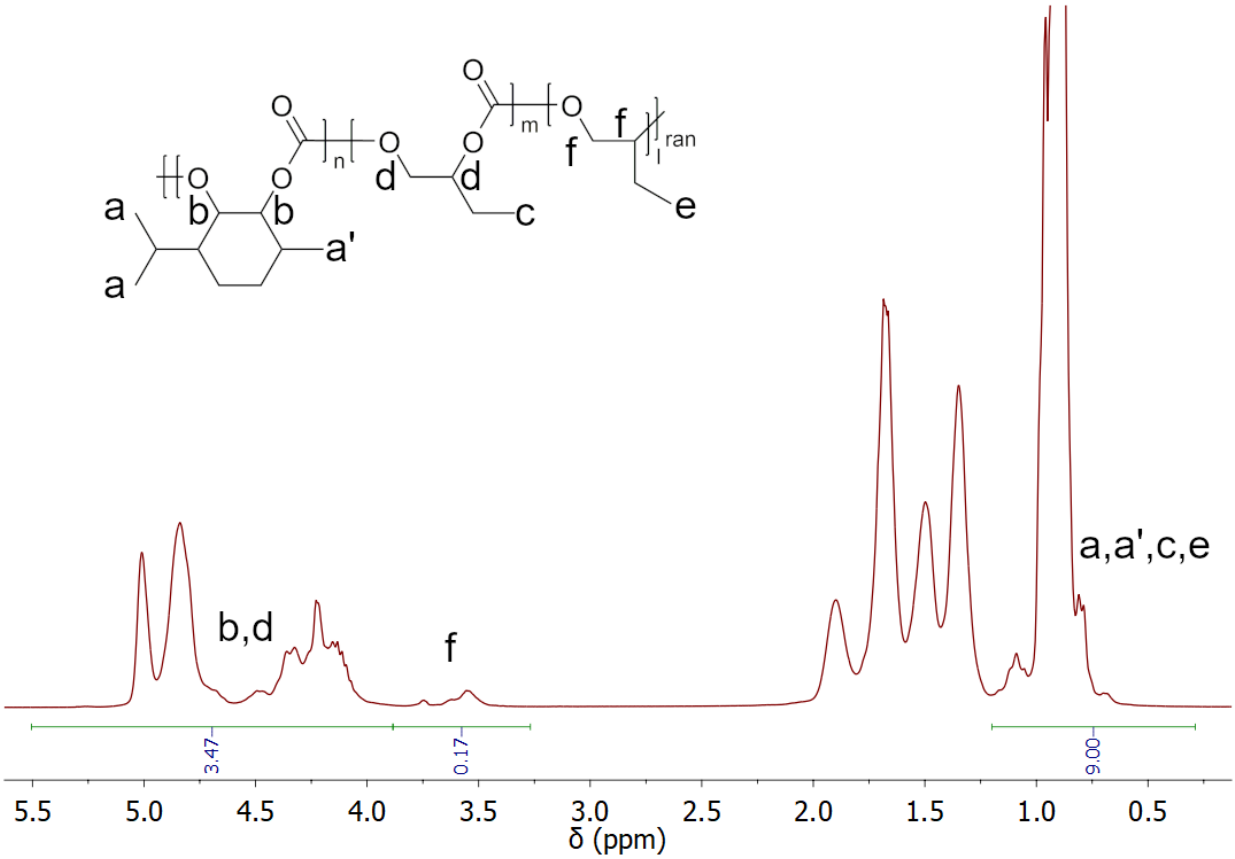

Figure 47. ^{1}H NMR spectrum of Table 6, Entry 3 with the assignment of the major peaks. Determination of the composition according to Formulas 1-4.

$$n(PMenC) = \frac{M-C-E}{7} \quad with\ M = I(a,a',c,e), C = I(b,d)\ and\ E = I(f) \tag{1}$$

$$n(PBC) = \frac{C-2\,n(PMenC)}{3} \tag{2}$$

$$n(PBO) = \frac{E}{3} \tag{3}$$

$$x(PMenC) = \frac{n(PMenC)}{\sum n} \tag{4}$$

$$T_g(Fox) = \frac{1}{\sum_{i=0}^{n} \frac{\omega(i)}{T_g(i)}} \tag{5}$$

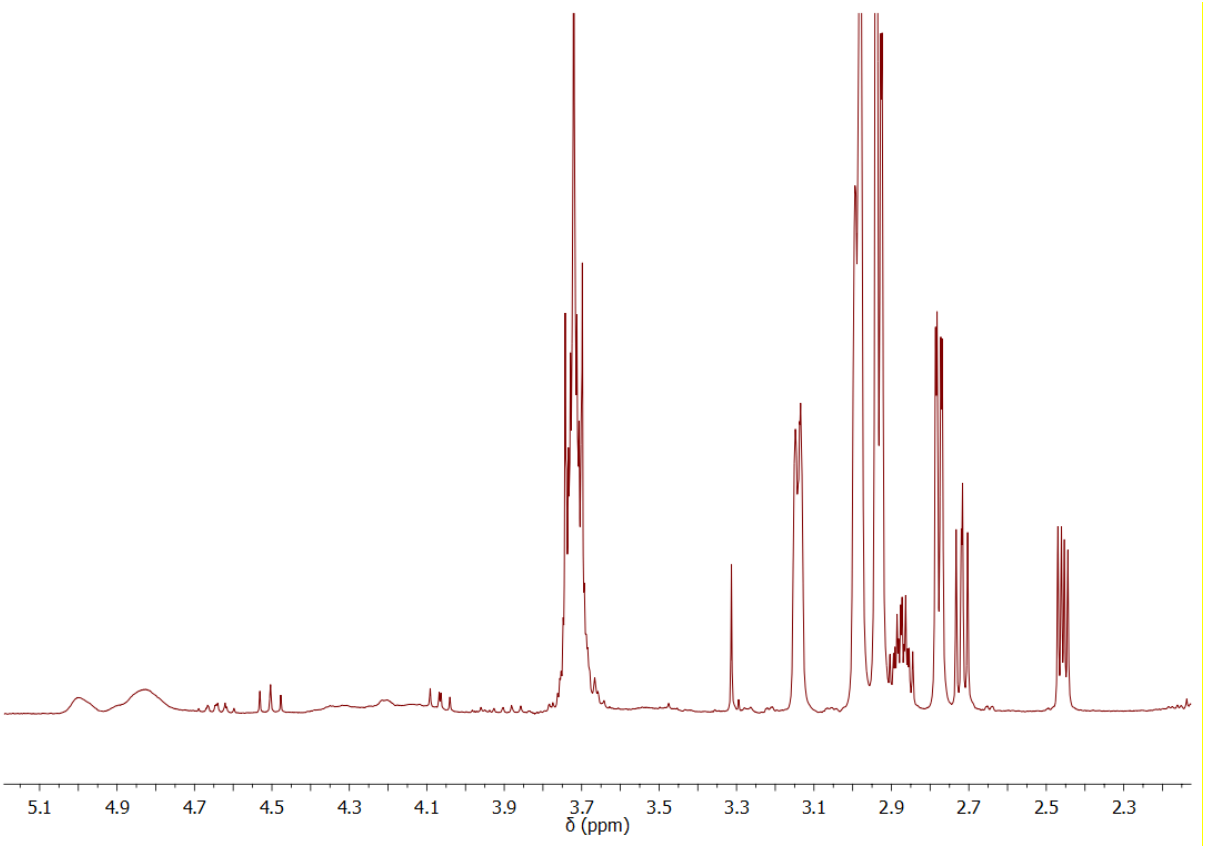

Figure 48. ^{1}H NMR of a reaction mixture of the terpolymerization of PMenBC with incomplete conversion.

10.4 Supplementary Data for Chapter 5.3

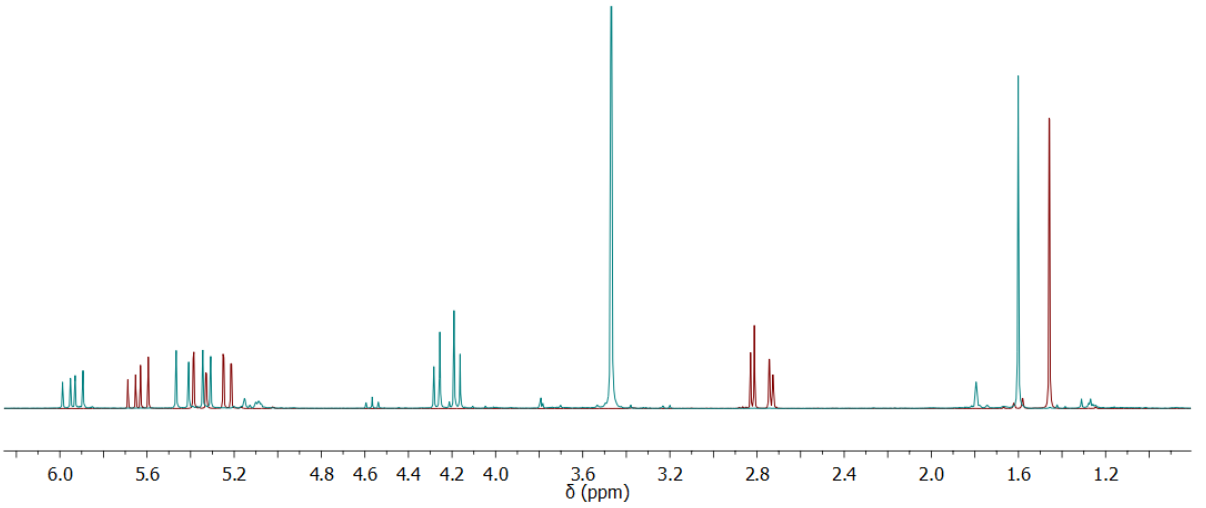

Figure 49. Comparison of the ^{1}H NMR spectra of isoprene oxide (red) and the product of the reaction with CO_2 (cyan).

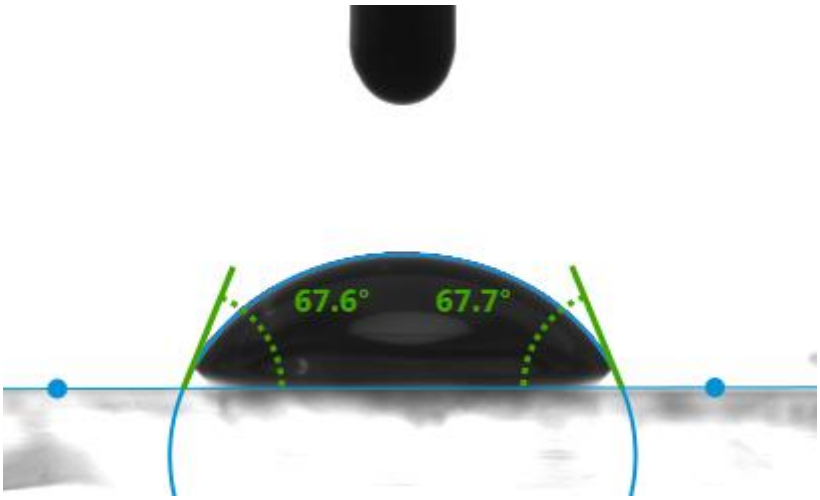

Figure 50. Contact angle measurement of water on a plasma-treated low T_g PMenC surface.

10.5 Supplementary Data for Chapter 5.4

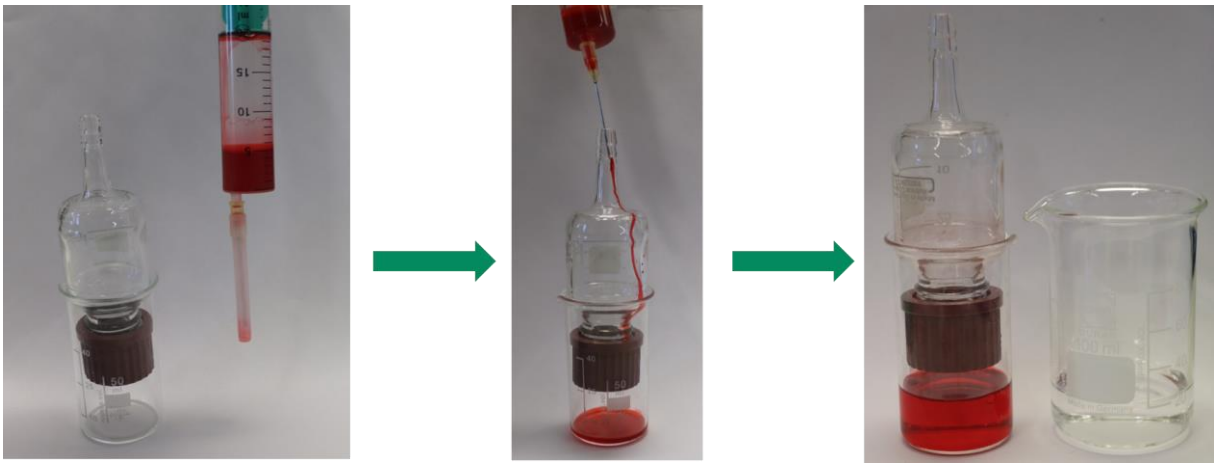

Figure 51. Separation of DCM (red) and water with an electrospun membrane of crosslinked PMenBC.

11 References

(1) UN General Assembly. https://www.unfpa.org/sites/default/files/resourc-pdf/Resolution_A_RES_70_1_EN.pdf (accessed 2021-12-16).

(2) https://www.bp.com/content/dam/bp/business-sites/en/global/corporate/pdfs/energy-economics/statistical-review/bp-stats-review-2021-full-report.pdf (accessed 2021-12-16).

(3) https://woo.opec.org/chapter.php?chapterNr=207&tableID=202 (accessed 2021-12-16).

(4) https://plasticseurope.org/wp-content/uploads/2021/09/Plastics_the_facts-WEB-2020_versionJun21final.pdf (accessed 2021-12-16).

(5) https://www.european-bioplastics.org/wp-content/uploads/2019/11/Report_Bioplastics-Market-Data_2019_short_version.pdf (accessed 2021-12-16).

(6) European Bioplastics. *Report Bioplastics*. https://docs.european-bioplastics.org/publications/market_data/Report_Bioplastics_Market_Data_2021_short_version.pdf (accessed 2022-01-06).

(7) Zhang, M.; Yu, Y. Dehydration of Ethanol to Ethylene. *Ind. Eng. Chem. Res.* **2013**, *52* (28), 9505–9514. DOI: 10.1021/ie401157c.

(8) Pang, J.; Zheng, M.; Sun, R.; Wang, A.; Wang, X.; Zhang, T. Synthesis of ethylene glycol and terephthalic acid from biomass for producing PET. *Green Chem.* **2016**, *18* (2), 342–359. DOI: 10.1039/C5GC01771H.

(9) Auras, R.; Harte, B.; Selke, S. An overview of polylactides as packaging materials. *Macromol. Biosci.* **2004**, *4* (9), 835–864. DOI: 10.1002/mabi.200400043.

(10) Stempfle, F.; Ortmann, P.; Mecking, S. Long-Chain Aliphatic Polymers To Bridge the Gap between Semicrystalline Polyolefins and Traditional Polycondensates. *Chem. Rev.* **2016**, *116* (7), 4597–4641. DOI: 10.1021/acs.chemrev.5b00705.

(11) Häußler, M.; Eck, M.; Rothauer, D.; Mecking, S. Closed-loop recycling of polyethylene-like materials. *Nature* **2021**, *590* (7846), 423–427. DOI: 10.1038/s41586-020-03149-9.

(12) Zhu, Y.; Romain, C.; Williams, C. K. Sustainable polymers from renewable resources. *Nature* **2016**, *540* (7633), 354–362. DOI: 10.1038/nature21001.

(13) Satoh, K.; Nakahara, A.; Mukunoki, K.; Sugiyama, H.; Saito, H.; Kamigaito, M. Sustainable cycloolefin polymer from pine tree oil for optoelectronics material:

living cationic polymerization of β-pinene and catalytic hydrogenation of high-molecular-weight hydrogenated poly(β-pinene). *Polym. Chem.* **2014**, *5* (9), 3222–3230. DOI: 10.1039/C3PY01320K.

(14) Sharma, S.; Srivastava, A. K. Alternating Copolymers of Limonene with Methyl Methacrylate: Kinetics and Mechanism. *J. Macromol. Sci., Part A* **2003**, *40* (6), 593–603. DOI: 10.1081/MA-120020867.

(15) Hillmyer, M. A.; Tolman, W. B. Aliphatic polyester block polymers: renewable, degradable, and sustainable. *Acc. Chem. Res.* **2014**, *47* (8), 2390–2396. DOI: 10.1021/ar500121d.

(16) Byrne, C. M.; Allen, S. D.; Lobkovsky, E. B.; Coates, G. W. Alternating copolymerization of limonene oxide and carbon dioxide. *J. Am. Chem. Soc.* **2004**, *126* (37), 11404–11405. DOI: 10.1021/ja0472580.

(17) Hauenstein, O.; Reiter, M.; Agarwal, S.; Rieger, B.; Greiner, A. Bio-based polycarbonate from limonene oxide and CO_2 with high molecular weight, excellent thermal resistance, hardness and transparency. *Green Chem.* **2016**, *18* (3), 760–770. DOI: 10.1039/C5GC01694K.

(18) Einhorn, A. Ueber die Carbonate der Dioxybenzole. *Justus Liebigs Ann. Chem.* **1898**, *300* (2), 135–155. DOI: 10.1002/jlac.18983000202.

(19) Abts, G.; Eckel, T.; Wehrmann, R. Polycarbonates. In *Ullmann's Encyclopedia of Industrial Chemistry*; Wiley-VCH Verlag GmbH & Co. KGaA, 2000; pp 1–18. DOI: 10.1002/14356007.a21_207.pub2.

(20) Schnell, H. Linear Aromatic Polyesters of Carbonic Acid. *Ind. Eng. Chem.* **1959**, *51* (2), 157–160. DOI: 10.1021/ie50590a038.

(21) Schnell, H. Polycarbonate, eine Gruppe neuartiger thermoplastischer Kunststoffe. Herstellung und Eigenschaften aromatischer Polyester der Kohlensäure. *Angew. Chem.* **1956**, *68* (20), 633–640. DOI: 10.1002/ange.19560682002.

(22) LeGrand, D. G.; Bendler, J. T., Eds. *Handbook of polycarbonate science and technology*; Plastics engineering, Vol. 56; Marcel Dekker, 2000.

(23) Freitag, D.; Fengler, G.; Morbitzer, L. Routes to New Aromatic Polycarbonates with Special Material Properties. *Angew. Chem. Int. Ed.* **1991**, *30* (12), 1598–1610. DOI: 10.1002/anie.199115981.

(24) Zhu, W.; Huang, X.; Li, C.; Xiao, Y.; Zhang, D.; Guan, G. High-molecular-weight aliphatic polycarbonates by melt polycondensation of dimethyl carbonate and

aliphatic diols: synthesis and characterization. *Polym. Int.* **2011**, *60* (7), 1060–1067. DOI: 10.1002/pi.3043.

(25) *MSC unanimously agrees that Bisphenol A is an endocrine disruptor*. https://echa.europa.eu/-/msc-unanimously-agrees-that-bisphenol-a-is-an-endocrine-disruptor (accessed 2022-01-06).

(26) Mirmira, P.; Evans-Molina, C. Bisphenol A, obesity, and type 2 diabetes mellitus: genuine concern or unnecessary preoccupation? *Transl. Res.* **2014**, *164* (1), 13–21. DOI: 10.1016/j.trsl.2014.03.003.

(27) Xin, Y.; Uyama, H. Synthesis of new bio-based polycarbonates derived from terpene. *J. Polym. Res.* **2012**, *19* (12), 1–7. DOI: 10.1007/s10965-012-0015-2.

(28) Xia, H.; Suo, Z. Y.; Qiang, G. J.; Chang, C. J. Synthesis, characterization, and degradation of a novel L-tyrosine-derived polycarbonate for potential biomaterial applications. *J. Appl. Polym. Sci.* **2008**, *110* (4), 2168–2178. DOI: 10.1002/app.28755.

(29) Yokoe, M.; Aoi, K.; Okada, M. Biodegradable polymers based on renewable resources. IX. Synthesis and degradation behavior of polycarbonates based on 1,4:3,6-dianhydrohexitols and tartaric acid derivatives with pendant functional groups. *J. Polym. Sci. A Polym. Chem.* **2005**, *43* (17), 3909–3919. DOI: 10.1002/pola.20830.

(30) Park, J. E.; Kim, W. K.; Da Hwang, Y.; Choi, G. H.; Suh, D. H. Thermally Stable Bio-Based Aliphatic Polycarbonates with Quadra-Cyclic Diol from Renewable Sources. *Macromol. Res.* **2018**, *26* (3), 246–253. DOI: 10.1007/s13233-018-6038-8.

(31) Chatti, S.; Kricheldorf, H. R.; Schwarz, G. Copolycarbonates of isosorbide and various diols. *J. Polym. Sci. A Polym. Chem.* **2006**, *44* (11), 3616–3628. DOI: 10.1002/pola.21444.

(32) Metzger, E. D.; Brozek, C. K.; Comito, R. J.; Dincă, M. Selective Dimerization of Ethylene to 1-Butene with a Porous Catalyst. *ACS Cent. Sci.* **2016**, *2* (3), 148–153. DOI: 10.1021/acscentsci.6b00012.

(33) McGuinness, D. S. Olefin oligomerization via metallacycles: dimerization, trimerization, tetramerization, and beyond. *Chem. Rev.* **2011**, *111* (3), 2321–2341. DOI: 10.1021/cr100217q.

(34) Briggs, J. R. The selective trimerization of ethylene to hex-1-ene. *J. Chem. Soc., Chem. Commun.* **1989** (11), 674. DOI: 10.1039/c39890000674.

(35) Bollmann, A.; Blann, K.; Dixon, J. T.; Hess, F. M.; Killian, E.; Maumela, H.; McGuinness, D. S.; Morgan, D. H.; Neveling, A.; Otto, S.; Overett, M.; Slawin, A. M. Z.; Wasserscheid, P.; Kuhlmann, S. Ethylene tetramerization: a new route to produce 1-octene in exceptionally high selectivities. *J. Am. Chem. Soc.* **2004**, *126* (45), 14712–14713. DOI: 10.1021/ja045602n.

(36) Okada, A.; Kikuchi, S.; Nakano, K.; Nishioka, K.; Nozaki, K.; Yamada, T. New Class of Catalysts for Alternating Copolymerization of Alkylene Oxide and Carbon Dioxide. *Chem. Lett.* **2010**, *39* (10), 1066–1068. DOI: 10.1246/cl.2010.1066.

(37) Langanke, J.; Wolf, A.; Hofmann, J.; Böhm, K.; Subhani, M. A.; Müller, T. E.; Leitner, W.; Gürtler, C. Carbon dioxide (CO_2) as sustainable feedstock for polyurethane production. *Green Chem.* **2014**, *16* (4), 1865–1870. DOI: 10.1039/C3GC41788C.

(38) Zhang, X.-H.; Wei, R.-J.; Zhang, Y.; Du, B.-Y.; Fan, Z.-Q. Carbon Dioxide/Epoxide Copolymerization via a Nanosized Zinc–Cobalt(III) Double Metal Cyanide Complex: Substituent Effects of Epoxides on Polycarbonate Selectivity, Regioselectivity and Glass Transition Temperatures. *Macromolecules* **2015**, *48* (3), 536–544. DOI: 10.1021/ma5023742.

(39) Nakano, K.; Kamada, T.; Nozaki, K. Selective formation of polycarbonate over cyclic carbonate: copolymerization of epoxides with carbon dioxide catalyzed by a cobalt(III) complex with a piperidinium end-capping arm. *Angew. Chem. Int. Ed.* **2006**, *45* (43), 7274–7277. DOI: 10.1002/anie.200603132.

(40) Seong, J. E.; Na, S. J.; Cyriac, A.; Kim, B.-W.; Lee, B. Y. Terpolymerizations of CO_2 , Propylene Oxide, and Various Epoxides Using a Cobalt(III) Complex of Salen-Type Ligand Tethered by Four Quaternary Ammonium Salts. *Macromolecules* **2010**, *43* (2), 903–908. DOI: 10.1021/ma902162n.

(41) Shaarani, F. W.; Bou, J. J. Synthesis of vegetable-oil based polymer by terpolymerization of epoxidized soybean oil, propylene oxide and carbon dioxide. *Sci. Total Environ.* **2017**, *598*, 931–936. DOI: 10.1016/j.scitotenv.2017.04.184.

(42) Bell, B. M.; Briggs, J. R.; Campbell, R. M.; Chambers, S. M.; Gaarenstroom, P. D.; Hippler, J. G.; Hook, B. D.; Kearns, K.; Kenney, J. M.; Kruper, W. J.; Schreck, D. J.; Theriault, C. N.; Wolfe, C. P. Glycerin as a Renewable Feedstock for Epichlorohydrin Production. The GTE Process. *Clean Soil Air Water* **2008**, *36* (8), 657–661. DOI: 10.1002/clen.200800067.

(43) Wei, R.-J.; Zhang, X.-H.; Du, B.-Y.; Fan, Z.-Q.; Qi, G.-R. Selective production of poly(carbonate–co–ether) over cyclic carbonate for epichlorohydrin and CO_2 copolymerization via heterogeneous catalysis of Zn–Co (III) double metal cyanide complex. *Polymer* **2013**, *54* (23), 6357–6362. DOI: 10.1016/j.polymer.2013.09.040.

(44) Wu, G.-P.; Xu, P.-X.; Lu, X.-B.; Zu, Y.-P.; Wei, S.-H.; Ren, W.-M.; Darensbourg, D. J. Crystalline CO_2 Copolymer from Epichlorohydrin via Co(III)-Complex-Mediated Stereospecific Polymerization. *Macromolecules* **2013**, *46* (6), 2128–2133. DOI: 10.1021/ma400252h.

(45) Yang, G.-W.; Xu, C.-K.; Xie, R.; Zhang, Y.-Y.; Zhu, X.-F.; Wu, G.-P. Pinwheel-Shaped Tetranuclear Organoboron Catalysts for Perfectly Alternating Copolymerization of CO_2 and Epichlorohydrin. *J. Am. Chem. Soc.* **2021**, *143* (9), 3455–3465. DOI: 10.1021/jacs.0c12425.

(46) Hilf, J.; Scharfenberg, M.; Poon, J.; Moers, C.; Frey, H. Aliphatic polycarbonates based on carbon dioxide, furfuryl glycidyl ether, and glycidyl methyl ether: reversible functionalization and cross-linking. *Macromol. Rapid Commun.* **2015**, *36* (2), 174–179. DOI: 10.1002/marc.201400504.

(47) Hu, Y.; Qiao, L.; Qin, Y.; Zhao, X.; Chen, X.; Wang, X.; Wang, F. Synthesis and Stabilization of Novel Aliphatic Polycarbonate from Renewable Resource. *Macromolecules* **2009**, *42* (23), 9251–9254. DOI: 10.1021/ma901791a.

(48) Darensbourg, D. J.; Chung, W.-C.; Arp, C. J.; Tsai, F.-T.; Kyran, S. J. Copolymerization and Cycloaddition Products Derived from Coupling Reactions of 1,2-Epoxy-4-cyclohexene and Carbon Dioxide. Postpolymerization Functionalization via Thiol–Ene Click Reactions. *Macromolecules* **2014**, *47* (21), 7347–7353. DOI: 10.1021/ma501781k.

(49) Honda, S.; Mori, T.; Goto, H.; Sugimoto, H. Carbon-dioxide-derived unsaturated alicyclic polycarbonate: Synthesis, characterization, and post-polymerization modification. *Polymer* **2014**, *55* (19), 4832–4836. DOI: 10.1016/j.polymer.2014.08.002.

(50) Hauenstein, O.; Agarwal, S.; Greiner, A. Bio-based polycarbonate as synthetic toolbox. *Nat. Commun.* **2016**, *7* (1), 11862. DOI: 10.1038/ncomms11862.

(51) Stößer, T.; Li, C.; Unruangsri, J.; Saini, P. K.; Sablong, R. J.; Meier, M. A. R.; Williams, C. K.; Koning, C. Bio-derived polymers for coating applications:

comparing poly(limonene carbonate) and poly(cyclohexadiene carbonate). *Polym. Chem.* **2017**, *8* (39), 6099–6105. DOI: 10.1039/C7PY01223C.

(52) Kindermann, N.; Cristòfol, À.; Kleij, A. W. Access to Biorenewable Polycarbonates with Unusual Glass-Transition Temperature (T_g) Modulation. *ACS Catal.* **2017**, *7* (6), 3860–3863. DOI: 10.1021/acscatal.7b00770.

(53) Li, C.; Johansson, M.; Sablong, R. J.; Koning, C. E. High performance thiol-ene thermosets based on fully bio-based poly(limonene carbonate)s. *Eur. Polym. J.* **2017**, *96*, 337–349. DOI: 10.1016/j.eurpolymj.2017.09.034.

(54) Inoue, S.; Koinuma, H.; Tsuruta, T. Copolymerization of carbon dioxide and epoxide. *J. Polym. Sci. B Polym. Lett.* **1969**, *7* (4), 287–292. DOI: 10.1002/pol.1969.110070408.

(55) Kuran, W.; Pasynkiewicz, S.; Skupińska, J. Investigations on the Catalytic Systems Diethylzinc/Di- and Trihydroxybenzenes in the Copolymerization of Carbon Dioxide with Propylene Oxide. *Makromol. Chem.* **1976**, *177* (5), 1283–1292. DOI: 10.1002/macp.1976.021770505.

(56) Kuran, W.; Pasynkiewicz, S.; Skupińska, J. Organozinc Catalyst Systems for the Copolymerization of Carbon Dioxide with Propylene Oxide. *Makromol. Chem.* **1977**, *178* (1), 47–54. DOI: 10.1002/macp.1977.021780106.

(57) Kobayashi, M.; Tang, Y.-L.; Tsuruta, T.; Inoue, S. Copolymerization of carbon dioxide and epoxide using dialkylzinc/dihydric phenol system as catalyst. *Makromol. Chem.* **1973**, *169* (1), 69–81. DOI: 10.1002/macp.1973.021690107.

(58) Inoue, S.; Kobayashi, M.; Koinuma, H.; Tsuruta, T. Reactivities of some organozinc initiators for copolymerization of carbon dioxide and propylene oxide. *Makromol. Chem.* **1972**, *155* (1), 61–73. DOI: 10.1002/macp.1972.021550107.

(59) Sugimoto, H.; Inoue, S. Copolymerization of carbon dioxide and epoxide. *J. Polym. Sci. A Polym. Chem.* **2004**, *42* (22), 5561–5573. DOI: 10.1002/pola.20319.

(60) Varghese, J. K.; Park, D. S.; Jeon, J. Y.; Lee, B. Y. Double metal cyanide catalyst prepared using H 3 Co(CN) 6 for high carbonate fraction and molecular weight control in carbon dioxide/propylene oxide copolymerization. *J. Polym. Sci. A Polym. Chem.* **2013**, *51* (22), 4811–4818. DOI: 10.1002/pola.26905.

(61) Kim, I.; Yi, M. J.; Lee, K. J.; Park, D.-W.; Kim, B. U.; Ha, C.-S. Aliphatic polycarbonate synthesis by copolymerization of carbon dioxide with epoxides

over double metal cyanide catalysts prepared by using ZnX_2 (X=F, Cl, Br, I). *Catal. Today* **2006**, *111* (3-4), 292–296. DOI: 10.1016/j.cattod.2005.10.039.

(62) Soga, K.; Imai, E.; Hattori, I. Alternating Copolymerization of CO_2 and Propylene Oxide with the Catalysts Prepared from $Zn(OH)_2$ and Various Dicarboxylic Acids. *Polym. J.* **1981**, *13* (4), 407–410. DOI: 10.1295/polymj.13.407.

(63) Ree, M.; Bae, J. Y.; Jung, J. H.; Shin, T. J. A new copolymerization process leading to poly(propylene carbonate) with a highly enhanced yield from carbon dioxide and propylene oxide. *J. Polym. Sci. A Polym. Chem.* **1999**, *37* (12), 1863–1876. DOI: 10.1002/(SICI)1099-0518(19990615)37:12<1863:AID-POLA16>3.0.CO;2-K.

(64) Soga, K.; Uenishi, K.; Hosoda, S.; Ikeda, S. Copolymerization of carbon dioxide and propylene oxide with new catalysts. *Makromol. Chem.* **1977**, *178* (3), 893–897. DOI: 10.1002/macp.1977.021780325.

(65) Zhang, D.; Zhang, H.; Hadjichristidis, N.; Gnanou, Y.; Feng, X. Lithium-Assisted Copolymerization of CO_2 /Cyclohexene Oxide: A Novel and Straightforward Route to Polycarbonates and Related Block Copolymers. *Macromolecules* **2016**, *49* (7), 2484–2492. DOI: 10.1021/acs.macromol.6b00203.

(66) Koinuma, H.; Hirai, H. Copolymerization of carbon dioxide and some oxiranes by organoaluminium catalysts. *Makromol. Chem.* **1977**, *178* (5), 1283–1294. DOI: 10.1002/macp.1977.021780507.

(67) Zhang, D.; Boopathi, S. K.; Hadjichristidis, N.; Gnanou, Y.; Feng, X. Metal-Free Alternating Copolymerization of CO_2 with Epoxides: Fulfilling “Green” Synthesis and Activity. *J. Am. Chem. Soc.* **2016**, *138* (35), 11117–11120. DOI: 10.1021/jacs.6b06679.

(68) Aida, T.; Ishikawa, M.; Inoue, S. Alternating copolymerization of carbon dioxide and epoxide catalyzed by the aluminum porphyrin-quaternary organic salt or-triphenylphosphine system … *Macromolecules* **1986** (19), 8–13.

(69) Coates, G. W.; Moore, D. R. Discrete metal-based catalysts for the copolymerization of CO_2 and epoxides: discovery, reactivity, optimization, and mechanism. *Angew. Chem. Int. Ed.* **2004**, *43* (48), 6618–6639. DOI: 10.1002/anie.200460442.

(70) Kruper, W. J.; Dellar, D. D. Catalytic Formation of Cyclic Carbonates from Epoxides and CO_2 with Chromium Metalloporphyrinates. *J. Org. Chem.* **1995**, *60* (3), 725–727. DOI: 10.1021/jo00108a042.

(71) Darensbourg, D. J.; Yarbrough, J. C. Mechanistic aspects of the copolymerization reaction of carbon dioxide and epoxides, using a chiral salen chromium chloride catalyst. *J. Am. Chem. Soc.* **2002**, *124* (22), 6335–6342. DOI: 10.1021/ja012714v.

(72) Eberhardt, R.; Allmendinger, M.; Rieger, B. DMAP/Cr(III) Catalyst Ratio: The Decisive Factor for Poly(propylene carbonate) Formation in the Coupling of CO_2 and Propylene Oxide. *Macromol. Rapid Commun.* **2003**, *24* (2), 194–196. DOI: 10.1002/marc.200390022.

(73) Qin, Z.; Thomas, C. M.; Lee, S.; Coates, G. W. Cobalt-Based Complexes for the Copolymerization of Propylene Oxide and CO_2: Active and Selective Catalysts for Polycarbonate Synthesis. *Angew. Chem.* **2003**, *115* (44), 5642–5645. DOI: 10.1002/ange.200352605.

(74) Lu, X.-B.; Wang, Y. Highly active, binary catalyst systems for the alternating copolymerization of CO_2 and epoxides under mild conditions. *Angew. Chem. Int. Ed.* **2004**, *43* (27), 3574–3577. DOI: 10.1002/anie.200453998.

(75) Sujith, S.; Min, J. K.; Seong, J. E.; Na, S. J.; Lee, B. Y. A highly active and recyclable catalytic system for CO_2/propylene oxide copolymerization. *Angew. Chem. Int. Ed.* **2008**, *47* (38), 7306–7309. DOI: 10.1002/anie.200801852.

(76) Liu, J.; Ren, W.-M.; Liu, Y.; Lu, X.-B. Kinetic Study on the Coupling of CO_2 and Epoxides Catalyzed by Co(III) Complex with an Inter- or Intramolecular Nucleophilic Cocatalyst. *Macromolecules* **2013**, *46* (4), 1343–1349. DOI: 10.1021/ma302580s.

(77) Darensbourg, D. J.; Holtcamp, M. W. Catalytic Activity of Zinc(II) Phenoxides Which Possess Readily Accessible Coordination Sites. Copolymerization and Terpolymerization of Epoxides and Carbon Dioxide. *Macromolecules* **1995**, *28* (22), 7577–7579. DOI: 10.1021/ma00126a043.

(78) Darensbourg, D. J.; Wildeson, J. R.; Yarbrough, J. C. Solid-state structures of zinc(II) benzoate complexes. Catalyst precursors for the coupling of carbon dioxide and epoxides. *Inorg. Chem.* **2002**, *41* (4), 973–980. DOI: 10.1021/ic0107983.

(79) Darensbourg, D. J.; Rainey, P.; Yarbrough, J. Bis-Salicylaldiminato Complexes of Zinc. Examination of the Catalyzed Epoxide/ CO_2 Copolymerization. *Inorg. Chem.* **2001**, *40* (5), 986–993. DOI: 10.1021/ic0006403.

(80) Darensbourg, D. J.; Wildeson, J. R.; Yarbrough, J. C. Synthesis and Structures of (Dialkylamino)ethylcyclopentadienyl Derivatives of Zinc. *Organometallics* **2001**, *20* (21), 4413–4417. DOI: 10.1021/om010519j.

(81) Kim, I.; Kim, S. M.; Ha, C.-S.; Park, D.-W. Synthesis and Cyclohexene Oxide/Carbon Dioxide Copolymerizations of Zinc Acetate Complexes Bearing Bidentate Pyridine-Alkoxide Ligands. *Macromol. Rapid Commun.* **2004**, *25* (8), 888–893. DOI: 10.1002/marc.200300287.

(82) Moore, D. R.; Cheng, M.; Lobkovsky, E. B.; Coates, G. W. Mechanism of the alternating copolymerization of epoxides and CO_2 using beta-diiminate zinc catalysts: evidence for a bimetallic epoxide enchainment. *J. Am. Chem. Soc.* **2003**, *125* (39), 11911–11924. DOI: 10.1021/ja030085e.

(83) Cheng, M.; Lobkovsky, E. B.; Coates, G. W. Catalytic Reactions Involving C 1 Feedstocks: New High-Activity Zn(II)-Based Catalysts for the Alternating Copolymerization of Carbon Dioxide and Epoxides. *J. Am. Chem. Soc.* **1998**, *120* (42), 11018–11019. DOI: 10.1021/ja982601k.

(84) Cheng, M.; Moore, D. R.; Reczek, J. J.; Chamberlain, B. M.; Lobkovsky, E. B.; Coates, G. W. Single-site beta-diiminate zinc catalysts for the alternating copolymerization of CO_2 and epoxides: catalyst synthesis and unprecedented polymerization activity. *J. Am. Chem. Soc.* **2001**, *123* (36), 8738–8749. DOI: 10.1021/ja003850n.

(85) Rieth, L. R.; Moore, D. R.; Lobkovsky, E. B.; Coates, G. W. Single-site beta-diiminate zinc catalysts for the ring-opening polymerization of beta-butyrolactone and beta-valerolactone to poly(3-hydroxyalkanoates). *J. Am. Chem. Soc.* **2002**, *124* (51), 15239–15248. DOI: 10.1021/ja020978r.

(86) Lee, B. Y.; Kwon, H. Y.; Lee, S. Y.; Na, S. J.; Han, S.-I.; Yun, H.; Lee, H.; Park, Y.-W. Bimetallic anilido-aldimine zinc complexes for epoxide/ CO_2 copolymerization. *J. Am. Chem. Soc.* **2005**, *127* (9), 3031–3037. DOI: 10.1021/ja0435135.

(87) Lehenmeier, M. W.; Kissling, S.; Altenbuchner, P. T.; Bruckmeier, C.; Deglmann, P.; Brym, A.-K.; Rieger, B. Flexibly tethered dinuclear zinc complexes: a solution to the entropy problem in CO_2/epoxide copolymerization catalysis? *Angew. Chem. Int. Ed.* **2013**, *52* (37), 9821–9826. DOI: 10.1002/anie.201302157.

(88) Kember, M. R.; Williams, C. K. Efficient magnesium catalysts for the copolymerization of epoxides and CO_2; using water to synthesize polycarbonate

polyols. *J. Am. Chem. Soc.* **2012**, *134* (38), 15676–15679. DOI: 10.1021/ja307096m.

(89) Buchard, A.; Kember, M. R.; Sandeman, K. G.; Williams, C. K. A bimetallic iron(III) catalyst for CO_2/epoxide coupling. *Chem. Commun. (Cambridge, England)* **2011**, *47* (1), 212–214. DOI: 10.1039/c0cc02205e.

(90) Kember, M. R.; Jutz, F.; Buchard, A.; White, A. J. P.; Williams, C. K. Di-cobalt(ii) catalysts for the copolymerisation of CO_2 and cyclohexene oxide: support for a dinuclear mechanism? *Chem. Sci.* **2012**, *3* (4), 1245. DOI: 10.1039/c2sc00802e.

(91) Buchard, A.; Jutz, F.; Kember, M. R.; White, A. J. P.; Rzepa, H. S.; Williams, C. K. Experimental and Computational Investigation of the Mechanism of Carbon Dioxide/Cyclohexene Oxide Copolymerization Using a Dizinc Catalyst. *Macromolecules* **2012**, *45* (17), 6781–6795. DOI: 10.1021/ma300803b.

(92) Garden, J. A.; Saini, P. K.; Williams, C. K. Greater than the Sum of Its Parts: A Heterodinuclear Polymerization Catalyst. *J. Am. Chem. Soc.* **2015**, *137* (48), 15078–15081. DOI: 10.1021/jacs.5b09913.

(93) Nagae, H.; Aoki, R.; Akutagawa, S.-N.; Kleemann, J.; Tagawa, R.; Schindler, T.; Choi, G.; Spaniol, T. P.; Tsurugi, H.; Okuda, J.; Mashima, K. Lanthanide Complexes Supported by a Trizinc Crown Ether as Catalysts for Alternating Copolymerization of Epoxide and CO_2 : Telomerization Controlled by Carboxylate Anions. *Angew. Chem. Int. Ed.* **2018**, *57* (9), 2492–2496. DOI: 10.1002/anie.201709218.

(94) Deacy, A. C.; Moreby, E.; Phanopoulos, A.; Williams, C. K. Co(III)/Alkali-Metal(I) Heterodinuclear Catalysts for the Ring-Opening Copolymerization of CO_2 and Propylene Oxide. *J. Am. Chem. Soc.* **2020**, *142* (45), 19150–19160. DOI: 10.1021/jacs.0c07980.

(95) Deacy, A. C.; Kilpatrick, A. F. R.; Regoutz, A.; Williams, C. K. Understanding metal synergy in heterodinuclear catalysts for the copolymerization of CO_2 and epoxides. *Nat. Chem.* **2020**, *12* (4), 372–380. DOI: 10.1038/s41557-020-0450-3.

(96) Williams, C. K.; Plajer, A. Heterocycle/Heteroallene Ring Opening Copolymerisation: Selective Catalysis Delivering Alternating Copolymers. *Angew. Chem. Int. Ed.* **2021.** DOI: 10.1002/anie.202104495.

(97) Jia, M.; Hadjichristidis, N.; Gnanou, Y.; Feng, X. Monomodal Ultrahigh-Molar-Mass Polycarbonate Homopolymers and Diblock Copolymers by Anionic

Copolymerization of Epoxides with CO_2. *ACS Macro Lett.* **2019**, *8* (12), 1594–1598. DOI: 10.1021/acsmacrolett.9b00854.

(98) Zhang, D.-D.; Feng, X.; Gnanou, Y.; Huang, K.-W. Theoretical Mechanistic Investigation into Metal-Free Alternating Copolymerization of CO_2 and Epoxides: The Key Role of Triethylborane. *Macromolecules* **2018**, *51* (15), 5600–5607. DOI: 10.1021/acs.macromol.8b00471.

(99) Chen, Z.; Yang, J.-L.; Lu, X.-Y.; Hu, L.-F.; Cao, X.-H.; Wu, G.-P.; Zhang, X.-H. Triethyl borane-regulated selective production of polycarbonates and cyclic carbonates for the coupling reaction of CO_2 with epoxides. *Polym. Chem.* **2019**, *10* (26), 3621–3628. DOI: 10.1039/C9PY00398C.

(100) Patil, N.; Bhoopathi, S.; Chidara, V.; Hadjichristidis, N.; Gnanou, Y.; Feng, X. Recycling a Borate Complex for Synthesis of Polycarbonate Polyols: Towards an Environmentally Friendly and Cost-Effective Process. *ChemSusChem* **2020**, *13* (18), 5080–5087. DOI: 10.1002/cssc.202001395.

(101) Patil, N. G.; Boopathi, S. K.; Alagi, P.; Hadjichristidis, N.; Gnanou, Y.; Feng, X. Carboxylate Salts as Ideal Initiators for the Metal-Free Copolymerization of CO_2 with Epoxides: Synthesis of Well-Defined Polycarbonates Diols and Polyols. *Macromolecules* **2019**, *52* (6), 2431–2438. DOI: 10.1021/acs.macromol.9b00122.

(102) Alagi, P.; Zapsas, G.; Hadjichristidis, N.; Hong, S. C.; Gnanou, Y.; Feng, X. All-Polycarbonate Graft Copolymers with Tunable Morphologies by Metal-Free Copolymerization of CO_2 with Epoxides. *Macromolecules* **2021.** DOI: 10.1021/acs.macromol.1c00659.

(103) Yang, G.-W.; Zhang, Y.-Y.; Xie, R.; Wu, G.-P. High-Activity Organocatalysts for Polyether Synthesis via Intramolecular Ammonium Cation Assisted SN 2 Ring-Opening Polymerization. *Angew. Chem. Int. Ed.* **2020**, *59* (39), 16910–16917. DOI: 10.1002/anie.202002815.

(104) Hu, L.-F.; Zhang, C.-J.; Wu, H.-L.; Yang, J.-L.; Liu, B.; Duan, H.-Y.; Zhang, X.-H. Highly Active Organic Lewis Pairs for the Copolymerization of Epoxides with Cyclic Anhydrides: Metal-Free Access to Well-Defined Aliphatic Polyesters. *Macromolecules* **2018**, *51* (8), 3126–3134. DOI: 10.1021/acs.macromol.8b00499.

(105) Jia, M.; Zhang, D.; Kort, G. W. de; Wilsens, C. H. R. M.; Rastogi, S.; Hadjichristidis, N.; Gnanou, Y.; Feng, X. All-Polycarbonate Thermoplastic Elastomers Based on Triblock Copolymers Derived from Triethylborane-Mediated

Sequential Copolymerization of CO_2 with Various Epoxides. *Macromolecules* **2020**, *53* (13), 5297–5307. DOI: 10.1021/acs.macromol.0c01068.

(106) Chidara, V. K.; Boopathi, S. K.; Hadjichristidis, N.; Gnanou, Y.; Feng, X. Triethylborane-Assisted Synthesis of Random and Block Poly(ester-carbonate)s through One-Pot Terpolymerization of Epoxides, CO_2 , and Cyclic Anhydrides. *Macromolecules* **2021**, *54* (6), 2711–2719. DOI: 10.1021/acs.macromol.0c02825.

(107) Zhang, J.; Wang, L.; Liu, S.; Kang, X.; Li, Z. A Lewis Pair as Organocatalyst for One-Pot Synthesis of Block Copolymers from a Mixture of Epoxide, Anhydride, and CO_2. *Macromolecules* **2021**, *54* (2), 763–772. DOI: 10.1021/acs.macromol.0c02647.

(108) Ye, S.; Wang, W.; Liang, J.; Wang, S.; Xiao, M.; Meng, Y. Metal-Free Approach for a One-Pot Construction of Biodegradable Block Copolymers from Epoxides, Phthalic Anhydride, and CO_2. *ACS Sustainable Chem. Eng.* **2020**, *8* (48), 17860–17867. DOI: 10.1021/acssuschemeng.0c07283.

(109) Ji, H.-Y.; Song, D.-P.; Wang, B.; Pan, L.; Li, Y.-S. Organic Lewis pairs for selective copolymerization of epoxides with anhydrides to access sequence-controlled block copolymers. *Green Chem.* **2019**, *21* (22), 6123–6132. DOI: 10.1039/C9GC02429H.

(110) Augustine, D.; Hadjichristidis, N.; Gnanou, Y.; Feng, X. Hydrophilic Stars, Amphiphilic Star Block Copolymers, and Miktoarm Stars with Degradable Polycarbonate Cores. *Macromolecules* **2020**, *53* (3), 895–904. DOI: 10.1021/acs.macromol.9b02658.

(111) Jia, M.; Hadjichristidis, N.; Gnanou, Y.; Feng, X. Polyurethanes from Direct Organocatalytic Copolymerization of p -Tosyl Isocyanate with Epoxides. *Angew. Chem.* **2021**, *133* (3), 1617–1622. DOI: 10.1002/ange.202011902.

(112) Yang, J.-L.; Wu, H.-L.; Li, Y.; Zhang, X.-H.; Darensbourg, D. J. Perfectly Alternating and Regioselective Copolymerization of Carbonyl Sulfide and Epoxides by Metal-Free Lewis Pairs. *Angew. Chem. Int. Ed.* **2017**, *56* (21), 5774–5779. DOI: 10.1002/anie.201701780.

(113) Noh, E. K.; Na, S. J.; S, S.; Kim, S.-W.; Lee, B. Y. Two components in a molecule: highly efficient and thermally robust catalytic system for CO_2/epoxide copolymerization. *J. Am. Chem. Soc.* **2007**, *129* (26), 8082–8083. DOI: 10.1021/ja071290n.

(114) Yang, G.-W.; Zhang, Y.-Y.; Xie, R.; Wu, G.-P. Scalable Bifunctional Organoboron Catalysts for Copolymerization of CO_2 and Epoxides with Unprecedented Efficiency. *J. Am. Chem. Soc.* **2020**, *142* (28), 12245–12255. DOI: 10.1021/jacs.0c03651.

(115) Zhang, Y.-Y.; Yang, G.-W.; Xie, R.; Yang, L.; Li, B.; Wu, G.-P. Scalable, Durable, and Recyclable Metal-Free Catalysts for Highly Efficient Conversion of CO_2 to Cyclic Carbonates *Angew. Chem. Int. Ed.* **2020**, *59* (51), 23291–23298. DOI: 10.1002/anie.202010651.

(116) *Kirk-Othmer chemical technology of cosmetics*; Wiley, 2013.

(117) Oertling, H.; Reckziegel, A.; Surburg, H.; Bertram, H.-J. Applications of menthol in synthetic chemistry. *Chem. Rev.* **2007**, *107* (5), 2136–2164. DOI: 10.1021/cr068409f.

(118) Klunder, J. M.; Sharpless, K. B. Convenient synthesis of sulfinate esters from sulfonyl chlorides. *J. Org. Chem.* **1987**, *52* (12), 2598–2602. DOI: 10.1021/jo00388a051.

(119) https://www.360marketupdates.com/global-l-menthol-market-14845507.

(120) *Mint*:*The genus mentha*; Medicinal and aromatic plants, Vol. 44; CRC Press, 2007.

(121) Brenna, E.; Fuganti, C.; Serra, S. From commercial racemic fragrances to odour active enantiopure compounds: the ten isomers of irone. *C. R. Chim.* **2003**, *6* (5-6), 529–546. DOI: 10.1016/S1631-0748(03)00087-0.

(122) Schäfer, B. *Natural products in the chemical industry*, 2. Ed.; Springer, 2014. DOI: 10.1007/978-3-642-54461-3.

(123) Kalita, H.; Selvakumar, S.; Jayasooriyamu, A.; Fernando, S.; Samanta, S.; Bahr, J.; Alam, S.; Sibi, M.; Vold, J.; Ulven, C.; Chisholm, B. J. Bio-based poly(vinyl ether)s and their application as alkyd-type surface coatings. *Green Chem.* **2014**, *16* (4), 1974. DOI: 10.1039/c3gc41868e.

(124) Lee, Y.-K.; Onimura, K.; Tsutsumi, H.; Oishi, T. Synthesis and polymerization of chiral methacrylates bearing a cholesteryl or menthyl group. *J. Polym. Sci. A Polym. Chem.* **2000**, *38* (23), 4315–4325. DOI: 10.1002/1099-0518(20001201)38:23<4315:AID-POLA180>3.0.CO;2-A.

(125) Metlyaeva, S. A.; Rodygin, K. S.; Lotsman, K. A.; Samoylenko, D. E.; Ananikov, V. P. Biomass- and calcium carbide-based recyclable polymers. *Green Chem.* **2021**, *23* (6), 2487–2495. DOI: 10.1039/d0gc04170j.

(126) Zhang, D.; Hillmyer, M. A.; Tolman, W. B. Catalytic polymerization of a cyclic ester derived from a “cool” natural precursor. *Biomacromolecules* **2005**, *6* (4), 2091–2095. DOI: 10.1021/bm050076t.

(127) Winnacker, M.; Vagin, S.; Auer, V.; Rieger, B. Synthesis of Novel Sustainable Oligoamides Via Ring-Opening Polymerization of Lactams Based on (−)-Menthone. *Macromol. Chem. Phys.* **2014**, *215* (17), 1654–1660. DOI: 10.1002/macp.201400324.

(128) Winnacker, M.; Tischner, A.; Neumeier, M.; Rieger, B. New insights into synthesis and oligomerization of ε-lactams derived from the terpenoid ketone (−)-menthone. *RSC Adv.* **2015**, *5* (95), 77699–77705. DOI: 10.1039/C5RA15656D.

(129) Winnacker, M.; Neumeier, M.; Zhang, X.; Papadakis, C. M.; Rieger, B. Sustainable Chiral Polyamides with High Melting Temperature via Enhanced Anionic Polymerization of a Menthone-Derived Lactam. *Macromol. Rapid Commun.* **2016**, *37* (10), 851–857. DOI: 10.1002/marc.201600056.

(130) Boys, C. V. On the Production, Properties, and some suggested Uses of the Finest Threads. *Proc. Phys. Soc. London* **1887**, *9* (1), 8–19. DOI: 10.1088/1478-7814/9/1/303.

(131) John, F. C. Apparatus for Electrically Dispersing Fluids. US18990019625 18991005.

(132) Morton, W. J. Method of Dispersing Fluids. US705691A.

(133) Formhals, A. Method and apparatus for the production of artificial fibers. US19370156169 19370728.

(134) Taylor, G. Disintegration of water drops in an electric field. *Proc. R. Soc. Lond. A* **1964**, *280* (1382), 383–397. DOI: 10.1098/rspa.1964.0151.

(135) Doshi, J.; Reneker, D. H. Electrospinning process and applications of electrospun fibers. *Journal of Electrostatics* **1995**, *35* (2-3), 151–160. DOI: 10.1016/0304-3886(95)00041-8.

(136) *Results SciFinder “electrospinning”*. https://scifinder-n.cas.org/search/reference/61d55e5bbb8a1359efdaf6a0/1 (accessed 2021-05-05).

(137) Reneker, D. H.; Yarin, A. L. Electrospinning jets and polymer nanofibers. *Polymer* **2008**, *49* (10), 2387–2425. DOI: 10.1016/j.polymer.2008.02.002.

(138) Agarwal, S.; Burgard, M.; Greiner, A.; Wendorff, J. H. *Electrospinning*:*A practical guide to nanofibers*; De Gruyter graduate; De Gruyter, 2016. DOI: 10.1515/9783110333510.

(139) Zhu, M.; Han, J.; Wang, F.; Shao, W.; Xiong, R.; Zhang, Q.; Pan, H.; Yang, Y.; Samal, S. K.; Zhang, F.; Huang, C. Electrospun Nanofibers Membranes for Effective Air Filtration. *Macromol. Mater. Eng.* **2017**, *302* (1), 1600353. DOI: 10.1002/mame.201600353.

(140) Gopal, R.; Kaur, S.; Feng, C. Y.; Chan, C.; Ramakrishna, S.; Tabe, S.; Matsuura, T. Electrospun nanofibrous polysulfone membranes as pre-filters: Particulate removal. *J. Membr. Sci.* **2007**, *289* (1-2), 210–219. DOI: 10.1016/j.memsci.2006.11.056.

(141) Gopal, R.; Kaur, S.; Ma, Z.; Chan, C.; Ramakrishna, S.; Matsuura, T. Electrospun nanofibrous filtration membrane. *J. Membr. Sci.* **2006**, *281* (1-2), 581–586. DOI: 10.1016/j.memsci.2006.04.026.

(142) Hota, G.; Kumar, B. R.; Ng, W. J.; Ramakrishna, S. Fabrication and characterization of a boehmite nanoparticle impregnated electrospun fiber membrane for removal of metal ions. *J Mater Sci* **2008**, *43* (1), 212–217. DOI: 10.1007/s10853-007-2142-4.

(143) Müller, A.-K.; Xu, Z.-K.; Greiner, A. Preparation and Performance Assessment of Low-Pressure Affinity Membranes Based on Functionalized, Electrospun Polyacrylates for Gold Nanoparticle Filtration. *ACS Appl. Mater. Interfaces* **2021**, *13* (13), 15659–15667. DOI: 10.1021/acsami.1c01217.

(144) Shin, C.; Chase, G. G. Water-in-oil coalescence in micro-nanofiber composite filters. *AIChE J.* **2004**, *50* (2), 343–350. DOI: 10.1002/aic.10031.

(145) Luraghi, A.; Peri, F.; Moroni, L. Electrospinning for drug delivery applications: A Review. *J. Control. Release* **2021**, *334*, 463–484. DOI: 10.1016/j.jconrel.2021.03.033.

(146) Beck-Broichsitter, M.; Thieme, M.; Nguyen, J.; Schmehl, T.; Gessler, T.; Seeger, W.; Agarwal, S.; Greiner, A.; Kissel, T. Novel ‘nano in nano’ composites for sustained drug delivery: biodegradable nanoparticles encapsulated into nanofiber non-wovens. *Macromol. Biosci.* **2010**, *10* (12), 1527–1535. DOI: 10.1002/mabi.201000100.

(147) Li, C.; Vepari, C.; Jin, H.-J.; Kim, H. J.; Kaplan, D. L. Electrospun silk-BMP-2 scaffolds for bone tissue engineering. *Biomaterials* **2006**, *27* (16), 3115–3124. DOI: 10.1016/j.biomaterials.2006.01.022.

(148) Hwang, T. H.; Lee, Y. M.; Kong, B.-S.; Seo, J.-S.; Choi, J. W. Electrospun core-shell fibers for robust silicon nanoparticle-based lithium ion battery anodes. *Nano Lett.* **2012**, *12* (2), 802–807. DOI: 10.1021/nl203817r.

(149) Croce, F.; Focarete, M. L.; Hassoun, J.; Meschini, I.; Scrosati, B. A safe, high-rate and high-energy polymer lithium-ion battery based on gelled membranes prepared by electrospinning. *Energy Environ. Sci.* **2011**, *4* (3), 921. DOI: 10.1039/c0ee00348d.

(150) Kayarkatte, M. K.; Delikaya, Ö.; Roth, C. Freestanding Catalyst Layers: A Novel Electrode Fabrication Technique for PEM Fuel Cells via Electrospinning. *ChemElectroChem* **2017**, *4* (2), 404–411. DOI: 10.1002/celc.201600530.

(151) Jiang, S.; Cheong, J. Y.; Nam, J. S.; Kim, I.-D.; Agarwal, S.; Greiner, A. High-density Fibrous Polyimide Sponges with Superior Mechanical and Thermal Properties. *ACS Appl. Mater. Interfaces* **2020**, *12* (16), 19006–19014. DOI: 10.1021/acsami.0c02004.

(152) Tai, M. H.; Tan, B. Y. L.; Juay, J.; Sun, D. D.; Leckie, J. O. A self-assembled superhydrophobic electrospun carbon-silica nanofiber sponge for selective removal and recovery of oils and organic solvents. *Chem. Eur. J.* **2015**, *21* (14), 5395–5402. DOI: 10.1002/chem.201405670.

(153) Ding, C.; Breunig, M.; Timm, J.; Marschall, R.; Senker, J.; Agarwal, S. Flexible, Mechanically Stable, Porous Self-Standing Microfiber Network Membranes of Covalent Organic Frameworks: Preparation Method and Characterization. *Adv. Funct. Mater.* **2021**, 2106507. DOI: 10.1002/adfm.202106507.

(154) Kronawitt, J.; Dulle, M.; Schmalz, H.; Agarwal, S.; Greiner, A. Poly(p -xylylene) Nanotubes Decorated with Nonagglomerated Gold Nanoparticles for the Alcoholysis of Dimethylphenylsilane. *ACS Appl. Nano Mater.* **2020**, *3* (3), 2766–2773. DOI: 10.1021/acsanm.0c00103.

(155) Li, D.; Xia, Y. Fabrication of Titania Nanofibers by Electrospinning. *Nano Lett.* **2003**, *3* (4), 555–560. DOI: 10.1021/nl034039o.

(156) Bognitzki, M.; Becker, M.; Graeser, M.; Massa, W.; Wendorff, J. H.; Schaper, A.; Weber, D.; Beyer, A.; Gölzhäuser, A.; Greiner, A. Preparation of Sub-

micrometer Copper Fibers via Electrospinning. *Adv. Mater.* **2006**, *18* (18), 2384–2386. DOI: 10.1002/adma.200600103.

(157) Venugopal, J.; Ramakrishna, S. Applications of Polymer Nanofibers in Biomedicine and Biotechnology. *ABAB* **2005**, *125* (3), 147–158. DOI: 10.1385/ABAB:125:3:147.

(158) O'Connor, G. L.; Nace, H. R. The Boric Acid Dehydration of Alcohols. *J. Am. Chem. Soc.* **1955**, *77* (6), 1578–1581. DOI: 10.1021/ja01611a052.

(159) Rudloff, E. von. A simple reagent for the specific dehydration of terpene alcohols. *Can. J. Chem.* **1961**, *39* (9), 1860–1864. DOI: 10.1139/v61-249.

(160) Brieger, G.; Watson, S. W.; Barar, D. G.; Shene, A. L. Thermal decomposition of aluminum alkoxides. *J. Org. Chem.* **1979**, *44* (8), 1340–1342. DOI: 10.1021/jo01322a032.

(161) Korstanje, T. J.; Waard, E. F. de; Jastrzebski, Johann T. B. H.; Klein Gebbink, Robertus J. M. Rhenium-Catalyzed Dehydration of Nonbenzylic and Terpene Alcohols to Olefins. *ACS Catal.* **2012**, *2* (10), 2173–2181. DOI: 10.1021/cs300455w.

(162) Majetich, G.; Irvin, T. C.; Thompson, S. B. One-pot dehydrations using phenyl isothiocyanate. *Tetrahedron Lett.* **2015**, *56* (23), 3326–3329. DOI: 10.1016/j.tetlet.2015.01.086.

(163) Fiorani, G.; Stuck, M.; Martín, C.; Belmonte, M. M.; Martin, E.; Escudero-Adán, E. C.; Kleij, A. W. Catalytic Coupling of Carbon Dioxide with Terpene Scaffolds: Access to Challenging Bio-Based Organic Carbonates. *ChemSusChem* **2016**, *9* (11), 1304–1311. DOI: 10.1002/cssc.201600238.

(164) Kiguchi, T.; Tsurusaki, Y.; Yamada, S.; Aso, M.; Tanaka, M.; Sakai, K.; Suemune, H. Insight into acid-mediated asymmetric spirocyclization in the presence of a chiral diol. *Chem. Pharm. Bull.* **2000**, *48* (10), 1536–1540. DOI: 10.1248/cpb.48.1536.

(165) Wambach, A.; Agarwal, S.; Greiner, A. Synthesis of Biobased Polycarbonate by Copolymerization of Menth-2-ene Oxide and CO_2 with Exceptional Thermal Stability. *ACS Sustainable Chem. Eng.* **2020**, *8* (39), 14690–14693. DOI: 10.1021/acssuschemeng.0c04335.

(166) Sulley, G. S.; Gregory, G. L.; Chen, T. T. D.; Peña Carrodeguas, L.; Trott, G.; Santmarti, A.; Lee, K.-Y.; Terrill, N. J.; Williams, C. K. Switchable Catalysis Improves the Properties of CO_2-Derived Polymers: Poly(cyclohexene carbonate-

b-ε-decalactone-b-cyclohexene carbonate) Adhesives, Elastomers, and Toughened Plastics. *J. Am. Chem. Soc.* **2020**, *142* (9), 4367–4378. DOI: 10.1021/jacs.9b13106.

(167) Ren, W.-M.; Zhang, X.; Liu, Y.; Li, J.-F.; Wang, H.; Lu, X.-B. Highly Active, Bifunctional Co(III)-Salen Catalyst for Alternating Copolymerization of CO_2 with Cyclohexene Oxide and Terpolymerization with Aliphatic Epoxides. *Macromolecules* **2010**, *43* (3), 1396–1402. DOI: 10.1021/ma902321g.

(168) Quan, Z.; Min, J.; Zhou, Q.; Xie, D.; Liu, J.; Wang, X.; Zhao, X.; Wang, F. Synthesis and properties of carbon dioxide – epoxides copolymers from rare earth metal catalyst. *Macromol. Symp.* **2003**, *195* (1), 281–286. DOI: 10.1002/masy.200390135.

(169) Poland, S. J.; Darensbourg, D. J. A quest for polycarbonates provided via sustainable epoxide/ CO_2 copolymerization processes. *Green Chem.* **2017**, *19* (21), 4990–5011. DOI: 10.1039/C7GC02560B.

(170) Makarova, M. A.; Paukshtis, E. A.; Thomas, J. M.; Williams, C.; Zamaraev, K. I. Dehydration of n-Butanol on Zeolite H-ZSM-5 and Amorphous Aluminosilicate: Detailed Mechanistic Study and the Effect of Pore Confinement. *J. Catal.* **1994**, *149* (1), 36–51. DOI: 10.1006/jcat.1994.1270.

(171) Ji, H.-Y.; Chen, X.-L.; Wang, B.; Pan, L.; Li, Y.-S. Metal-free, regioselective and stereoregular alternating copolymerization of monosubstituted epoxides and tricyclic anhydrides. *Green Chem.* **2018**, *20* (17), 3963–3973. DOI: 10.1039/C8GC01641K.

(172) Labbé, A.; Brocas, A.-L.; Ibarboure, E.; Ishizone, T.; Hirao, A.; Deffieux, A.; Carlotti, S. Selective Ring-Opening Polymerization of Glycidyl Methacrylate: Toward the Synthesis of Cross-Linked (Co)polyethers with Thermoresponsive Properties. *Macromolecules* **2011**, *44* (16), 6356–6364. DOI: 10.1021/ma201075n.

(173) Gramlich, W. M.; Theryo, G.; Hillmyer, M. A. Copolymerization of isoprene and hydroxyl containing monomers by controlled radical and emulsion methods. *Polym. Chem.* **2012**, *3* (6), 1510. DOI: 10.1039/c2py20072d.

(174) Satake, Y.; Nishikawa, T.; Hiramatsu, T.; Araki, H.; Isobe, M. Scalable Synthesis of a New Dihydroxylated Intermediate for Tetrodotoxin and Its Analogues. *Synthesis* **2010**, *2010* (12), 1992–1998. DOI: 10.1055/s-0029-1218747.

(175) Chen, Y. L.; Rånby, B. Photocrosslinking of polyethylene. I. Photoinitiators, crosslinking agent, and reaction kinetics. *J. Polym. Sci. A Polym. Chem.* **1989**, *27* (12), 4051–4075. DOI: 10.1002/pola.1989.080271214.

(176) Mukherjee, S.; Xie, R.; Reynolds, V. G.; Uchiyama, T.; Levi, A. E.; Valois, E.; Wang, H.; Chabinyc, M. L.; Bates, C. M. Universal Approach to Photo-Crosslink Bottlebrush Polymers. *Macromolecules* **2020**, *53* (3), 1090–1097. DOI: 10.1021/acs.macromol.9b02210.

(177) Thavasi, V.; Singh, G.; Ramakrishna, S. Electrospun nanofibers in energy and environmental applications. *Energy Environ. Sci.* **2008**, *1* (2), 205. DOI: 10.1039/b809074m.

(178) Ramakrishna, S.; Fujihara, K.; Teo, W.-E.; Yong, T.; Ma, Z.; Ramaseshan, R. Electrospun nanofibers: solving global issues. *Mater. Today* **2006**, *9* (3), 40–50. DOI: 10.1016/S1369-7021(06)71389-X.

(179) Agarwal, S.; Wendorff, J. H.; Greiner, A. Progress in the field of electrospinning for tissue engineering applications. *Adv. Mater.* **2009**, *21* (32-33), 3343–3351. DOI: 10.1002/adma.200803092.

(180) Sas, I.; Gorga, R. E.; Joines, J. A.; Thoney, K. A. Literature review on superhydrophobic self-cleaning surfaces produced by electrospinning. *J. Polym. Sci. B Polym. Phys.* **2012**, *50* (12), 824–845. DOI: 10.1002/polb.23070.

(181) Han, D.; Steckl, A. J. Superhydrophobic and oleophobic fibers by coaxial electrospinning. *Langmuir* **2009**, *25* (16), 9454–9462. DOI: 10.1021/la900660v.

(182) Ma, M.; Mao, Y.; Gupta, M.; Gleason, K. K.; Rutledge, G. C. Superhydrophobic Fabrics Produced by Electrospinning and Chemical Vapor Deposition. *Macromolecules* **2005**, *38* (23), 9742–9748. DOI: 10.1021/ma0511189.

(183) Liao, X.; Dulle, M.; Souza E Silva, J. M. de; Wehrspohn, R. B.; Agarwal, S.; Förster, S.; Hou, H.; Smith, P.; Greiner, A. High strength in combination with high toughness in robust and sustainable polymeric materials. *Science (New York, N.Y.)* **2019**, *366* (6471), 1376–1379. DOI: 10.1126/science.aay9033.

(184) Tebyetekerwa, M.; Xu, Z.; Yang, S.; Ramakrishna, S. Electrospun Nanofibers-Based Face Masks. *Adv. Fiber Mater.* **2020**, *2* (3), 161–166. DOI: 10.1007/s42765-020-00049-5.

(185) Sio, L. de; Ding, B.; Focsan, M.; Kogermann, K.; Pascoal-Faria, P.; Petronela, F.; Mitchell, G.; Zussman, E.; Pierini, F. Personalized Reusable Face Masks with

Smart Nano-Assisted Destruction of Pathogens for COVID-19: A Visionary Road. *Chem. Eur. J.* **2021**, *27* (20), 6112–6130. DOI: 10.1002/chem.202004875.

(186) Kchaou, M.; Alquraish, M.; Abuhasel, K.; Abdullah, A.; Ali, A. A. Electrospun Nanofibrous Scaffolds: Review of Current Progress in the Properties and Manufacturing Process, and Possible Applications for COVID-19. *Polymers* **2021**, *13* (6). DOI: 10.3390/polym13060916.

(187) Ma, W.; Zhang, Q.; Hua, D.; Xiong, R.; Zhao, J.; Rao, W.; Huang, S.; Zhan, X.; Chen, F.; Huang, C. Electrospun fibers for oil–water separation. *RSC Adv.* **2016**, *6* (16), 12868–12884. DOI: 10.1039/C5RA27309A.

(188) Allen, S. D.; Moore, D. R.; Lobkovsky, E. B.; Coates, G. W. High-activity, single-site catalysts for the alternating copolymerization of CO_2 and propylene oxide. *J. Am. Chem. Soc.* **2002**, *124* (48), 14284–14285. DOI: 10.1021/ja028071g.

(189) Erker, G.; Aulbach, M.; Knickmeier, M.; Wingbermuehle, D.; Krueger, C.; Nolte, M.; Werner, S. The role of torsional isomers of planarly chiral nonbridged bis(indenyl)metal type complexes in stereoselective propene polymerization. *J. Am. Chem. Soc.* **1993**, *115* (11), 4590–4601. DOI: 10.1021/ja00064a022.

12 Danksagungen

Zuerst möchte ich Prof. Dr. Andreas Greiner danken. Er hat mir dieses Thema vorgeschlagen und mich mit allen Mitteln bei der Umsetzung unterstützt. Ihre Fähigkeit immer den richtigen Blickwinkel auf die Dinge zu behalten hat es mir wiederholt ermöglicht im Dschungel meiner Daten die wahrhaft interessanten Stücke zu finden. Unsere Gespräche, in denen wir viele optimistische Ziele und auch meine teilweise verrückten Ideen fachlich diskutieren konnten, waren oftmals eine Quelle der Motivation und Orientierung. Vielen Dank für die Freiheiten meines Themas und das verbundene Vertrauen, das Sie in mich gesetzt haben.

Prof. Dr. Seema Agarwal ist auch natürlich auch zu danken. Sie haben immer die richtigen Worte gefunden, um Denkanstöße oder Inspiration für weitere Experimente zu geben oder mich daran zu erinnern, dass meine Ergebnisse trotz Rückschlägen brauchbar sind. Gerade Ihre Anmerkungen zu meinem Paper habe dieses erst auf das Niveau gebracht auf dem es veröffentlicht wurde.

Ohne meine Familie würde ich diese Danksagungen heute nicht schreiben. Meine Eltern haben mich immer in jeglicher Hinsicht unterstützt, von Kindesbeinen, durch Schule und Studium, bis hierher und ich bin mir sicher sie werden es auch in Zukunft immer tun. Ihr habt mir alle Freiheiten gegeben meinen Weg zu finden, meine Fehler zu machen und meine Träume zu verfolgen. Der immerwährende Wettstreit mit meinem Bruder stets schneller, schlauer oder kurz besser zu sein hat bestimmt auch seinen Teil beigetragen.

Natürlich muss ich auch unserem tollem Sekretariat Gaby, Niko, Christina und Ramona danken. Die viele Zeit, die ich mit Euch verbracht habe, war wirklich unterhaltsam und Ihr habt mich genauso unterstützt wie ich Euch.

Ein dank geht natürlich auch an meine Studenten Markus, Heiko, Andreas, Christoph und Matthias. Ihr habt alle außerordentliches Durchhaltevermögen bewiesen. Jeder von Euch hat in seiner eigen Weise diese Arbeit bereichert und es war wirklich angenehm mit Euch zu arbeiten.

Ein weiterer Dank an meine Hiwis Markus und Joan. Ihr habt mir so viel Arbeit abgenommen und Euch selbst übertroffen. Ihr habt deutlich mehr geleistet, als ich anfangs dachte. Nicht jeder kocht die Reserven der Universität leer!

Ich muss auch Felix, Nina, Marius, Elmar, Liao, Rika, Thomas und Martin danken. Die hervorragenden Messungen, die Ihr mir abgenommen habt, haben maßgeblich zu einem besseren Verständnis meiner Daten verholfen.

Gerade in Sachen Electrospinning muss ich einen Dank an Chengzhang und Felix aussprechen. Sie haben mir die Methode in kürzester Zeit erklärt und standen auch danach immer mit Rat, Tat, Material und ihrer Zeit zur Verfügung.

Danke auch an Holger, der immer richtigen Moment die Augenbraue gehoben hat, damit man weiß, dass man auf dem Holzweg ist. Sein Wissen über Arbeiten unter Schutzgas, die Unterstützung bei der Trocknung des CO_2 und seine allgemeine Erfahrung im Labor haben große Teile dieser Arbeit erst möglich gemacht.

Danke Thomas für all die Runden „Namensreaktionraten“, Diskussionen über verrückte Synthesen oder Verbindungen, den tollen Urlaub in Prag, nerdige Gespräche und generell für die Freundschaft, die sich in den letzten Jahre mit Dir entwickelt hat.

Danke auch an meine Lab-Buddies im PNS und Chris. Neben der Arbeit auch mal quatschen zu können, einfach mal seltsame Musik laufen zu lassen und gemeinsame Aufräumaktionen haben für einige unvergessliche Momente gesorgt.

Ein besonderer Dank erneut an Thomas, Felix und Marcel, die diese Arbeit vor der Abgabe nochmal genau untersucht und jeden erdenklichen Fehler rot angestrichen haben. Wärt ihr nicht gewesen, hätte diese Arbeit einiges weniger an Biss. Danke, dass Ihr Euch die Zeit genommen habt!

Der letzte Dank geht an den ganzen Lehrstuhl, der mich die ganzen Jahre begleitet, mit mir gefeiert, diskutiert, geschuftet, gegessen und gelacht hat. Ohne euch wäre diese Zeit bei weitem nicht so schön und spannend gewesen.

(Eidesstattliche) Versicherungen und Erklärungen

(§ 9 Satz 2 Nr. 3 PromO BayNAT)

Hiermit versichere ich eidesstattlich, dass ich die Arbeit selbstständig verfasst und keine anderen als die von mir angegebenen Quellen und Hilfsmittel benutzt habe (vgl. Art. 64 Abs. 1 Satz 6 BayHSchG).

(§ 9 Satz 2 Nr. 3 PromO BayNAT)

Hiermit erkläre ich, dass ich die Dissertation nicht bereits zur Erlangung eines akademischen Grades eingereicht habe und dass ich nicht bereits diese oder eine gleichartige Doktorprüfung endgültig nicht bestanden habe.

(§ 9 Satz 2 Nr. 4 PromO BayNAT)

Hiermit erkläre ich, dass ich Hilfe von gewerblichen Promotionsberatern bzw. -vermittlern oder ähnlichen Dienstleistern weder bisher in Anspruch genommen habe noch künftig in Anspruch nehmen werde.

(§ 9 Satz 2 Nr. 7 PromO BayNAT)

Hiermit erkläre ich mein Einverständnis, dass die elektronische Fassung meiner Dissertation unter Wahrung meiner Urheberrechte und des Datenschutzes einer gesonderten Überprüfung unterzogen werden kann.

(§ 9 Satz 2 Nr. 8 PromO BayNAT)

Hiermit erkläre ich mein Einverständnis, dass bei Verdacht wissenschaftlichen Fehlverhaltens Ermittlungen durch universitätsinterne Organe der wissenschaftlichen Selbstkontrolle stattfinden können.

…….
Ort, Datum, Unterschrift